UNIVERSITÀ DEGLI STUDI DI SALERNO

DIPARTIMENTO DI CHIMICA E BIOLOGIA "A. ZAMBELLI"

PHD THESIS – XXXI CYCLE
2017/2018

SYNTHESIS OF SUSTAINABLE POLYESTERS VIA RING OPENING POLYMERIZATION PROMOTED BY PHENOXY-IMINE ALUMINUM COMPLEXES

FLORENCE ISNARD

TUTOR:
PROF. MINA MAZZEO

CO-TUTOR:
PROF. MARINA LAMBERTI

COORDINATOR: PROF. GAETANO GUERRA

A ma famille,

« Savoir s'étonner à propos est le premier pas fait sur la route de la découverte. » Louis Pasteur.

INDEX

LIST OF ABBREVIATIONS.

°C	Celsius degree
Ar	Aryl
BDI	β-diiminate
BL	β-butyrolactone
Cat	Catalyst
CHO	Cyclohexene oxide
CL	Caprolactone
Conv.	Conversion
Đ	Polydispersity index
DMAP	4-(N,N-dimethylamino)pyridine
DSC	Differential Scanning Calorimetry
GPC	Gel Permeation Chromatography
h	Hours
^{i}Pr	Isopropyl
LA	Lactide
LO	Limonene oxide
MA	Maleic anhydride
MALDI-ToF-MS	Matrix assisted laser desorption/ionization-Time of Flight Mass
Me	Methyl
min	Minute
M_n	Number average molecular weight
NMR	Nuclear Magnetic Resonance
PA	Phthalic anhydride
PCHO	Poly(cyclohexene oxide)
PCL	Poly(ε-capolactone)
Ph	Phenyl
PHB	Poly(β-butyrolactone)
PLA	Poly(lactic acid)
PPN	bis(triphenylphosphine)iminium
ROCOP	Ring-opening co-polymerization
ROP	Ring-opening polymerization
RT	Room temperature
SA	Succinic anhydride
T	Temperature
t	Time
TBA	Tetrabutylammonium
^{t}Bu	*tertio*-Butyl
T_g	Glass transition temperature
THF	Tetrahydrofuran
TOF	Turnover frequency
TON	Turnover number

SUMMARY.

Aliphatic polyesters are emerging as an important class of materials as alternatives to petroleum-based polymers.[1] They are biodegradable and, in some cases, are produced from renewable feedstocks. In this context, the development of efficient polymerization routes to produce polyesters with controlled macromolecular parameters is of great interest. To this purpose, the most effective methods are the ring-opening polymerization (ROP) of cyclic esters and the ring-opening co-polymerization (ROCOP) between epoxides and anhydrides.

In the ROP of cyclic esters, salen complexes based on five-coordinate aluminum are among the most successful catalysts.[2] Recently, bimetallic complexes have attracted great attention as they have different catalytic behaviours in comparison to their related monometallic derivatives because of the presence of two proximal reactive centres within the same complex that can act in a concerted mode.[3]

In the parallel field of the ROCOP between epoxides and anhydrides, the literature suggests a bimetallic mechanism to explain the greater performances of bimetallic complexes.[4,5]

On the other hand, the use of dianionic [ONNO]-type ligands as binucleating ligands for the formation of bimetallic species is definitively less explored.[6]

The aim of the thesis is to develop simple and efficient aluminum catalysts for the ROP of cyclic esters, as well as for the ROCOP between epoxides/anhydrides exploring the possibility of a

synergistic effect when two reactive metal centres are in proximal positions.

Salen ligand framework is a platform of choice thanks to its facile synthesis and modifications. In addition, aluminum is an abundant and cheap metal with low toxicity.

We report the synthesis and the study of the catalytic behaviour of tetra-coordinate dinuclear aluminum complexes ligated by simple salen-type frameworks to explore the possibility of cooperation between the two aluminum centres in both catalytic processes ROP and ROCOP.

Since the distance between metal centres is a critical parameter to have cooperation, the salen ligands have been designed to feature two coordinative tasks at varying distances from one another, thanks to the variable alkyl backbone length between the imine functionalities (complexes **1**-**3**). In the same scope, the related hemi-salen monometallic complex **4** was designed (Scheme 1).

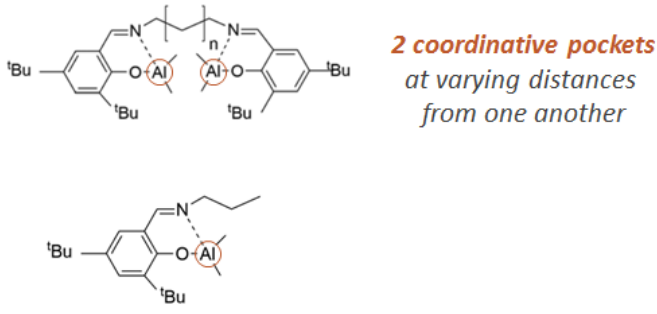

Scheme 1. Aluminum salen complexes investigated (n = 1, 3, 10).

Firstly, all complexes were tested as initiators in the ROP of several heterocyclic substrates: lactide (LA), ε-caprolactone (ε-CL), *rac*-β-butyrolactone (β-BL) and cyclohexene oxide (CHO).

The bimetallic complex **1** in which the two reactive centres are in proximal positions demonstrated the best activity towards all the monomers. In the polymerization of lactides and ε-caprolactone, its activity was about 50 times higher than that of the bimetallic species in which reactive centres are more distant (**2**-**3**) and of the related monometallic species **4** (scheme 2).

Strikingly, in the ROP of CHO and β-BL complex **1** was the only one active.

In the ROP of *rac*-lactide, complex **1** resulted the only one able to produce isotactic enriched PLA.

All these data suggested the existence of cooperative phenomena between the two vicinal metal centres in complex **1** (Chapter 2.3).[7]

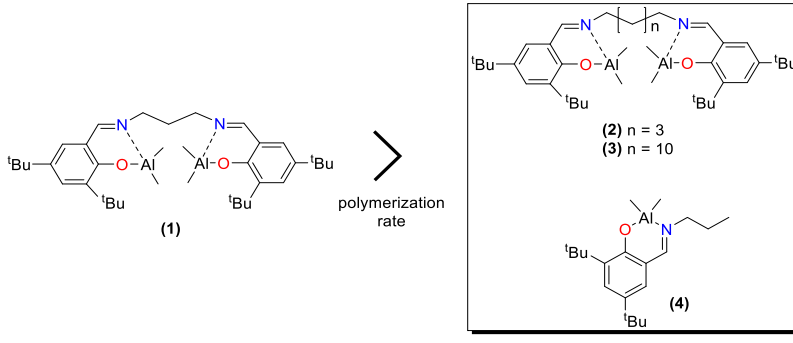

Scheme 2. Reactivities of the complexes in the ROP of *rac*-lactide.

Seeing the high activity of complex **1** in the ROP of several heterocyclic substrates, co-polymerization reactions were performed.

In the copolymerizations of cyclic esters, complex **1** produced polyesters ranging from gradient to blocky structure depending on the kinetic control.

In the co-polymerization of cyclic esters with cyclohexene oxide, a drastic chemoselectivity emerged, since only the homopolyesters could be produced when both monomers were present simultaneously in the reaction medium. Block polyether-co-polyester were successfully obtained by sequential addition of the monomers (Chapter 2.4).[8]

Afterwards, the same complexes, in combination with a nucleophilic co-catalyst, were found to be highly active in the ROCOP of cyclohexene oxide (CHO) and limonene oxide (LO) with different anhydrides.

The reaction conditions and in particular the optimal choice of co-catalyst, were studied revealing that non-ionic co-catalysts, such as 4-(N,N-dimethylamino)pyridine (DMAP), are more selective in apolar media and ionic co-catalysts are more efficient in polar solvents such as methylene chloride.

The copolymerization of LO with phthalic anhydride (PA) allowed to produce partially renewable semi-aromatic polyesters (Chapter 3.2).

From the copolymerization studies of epoxides and anhydrides emerged that the monometallic complex **4** and the bimetallic complex **1** have the same catalytic behaviour, in terms of both activity and selectivity. This suggested a monometallic pathway with our class of complexes in this catalysis.[9]

Since the bimetallic catalyst **1** with reactive centres in proximal positions exhibited the best performances both in the ROP and ROCOP processes, we explored the possibility to combine them

starting from a mixed monomer feedstock (CHO, SA and a cyclic ester).

Complex **1** revealed to be able to switch between the distinct polymerization cycles showing high monomer selectivity and producing block copolyesters from ROCOP of CHO/SA followed by ROP of the cyclic ester. Surprisingly, the portion of the copolymer obtained by copolymerization of CHO and SA showed a perfectly alternating structure without any addition of cocatalyst, suggesting that, during the production of the first block, the cyclic ester played the role of a co-catalyst (Chapter 3.4).[8]

The results obtained in the ROCOP of epoxides and anhydride revealed that the simple monometallic phenoxy-imine aluminum complex **4**, in combination with DMAP, was highly active and selective in this catalysis.

Thus, we studied the structure-performance relationship, both in terms of activity and selectivity, of tetra-coordinate phenoxy-based monometallic catalysts in the ROCOP. Phenoxy-imine, phenoxy-thioether and phenoxy-amine complexes have been tested (Scheme 3). Phenoxy-imine complexes resulted the most efficient with higher activities favoured by electron-donating substituents attached to the phenoxy-donor although when large substituents are in *ortho* positions the selectivity is compromised.

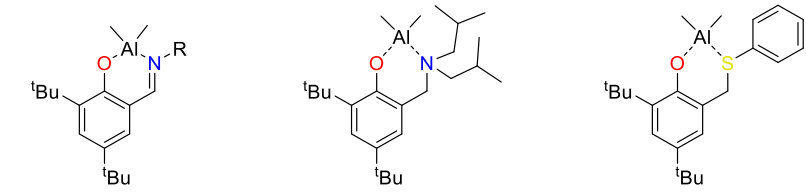

(4) R = *n*-propyl
(5a) R = Ph
(5b) R = 2,6-diisopropylphenyl
(5c) R = 2,6-dimethylphenyl
(5d) R = 4-methoxyphenyl
(5e) R = C_6F_5

Scheme 3. Phenoxy-based dimethyl-aluminum complexes **4-7**.

Finally, bifunctional catalysts which in addition to the reactive metal centre, present a nucleophilic portion, to simulate the cocatalyst, were synthetized. A pendant arm bearing an additional neutral donor was introduced on the ancillary ligand with the aim to incorporate the co-catalyst directly in the structure of the ligand (Scheme 4).

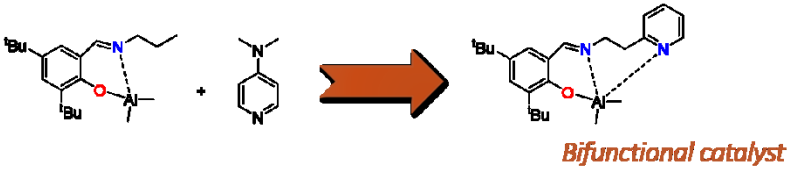

Scheme 4. Design of a bifunctional catalyst.

The effect of the structure of the ancillary ligand, modifying the substituents on the phenoxy ring and the nature of the neutral donor, on the performance of these [ON]-$AlMe_2$ complexes (Scheme 5) in terms of activity, as well as selectivity was discussed.

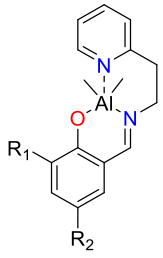

(8a) $R_1 = R_2 = {}^tBu$
(8b) $R_1 = H$, $R_2 = OMe$
(8c) $R_1 = R_2 = F$
(8d) $R_1 = R_2 = NO_2$

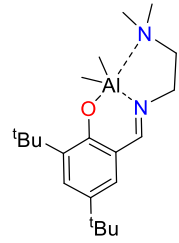

(9)

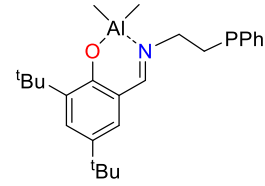

(10)

Scheme 5. Phenoxy-imine dimethyl-aluminum complexes with a pendant arm **8-10**.

From this study emerged that catalysts with a pyridine pendant arm and electron donating substituents (**8a-b**) on the phenoxide ring were the best ones for the ROCOP since they gave an excellent selectivity towards polyester formation (Chapter 4).

CHAPTER 1. INTRODUCTION.

Polyesters: An attractive class of polymers.

Plastic materials are widely used in our modern society: 335 million tons of plastics were produced worldwide in 2016, a 45% increase since 2005.[10] The vast majority of commodity materials are obtained from petrochemical feedstocks. However, fossil resources are limited. Furthermore, once introduced into the marketplace, the majority of these materials end up in the environment as waste, from which 4.8 to 12.7 million tons entering the ocean, damaging the marine environment.[11]

It is a growing market in need of innovation to minimize the impact on the environment. In particular, bio-sourced polyesters attract considerable interest with regard to sustainable development as alternatives to polymers derived from oil.[1] One of the current challenges is to develop bioderived polymers with competitive performance properties (thermal resistance, mechanical strength, processability) and that are cost efficient.

According to the structure of the repeating units of the main chain, polyesters are classified as aliphatic, semi-aromatic and aromatic. Aromatic portions improve the hardness, rigidity and heat resistance of the polymeric material, whereas aliphatic segments increase the flexibility and lower the melting temperature thus improving the processability.

The most important commercial polyesters are terephthalic polyesters such as poly(ethylene terephathalate) (PET) and poly(butylene terephthalate) (PBT). Both are semi-aromatic. They are thermoplastic materials that can be easily shaped to obtain films and fibers, and thanks to their good mechanical properties, they are largely used in daily life.

Aliphatic polyesters are materials with low melting and glass transition temperatures as well as poor hydrolytic stability. They are biodegradable and/or biocompatible. Traditionally, because of these properties they have found application in the biomedical and pharmaceutical fields but recently their use has been extended to different industrial areas such as packaging and fibers.

Some of the most successful aliphatic polyesters are certainly poly(glycolic acid) (PGA) and more recently poly(lactic acid) (PLA) (Scheme 1.1) thanks to the NatureWorks process for the scalable production of PLA from corn *via* fermentation technologies.[12,13,14] Their common uses include plastic films, bottles, and biodegradable medical devices for drug release and tissue engineering.[15] In this context, PLA is the leading bio-plastic which production capacities are predicted to grow up by 50 percent from 2017 to 2022.[16]

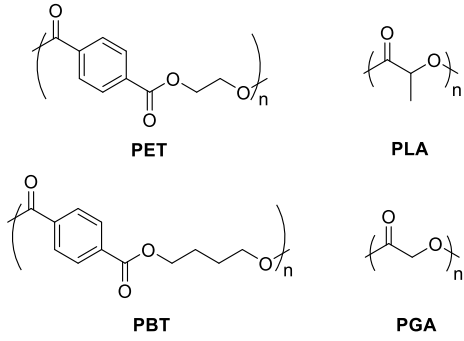

Scheme 1.1. Structures of some successful polyesters.

Using biomass can have both economic and environmental benefits. The discovery of efficient and selective processes for the synthesis of renewable polymers from biomass-derived feedstocks and that are suitable for recycling or biodegradation, is a crucial requirement for the sustained growth of the chemical industry.

1.1. SYNTHETIC APPROACHES TO POLYESTERS

Polyesters can be mainly produced *via* three synthetic methods (Scheme 1.2).

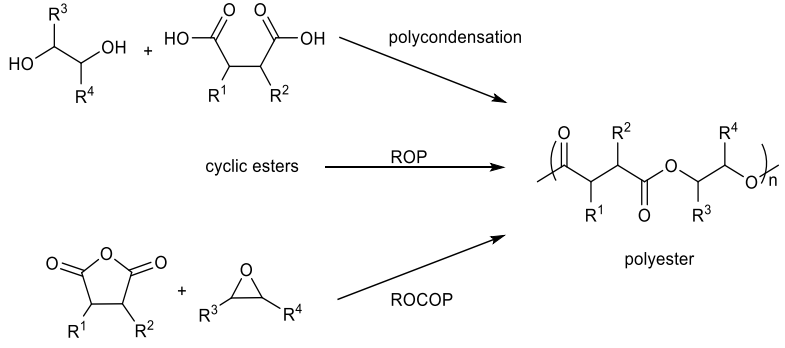

Scheme 1.2. Synthetic approaches to polyesters.

The traditional one is the polycondensation between a diol and a diacid. The advantages of this synthetic method are the access to a large monomer feedstock and thus the possibility to produce a wide range of polymers structurally diverse at low costs. Unfortunately, this method requires high temperatures to remove the by-products (most often water) to achieve high molecular weight polymers which has significant consequences on the energy demand and on the control of the polymerization process. This is the reason why the development of controlled polymerizations is of interest, especially for the production of more sophisticated polymers.

1.1.1. Ring-Opening Polymerization (ROP)

The ring-opening polymerization (ROP) of cyclic esters enables the preparation of high molecular weight polyesters with controlled microstructure under mild reaction conditions. The ring strain of the monomer is the thermodynamic driving force of the ROP.

Several metal-salts and well-defined single site catalysts have been described to promote ROP by coordination-insertion mechanism.[17] The catalyst's key parameters are the activity, the ability to control molar mass (and polydispersity) and if applicable, the regio- and stereo-selectivity during monomer enchainment.

Tin octanoate, tin triflate and aluminum isopropoxide for example have been applied with success in the ROP of cyclic esters.[18]

Single-site catalytic systems have a general formula L_nM-X where L_n is an ancillary ligand that minimizes aggregation reactions and modulates the electronic and steric properties of the catalyst. The metal M serves as a Lewis acid and -X is the initiator group

(commonly carboxylate, alkoxide or halide). Notably, aluminum complexes bearing tetraphenylporphyrin ligand[19] or salicylaldiminato ligands (salen)[20] have been reported in the ROP of cyclic esters. Salen aluminum catalysts display a great stereoselectivity in the ROP of *rac*-lactide.[20b-e] The use of salen aluminum catalysts in the ROP will be further discussed in the next Chapter.

Single-site catalysts promote ROP by coordination-insertion mechanism. The first step is the coordination of the monomer (*rac*-lactide for instance) to the metal centre, followed by the attack by the metal alkoxide group which will become one of the end-group of the polymer chain. This intermediate undergoes acyl bond cleavage of the lactide ring to generate a new metal alkoxide species on which will continue to grow the polymeric chain (Scheme 1.3).

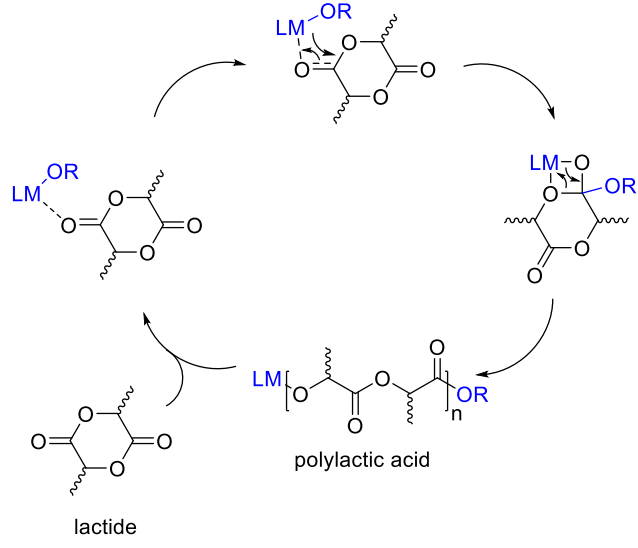

Scheme 1.3. Coordination-insertion mechanism for *rac*-lactide promoted by an alkoxide metal complex.

However, ROP usefulness is restricted by the limited number of structurally diverse monomers, in addition it is arduous to synthesize semi-aromatic polyesters.[21]

1.1.2. Ring-Opening Co-Polymerization between epoxides and anhydrides (ROCOP)

A versatile way for producing polyesters with variable architectures is the ring-opening co-polymerization (ROCOP) between epoxides and cyclic anhydrides. The ROCOP route is both energy and atom efficient, a key advantage in the context of green chemistry. Finally, the ROCOP enables the preparation of polyester backbones with aromatic/semi-aromatic repeat units, which cannot be accessed using ROP but are useful to improve the thermal–mechanical properties and to integrate functionality into polymers.

In contrast to the ROP, the ROCOP has been yet under-investigated, and only a limited number of catalytic systems described in the literature are able to produce high molecular weight polyesters.[22]

In the 60s, Inoue wrote the first mechanistic proposal with dialkyl zinc.[23] The initiation step is the ring-opening of the epoxide to form the metal alkoxide intermediate (Scheme 1.4). The formed intermediate attacks the anhydride to produce a metal carboxylate intermediate. Therefore, the copolymerization occurs by the continual cycling between metal alkoxide and carboxylate intermediates. The termination is achieved by manipulating the reaction conditions: lowering the temperature, complete consumption of the monomers or by addition of water or acids.

Perfectly alternating polyester structures will be formed by sequential epoxide/anhydride copolymerization. A detrimental side

reaction is the sequential enchainment of epoxides, producing ether linkages. The percentage of ester linkages determines the selectivity of the copolymerization.

Another side reaction is the chain transfer reaction, when the growing polymer chain reacts with protic compounds, such as alcohols. Chain transfer reaction can be beneficial to control the molar mass, end group and narrow the polydispersity. On the other side, the catalytic system has to be particularly robust to not be degraded by the protic compound.

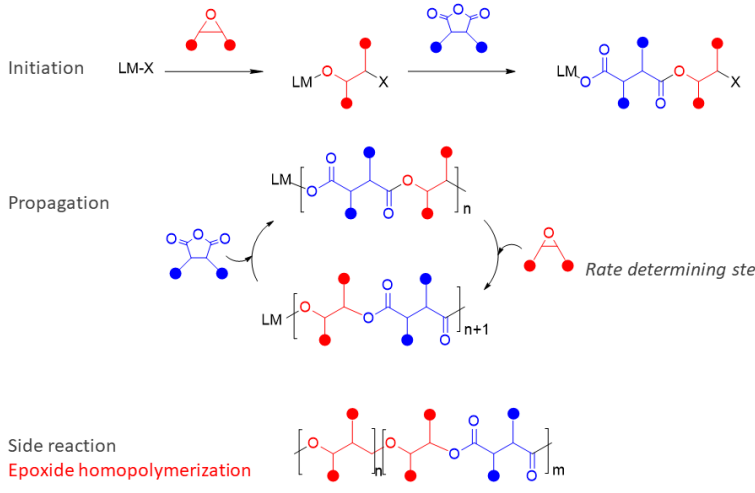

Scheme 1.4. Polymerization pathway.

One of the first remarkable examples of catalysts able to promote this reaction was the β-diiminate zinc complex, (BDI)ZnOAc, reported by Coates and co-workers in 2007 (Scheme 1.5).[24] Used in the copolymerization of diglycolic anhydride with cyclohexene oxide, it produced perfectly alternating polyesters with high molar masses and narrow distributions.

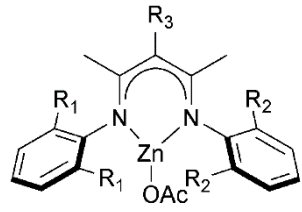

Scheme 1.5. β-diiminate zinc complex.

Indeed, few successful single catalysts active in the ROCOP of epoxides and anhydrides have been reported. The most significant examples include complexes of trivalent metals such as Cr^{III}, Co^{III}, Mn^{III}, or Al^{III} with tetradentate dianionic ligands such as porphyrinate or salen derivatives (Scheme 1.6).

In 1985, Inoue reported porphyrinato aluminum complexes with quaternary salts catalytic systems having low activity for the propylene oxide/ phthalic anhydride copolymerization. The polymers obtained displayed high ester linkage content but with low molar masses.[25]

In 2011, Duchateau used chromium tetraphenylporphyrinato complex and highlighted the positive effect of the addition of a co-catalyst (DMAP, 4-N,N-dimethylamino-pyridine) on both the activity and the selectivity.[26] Indeed, it is generally proposed that either the Lewis base or the anion coordinates to the metal catalyst, resulting in the labilizing of the initiating group (X) or the propagating polymer chain and thus accelerating polymerization. The authors also showed that the Cr^{III} complex performed better than the Co^{III} and Mn^{III} analogues.

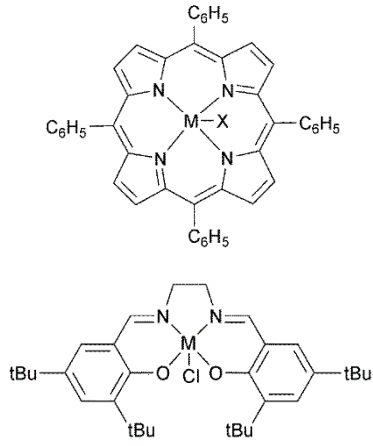

Scheme 1.6. Porphyrin (up) and salen-type (down) ligands with trivalent metals (M = Cr, Al, Co, Mn).

Coates reported the successful use of cobalt and chromium salen complexes for epoxide/maleic anhydride copolymerizations. They afforded perfectly alternating polyesters with high molar masses (up to 31 000 g/mol), reasonably narrow distributions (< 1.7) and moderate activities.[27] The alternating copolymerization of propylene oxide with terpene-based cyclic anhydrides was carried out by the same author, illustrating a sustainable route to aliphatic polyesters. The aluminum salen complex exhibited exceptional selectivity. The resulting polyesters had high molecular weights with narrow polydispersities.[28]

Duchateau and co-workers reported an extensive study of metal/co-catalyst combinations for cyclohexene oxide/anhydride copolymerization.[29]

They also investigated limonene oxide/phthalic anhydride copolymerization to yield partially renewable polyesters. The

chromium and aluminum catalysts performed best, leading to the formation of polyesters with tunable molecular weights and narrow polydispersities.[30]

Recent mechanistic studies suggested the interest of using dinuclear catalysts that are supposed to accommodate more easily the monomers. Moreover, dinuclear catalysts frequently showed superior performance compared to monometallic ones in the parallel field of CO_2-epoxides copolymerization.[31,32] In 2013, Lu *et al.* described a phenoxide dinuclear catalyst 4-7 times faster in the ROCOP of epoxide/maleic anhydride in comparison to the related monometallic one.[4] Williams[33] reported a bisphenoxide heterodinuclear (zinc and magnesium) catalyst showing good activity to produce perfectly alternate polyester without addition of a co-catalyst.

In conclusion, the huge asset of this synthetic way is the wide range of relatively cheap and often commercially available monomers. There is an incentive to develop synthetic routes to prepare epoxides and anhydrides from renewable feedstocks in order to produce renewable polymers. By taking advantage of the structural diversity, abundance and innocuousness of renewable monomers, and of the recent developments in ROCOP, new opportunities for the production of polyesters are emerging.[34]

1.2. MONOMERS FROM BIOMASS

Bio-based materials are defined as materials made from biological and renewable resources.[35] Nonetheless, it is important to note that not all bio-derived material will be biodegradable, and *vice versa*.[36]

There are many biomass sources that could be converted into renewable monomers to produce sustainable polymers, including simple sugars, starch, lignocelluloses, plant oils, and so on. The majority (60–90 wt%) of plant biomass are the biopolymer carbohydrates stored in the form of cellulose and hemicelluloses. Epoxides or anhydrides may be derived from naturally occurring sources such as carbohydrates, fatty acids, and terpenes (Scheme 1.7). The large and ubiquitous availability of these sources, generally as waste from the food and wood industries, is an attractive key point for the development of new sustainable polymers with enhanced properties.

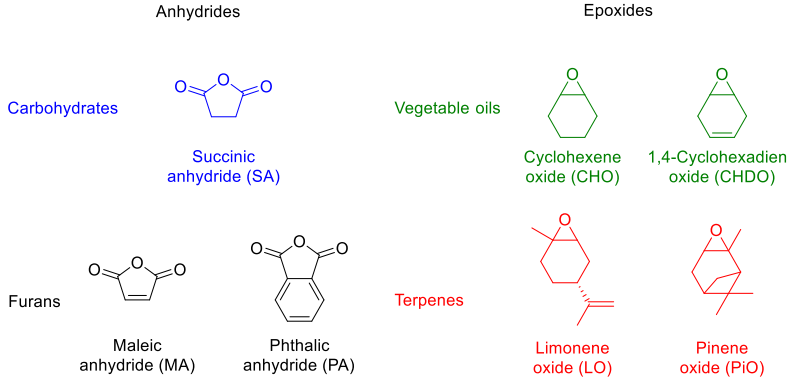

Scheme 1.7. Most investigated monomers in the ROCOP deriving from natural sources.

1.2.1. Lactide and Anhydrides from Carbohydrates

Most renewable carboxylic acids are prepared by fermentation of carbohydrates such as glucose. Glucose is transformed into building-block chemicals such as lactic acid or succinic acid which will be transformed into monomers. Bio-succinic acid has also been a hot

topic the last few years with four companies working on its production: Myriant, BioAmber, BASF-Purac (Succinity) and Reverdia (DSM-Roquette). For example, lactic acid leads to lactide and succinic acid to succinic anhydride, one of the most studied anhydride in the ROCOP, since the early discovery by Maeda *et al.* in 1997.[37] Thomas and co-workers reported in 2011 the synthesis of aliphatic polyesters *via* an auto-tandem catalytic transformation, where cyclic anhydrides (*e.g.*, camphoric, glutaric, pimelic, succinic anhydrides) are directly synthesized from dicarboxylic acids and subsequently copolymerized with epoxides.[38]

Maleic and phthalic anhydride, furan-derived monomers can be prepared from carbohydrate resources. Phthalic anhydride is of high interest since it allows the production of semi-aromatic polyesters thus improving the rigidity of the polymer backbone and the thermal properties.[39] The copolymerization of maleic anhydride with epoxides has been largely studied by Coates and co-workers, to produce unsaturated polyesters.[27]

1.2.2. Bio-based Epoxides

Vegetable oils are an important class of abundant natural resources and the literature already reports their use to make various monomers for polymerization. In 2015, Williams and co-workers showed that epoxides derived from 1,4-cyclohexadiene such as cyclohexene oxide (CHO) and 1,4-cyclohexadiene oxide (CHDO) can be synthesized from plant oil derivatives.[40]

Fully renewable options are limonene oxide and pinene oxide, derived from terpenes. Terpenes are found in many essential oils

from plants and trees, and represent a versatile chemical feedstock. The global turpentine production is more than 300 000 tons per year and its major constituents are α-pinene (45–97%) and β-pinene (0.5–28%). However, to date, the only example of a successful synthesis of aliphatic polyesters from these biorenewable substrates compounds was described by Thomas *et al.* who reported the alternating copolymerization of α-pinene oxide (α-PiO) and glutaric anhydride, to give the corresponding fully biodegradable copolymer.[38]

Produced by more than 300 plants, limonene is the most common terpene.[41] The *(R)*-enantiomer constitutes 90-96% of citrus peel oil,[42] and its world production is estimated to be more than 60 000 tons per year.[43] The corresponding epoxide is commercially available and its abundance, low cost, and structural similarity to CHO make *(R)*-limonene oxide (LO) an excellent choice as a non-food biorenewable epoxide monomer.

LO has been used as a comonomer for the synthesis of aliphatic polyesters by Coates[24] and Thomas[38]. More recently, Duchateau[30] reported the copolymerization of phthalic anhydride with LO to produce poly(limonene phthalate) a partially renewable semi-aromatic polyester. Additionally, bearing a vinyl pendant group as extra functionality, *(R)*-limonene offers the opportunity of post polymerization modifications to functional polymers, thereby increasing the range of potential uses. Taking advantage of these functional groups of raw natural biomass is of great interest. This usually requires the use of highly efficient chemistry for functionalization. The production of functional polymers is of

interest for many applications such as reactive substrates, coating resins, electronic and biomedical materials.[44]

Recently, Coates and co-workers reported the copolymerization of terpene-based cyclic anhydrides with propylene oxide using various metal salen catalysts, producing polyesters with T_g values up to 109 °C.[28, 45]

1.3. PRESENTATION OF THE PHD PROJECT

Aliphatic polyesters are emerging as an important class of materials alternatives to petroleum-based polymers.[1] They are often biodegradable and can be produced from renewable feedstocks. In this context, the development of controlled polymerization routes such as the ROP of cyclic esters and the ROCOP between epoxides and anhydrides, is of high interest.

As reported above, salen complexes based on five-coordinated aluminum have been widely studied to promote the ROP of cyclic esters such as lactide, and are among the most successful catalysts.[2] Salen ligand framework is a platform of choice thanks to its facile synthesis and modifications. In addition, aluminum is the most abundant of all metals in the earth's crust, a cheap metal with low toxicity.

Recently, bimetallic complexes have attracted great attention as they have different catalytic behaviours in comparison to their related monometallic derivatives because of the presence of two proximal reactive centres within the same complex that can act in a concerted mode.[3]

Moreover, in the parallel field of the ROCOP between epoxides and anhydrides, the literature suggests a bimetallic mechanism to explain the greater performances of bimetallic complexes.[4,5]
On the other hand, the use of dianionic "ONNO" type ligands as binucleating ligands for the formation of bimetallic species is definitively less explored.[6]

The aim of the thesis is to develop simple and efficient bimetallic salen-type aluminum catalysts for the ROP of cyclic esters, as well as for the ROCOP between epoxides/anhydrides exploring the possibility of a synergistic effect when two reactive metal centres are in proximal positions.

Since the distance between the metal centres is a critical parameter to have cooperation between them, dinuclear aluminum alkyl complexes of the general formula L-Al_2Me_4, where L are salen ligands with an alkyl backbone of different lengths between the nitrogen atoms have been prepared to investigate the possibility of cooperation between reactive centres in ring-opening polymerizations. The related tetra-coordinate hemi-salen, that is phenoxy-imine monometallic complex, was also synthesized (Scheme 1.8).

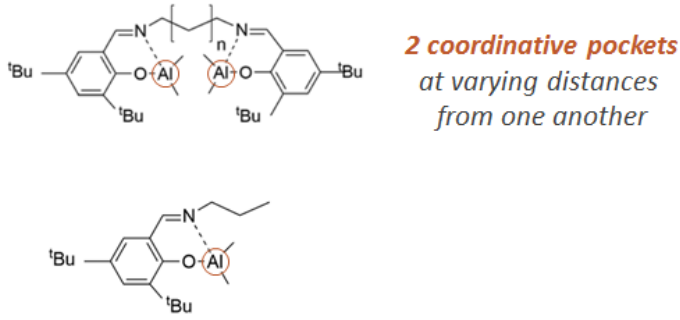

Scheme 1.8. Aluminum complexes investigated (n = 1, 3, 10).

The PhD project aimed at answering several questions:

- if the bimetallic complexes are more active than the related monometallic one,
- if the ROP and ROCOP mechanisms are involving a bimetallic or monometallic pathway,
- how the structure of the catalyst influences the selectivity in the ROCOP process.

The activities of these aluminum complexes have been analysed for the synthesis of polyesters via both catalytic processes. A comparison of the catalytic behaviour of the bimetallic aluminum complexes and of the related monometallic complex was performed to verify the hypothesis of bimetallic mechanism.

Firstly, all complexes were tested as initiators in the ROP of several heterocyclic substrates: lactide (LA), caprolactone (ε-CL) and butyrolactone (*rac*-β-BL), cyclohexene oxide (CHO). Copolymerizations were explored in an attempt to broaden the range of the polymers of controlled microstructure produced (Chapter 2).[7-8]

All complexes were subsequently used in the ROCOP of cyclohexene oxide and limonene oxide (LO) with anhydrides. The reaction conditions and in particular the optimal choice of co-catalyst, were studied.

The possibility of terpolymerization for the preparation of block polyesters by combining ROP and ROCOP processes was investigated (Chapter 3).[8-9]

Finally, the catalyst structure-performances relationship was further examined in the ROCOP. With the activity, an additional key parameter for a ROCOP catalyst is the selectivity. We worked on the ligand design to obtain efficient and rigorously selective catalytic system, leading to the design of a bifunctional catalyst (Chapter 4).

In the field of polyester synthesis promoted by metal-complexes, I carried out a period as a visiting PhD student in the Organometallic Chemistry and Polymerization Catalysis group at IRCP (Institut de Recherche de Chimie Paris) under the supervision of Prof. C. M. Thomas, focusing on the synthesis of divalent metal-based catalysts for the polymerization of *rac*-lactide (Chapter 5).

CHAPTER 2. BIMETALLIC SALEN ALUMINUM COMPLEXES IN THE ROP OF CYCLIC ESTERS.

2.1. INTRODUCTION

In the 90s, Spassky[20a, 46] reported the first example of salen aluminum complex able to produce moderately isotactic poly(lactic acid) (PLA) from *rac*-lactide. Feijen[20d] and Coates[20b] used chiral salen-type catalysts for the stereoselective polymerization of *rac*-lactide *via* enantiomorphic site control mechanism. Nomura[20c, 20e] and Gibson[47] reported achiral salen-type aluminum catalysts promoting isotactic polymerization of *rac*-lactide *via* chain-end control mechanism (Scheme 2.1).

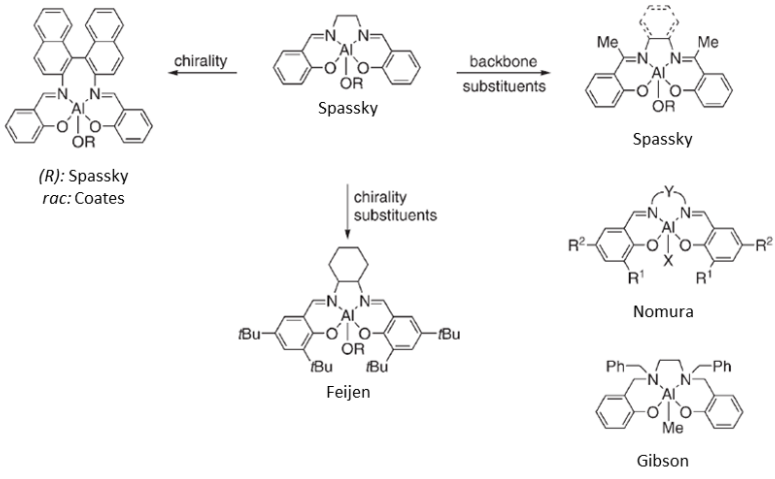

Scheme 2.1. Catalysts for the synthesis of isotactic polylactide from *rac*-lactide.

Numerous examples of structurally related dianionic tetradentate [ONNO]-type ligands such as salan[47-48], salalen[49] and dialkoxy-

diimino[50] ligands have been deeply investigated for the synthesis of monometallic five-coordinate aluminum complexes active in the ROP of cyclic esters. Some of these catalytic systems revealed uncommon abilities for controlling the stereochemistry in the ROP of *rac*-lactide, producing polymers with improved stereoregularities[51] or original microstructures.[52]

More recently, bimetallic aluminum complexes have attracted increasing attention thanks to their improved catalytic behaviours in comparison with their monometallic counterparts; since the two proximal Lewis acidic centres can act in a concerted way.[3]

Bimetallic five-coordinated salen-aluminum complexes have been investigated as initiators for controlled and stereoselective ROP of LA.[53] On the other hand, the use of dianionic "ONNO" type ligands as binucleating ligands for the formation of bimetallic species in which the aluminum centres are tetra-coordinate is definitively underexplored.[6] Carpentier *et al.* reported enantiomerically pure diphenylethylene salen ligands for the synthesis of monometallic five-coordinate and bimetallic tetra-coordinate aluminum complexes. All the complexes showed the same activity in the ROP of lactide, but the bimetallic complexes revealed inefficient in the stereocontrol of the process.[54] The same behaviour was observed with mononuclear and dinuclear aluminum complexes supported by 6,6'-dimethylbiphenyl-bridged salen ligands.[55] Binuclear tetra-coordinate salan aluminum complexes were recently described by Ma as efficient initiators for the copolymerization of L-lactide and ε-caprolactone, producing copolymers ranging from blocky to random microstructures.[56] Evidences about the cooperation between

two metal centres of dinuclear tetra-coordinate aluminum complexes with bis amine-phenolato ligands were recently discussed by Yao and Yuan.[3d]

2.2. Synthesis of a series of Salen Aluminum Complexes

In this project, simple dinuclear aluminum alkyl complexes of general formula L-Al_2Me_4, where L are salen ligands with alkyl backbone of different length between the nitrogen atoms (1,3-propylene (**1**), 1,5-pentylene (**2**) and 1,12-dodecaylene (**3**)), have been reported. Since the distance between metal centres is a critical parameter to have cooperation, the salen ligands have been designed to feature two coordinative pockets at varying distances from one another thanks to the variable alkyl backbone length between the imine functionalities.

The salen ligands have been obtained, in quantitative yield, by direct reaction between the appropriate diamine and two equivalents of 3,5-di-tert-butyl-2-hydroxybenzaldehyde.[57] The complexes have been synthesized through alkane elimination reactions between each pro-ligand and two equivalents of $AlMe_3$. The related hemi-salen aluminum complex (**4**) was prepared by an analogous reaction between the phenoxy-imine ligand and a single equivalent of $AlMe_3$ (Scheme 2.2).

All ligands and complexes have been characterized by ^{1}H and ^{13}C NMR spectroscopy, as well as elemental analysis for complexes **1**-**3**.

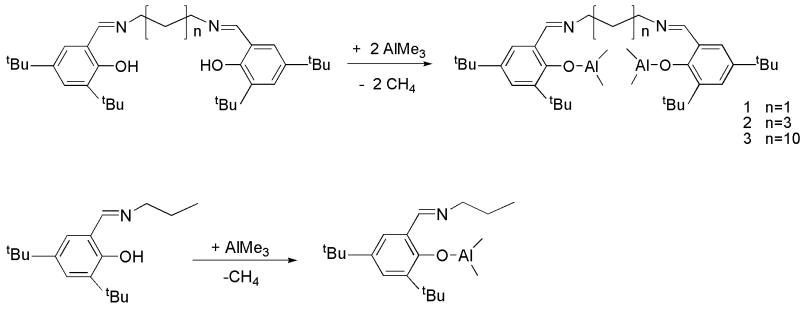

Scheme 2.2. Synthesis of salen aluminum complexes **1**–**3** and hemi-salen complex **4**.

The ^{1}H NMR spectra of the complexes **1**–**3** in C_6D_6 were all consistent with the presence of two aluminum atoms per ancillary ligand and pointed to symmetrical structures in solution. Diagnostic resonances in the protonic spectra include sharp singlets in the high-field region (between $\delta = -0.20$ and -0.29 ppm) assigned to the equivalent protons of the Al–Me groups. In the low-field region, singlets (between $\delta = 7.13$ and 7.29 ppm) are detected for the equivalent CH=N moieties.

The X-ray structural characterization reported by Atwood for analogous aluminum complexes, describes aluminum centres adopting a four-coordinate distorted tetrahedral geometry.[57]

On the ^{1}H NMR spectrum of complex **1** (Figure 2.1), the formation of the complex is confirmed by the signal at -0.29 ppm which integrates for 12 protons, corresponding to the methyl groups on the aluminum centres. In the aliphatic region, two singlets at 1.32 and 1.60 ppm can be found integrating for 18 protons and corresponding to the tert-butyl groups on the phenoxide rings. The signals of the protons of the propylene bridge between the two imine nitrogens

appears as a quintuplet and a triplet at 1.72 and 2.84 ppm integrating respectively for 2 and 4 protons. The signals in the aromatic region correspond to the two aromatic protons on the phenoxide rings as doublets at 6.79 and 7.70 ppm and the singlet at 7.14 ppm is the imine proton.

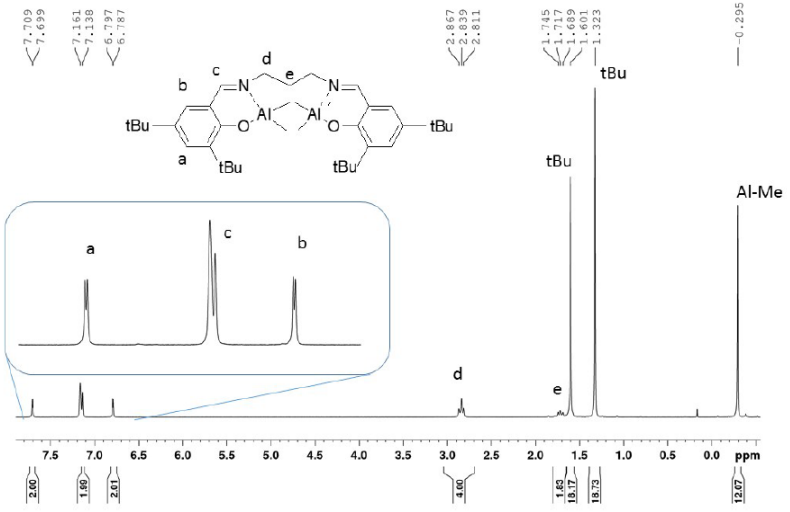

Figure 2.1. ^{1}H NMR of complex **1** (600 MHz, C_6D_6, 298 K).

All complexes were tested as initiators in the ROP of several heterocyclic substrates to explore the possibility of the cooperation between the two aluminum centres.

2.3. HOMOPOLYMERIZATIONS

2.3.1. ROP OF *RAC*- AND L-LACTIDE

First, the complexes were tested in the ROP of *rac*-lactide (Scheme 2.3). The ring-opening polymerizations were conducted at 70 °C, in toluene solution with four equivalents of isopropanol as an activator,

to convert all the aluminum-alkyl groups into more nucleophilic alkoxy groups.

Bimetallic complex **1** proved to be highly active in the ROP of *rac*-lactide and showed the complete conversion of 200 equivalents within 12 hours, an activity twice as high than for the related monometallic species reported by Nomura.[20e]

On the other hand, in the same reaction conditions, bimetallic complexes **2-3** with a longer alkyl bridge between the two nitrogens, required the double amount of time to achieve the same conversions (Table 2.1, entries 1-3).

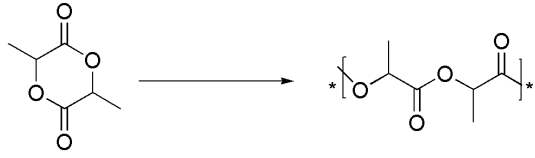

Scheme 2.3. ROP of *rac*-lactide.

In the ROP of L-LA (entry 6, Table 2.1), complex **1** revealed the same behaviour observed towards the racemic monomer.

All polymerizations proceeded in a controlled fashion: the polymers had monomodal and moderately narrow molecular mass distributions (Đ < 1.20). The molecular masses of the polymers produced by the bimetallic complex **1** were in good agreement with the theoretical value calculated hypothesizing the formation of a single PLA chain per catalyst unit: calculated M_n of PLA (in g/mol) = 144,14 x ([LA]/[cat]) x conversion of LA. Whereas the molecular masses of the polymers produced by complexes **2** and **3** were halved, thus coherent with the formation of two polymer chains per catalyst unit, one for each metal centre.

Table 2.1. Ring-Opening Polymerization of *rac*-LA by **1**-**4**.[a]

Run	Cat	Time (h)	Conv. (%)	M_{nGPC} [b] (kDa)	M_n^{th} [c] (kDa)	Đ[b]	P_m [d] (%)	T_m [e]
1	**1**	12	100	22.1	28.8	1.09	82	161.4
2	**2**	24	85	15.2	24.5	1.20	56	89.0
3	**3**	24	76	12.0	21.9	1.18	59	89.3
4[f]	**4**	24	91	12.8	13.6	1.20	57	89.0
5[g]	**1**	8	95	4.0	4.1[g]	1.07	83	-
6[h]	**1**	8	100	23.6	28.8	1.07	-	-

[a]All reactions were carried out with 9.6×10^{-6} mol of catalyst at 70 °C, in 2 mL of toluene, [cat]/[^{i}PrOH]/[*rac*-LA] = 1:4:200. [b]Experimental M_n (corrected using factor 0.58)[58] and Đ values were determined by GPC analysis, in THF *vs* polystyrene standards. [c]Calculated M_n of PLA (in g.mol^{-1}) = 144,14 x ([*rac*-LA]/[cat]) x conversion of LA. [d]P_m is the probability of *meso* linkages. [e]The melting temperature (T_m) was determined from the second heating at heating rate of 10 °C min^{-1}. [f]1.9×10^{-5} mol of cat [**4**]/[^{i}PrOH]= 1:2. [g][cat]/[^{i}PrOH]/[*rac*-LA] = 1:10:200; M_n^{th} = 144,14 x ([*rac*-LA]/[cat + ^{i}PrOH excess]) x conversion of LA. [h]L-LA was used instead of *rac*-LA.

The proximity of the two metal centres could explain these results. In the bimetallic complex **1** with the shortest alkyl bridge, the simultaneous growth of two polymer chains could be impeded by an excessive steric hindrance, maybe caused by interactions between the last lactate unit of the growing chain and the metal centres. At the same time, thanks to this proximity, a cooperation between the two reactive adjacent centres can take place and favours high activity.[59]
In complexes **2** and **3**, such interaction cannot take place because of the greater distance between the two centres, and the metal centres act independently.
With the hypothesis of the growth of a single chain for complex **1,** the latter has a TOF (turnover frequency) of 16.7 h^{-1}, thus a much

higher activity than complexes **2** and **3** (TOF of 3.5 h^{-1} and 3.1 h^{-1} respectively).

To confirm this hypothesis, the monometallic phenoxy–imine aluminum complex **4,** whose structure reproduces the coordinative environment of each aluminum centre in the dinuclear complexes **1**–**3**, was used. In the same concentration of aluminum centres of complexes **1**–**3**, complex **4** showed an activity close to complexes **2** and **3** (runs 2-4 of Table 2.1, Scheme 2.4). This confirmed unequivocally that in the bimetallic complexes **2** and **3**, the two aluminum centres act independently, as in the monometallic complex.

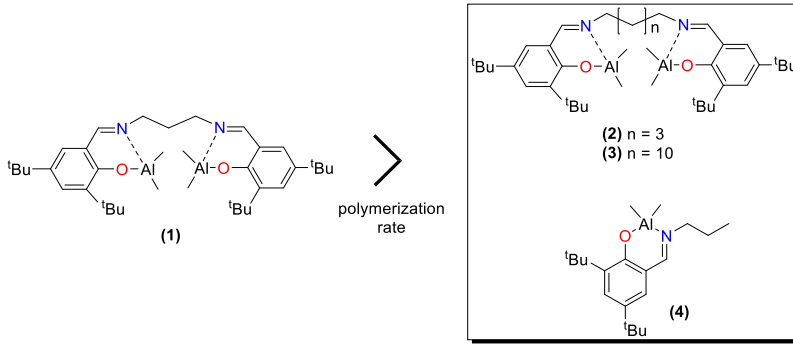

Scheme 2.4. Reactivities of the complexes **1**-**4** in the ROP of *rac*-lactide.

Analysis of the microstructure.

PLAs microstructures can be determined by analysis of the methine regions of the homonuclear decoupled ^{1}H NMR spectra. A PLA derived from *rac*-lactide can exhibit up to five tetrad sequences in relative ratios determined by the ability of the initiator to control *racemic* [*r*-diad] and *meso* [*m*-diad] linkage between each lactide unit (Scheme 2.5).

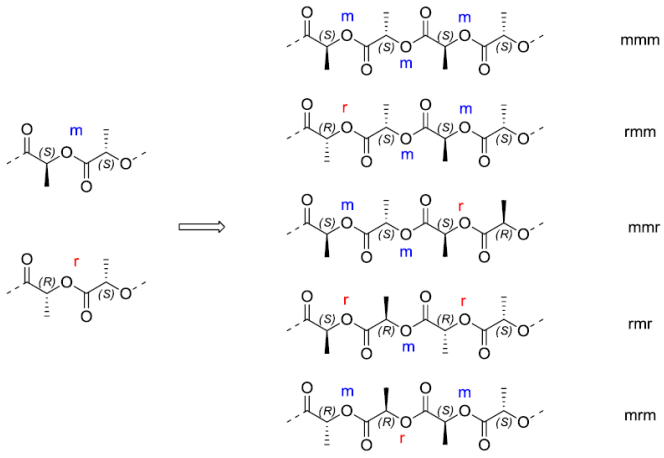

Scheme 2.5. Tetrad sequences from polymerization of *rac*-lactide.

The isotacticity of the polymer obtained is described by the probability of the formation of a *meso* linkage between lactide units during polymerization (P_m). In a chain-end control mechanism, the stereochemistry of *rac*-lactide enchainment is evaluated by comparing the integrals at the tetrad level in the homonuclear decoupled ^{1}H NMR spectra (Figure 2.2), with calculated values using Bernoullian statistics (Table 2.2).

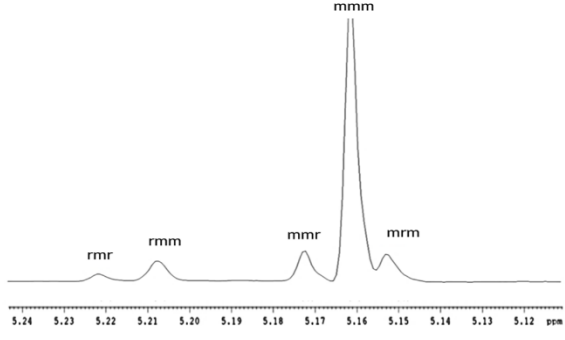

Figure 2.2. Homodecoupled ^{1}H NMR spectrum (600 MHz, $CDCl_3$, 298 K) of PLA obtained by run 1 of Table 2.1.

The concordance between the values suggests that the stereocontrol proceeds *via* a chain end control mechanism, whereby the stereochemistry of the last inserted LA unit in the growing chain induces the stereoselection of the incoming enantiomer. The spectrum of the PLA obtained by **1** in entry 1 of Table 2.1 indicated an isotactic multiblock microstructure with a $P_m = 0.82$ (Figure 2.2).

Table 2.2. Tetrad probabilities based on Bernoullian Statistic (Th) for a P_m of 0.82 and experimental values (Exp) as obtained by NMR analysis of PLA sample obtained by **1**.

Tetrad	Formula	Exp	Th
[*mmm*]	$P_m^2+P_rP_m/2$	0.75	0.75
[*mmr*]	$P_rP_m/2$	0.08	0.07
[*rmm*]	$P_rP_m/2$	0.07	0.07
[*rmr*]	$P_r^2/2$	0.02	0.02
[*mrm*]	$(P_r^2+P_rP_m)/2$	0.08	0.09

The tacticity was comparable to that observed for the PLAs produced by the related monometallic aluminum complexes reported by Gibson and Nomura for which the pentacoordination of the metal centre was considered crucial for the stereoselection.[20c, 20e, 47] Analogous stereoselectivity was observed with phenoxy-imine aluminum complexes having encumbered benzyl-type imino substituents.[60]

The stereoregularity of the PLAs obtained by **2** and **3** was significantly lower ($P_m = 0.56$ and 0.59, respectively) showing the

same behaviour of the hemi-salen catalyst **4** (P_m = 0.57) and analogous tetra-coordinate aluminum complexes bearing bidentate phenoxy-imine[59, 61] or phenoxy–amine[62] ligands. This is coherent with the reduced steric encumbrance around the reactive centres because of the greater flexibility imparted by the longer alkyl bridges.

As for the poly(L-lactide) (PLLA) produced in entry 6 of Table 2.1, the ^{1}H NMR spectrum did not show any racemization within the polymer.

Immortal polymerization.

The possibility of achieving "immortal" polymerization with these systems, i.e. to generate several PLA chains per metal centre by introducing several equivalents of a hexogen alcohol as a chain transfer agent, was explored with complex **1**. Ten equivalents of iso-propanol were used, four equivalents served for the *in situ* synthesis of the aluminum alkoxide derivative, while the alcohol in excess acted as an effective chain transfer agent (run 5, Table 2.1).

The ^{1}H NMR analysis of the PLA oligomers obtained revealed the existence of HOCH(CH_3)CO- and isopropoxy end-groups; and the stereoregularity was preserved (P_m = 0.83). The molecular weights increased monotonously with lactide conversion (Figure 2.3) and they were in strict agreement with the theoretical ones calculated from the initial monomer-to-alcohol molar ratio and the monomer conversion, confirming the immortal character of the polymerization.

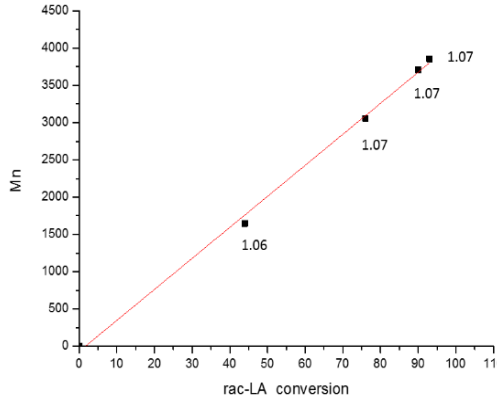

Figure 2.3. Dependence of the number-average molecular weights on *rac*-lactide conversions in the ROP promoted by complex **1**: [*rac*-LA]/[**1**]/[^{i}PrOH] = 200:1:10. R = 0.997.

NMR study of the active species.

In order to elucidate the modes of interaction between the two metals responsible for the different catalytic behaviour shown by complex **1**, we decided to study the structure of the active species. Experiments to elucidate the previous findings were performed in J-Young tube and followed by ^{1}H and 2D NMR spectroscopy.

A solution in deuterated benzene containing complex **1**, four equivalents of ^{i}PrOH and ten equivalents of L-LA was prepared. After 1 hour at room temperature, no alcoholysis of complex **1** was observed and no conversion of the monomer was achieved. This is consistent with the literature which reports a high activation energy for the formation of the alkoxide active species.[18, 63]

Increasing the temperature to 70 °C, the disappearance of the resonances for Al-Me protons and for the lactide monomer was observed within a few minutes. The ^{1}H NMR spectrum (Figure 2.4 and Figure 2.5) showed six different signals in the aromatic region

corresponding to four different aromatic protons and two imine protons of the coordinated ligand. In the aliphatic region, five signals were evident corresponding to the diastereotopic protons of the trimethylene bridge between the imine nitrogens. These evidences pointed to the loss of symmetry of the initial complex. In addition, three doublets, each integrating for six protons were observed between 0.90 - 0.93 ppm indicating the presence of three isopropoxy groups bound to the aluminum atoms. An additional doublet was observed at 1.11 ppm, for the methyl protons of the terminal isopropoxy group of the growing chain and a quartet, was observed for the methine proton of the repeating unit nearest to the aluminum of the growing chain. Finally, methine and methyl protons of the growing chain appeared at 5.09 and 1.37 ppm, respectively.

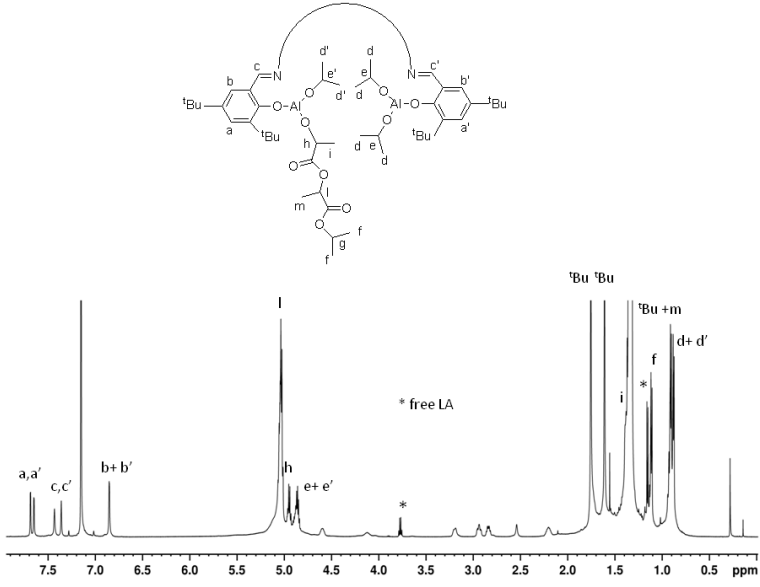

Figure 2.4. ^{1}H NMR spectrum (600 MHz, C_6D_6, 298 K) of the propagating species **1**-PLA.

Five more equivalents of lactide were added to the solution, after ten minutes the almost complete conversion of the monomer occurred, and the pattern of the propagating species remained unchanged in the ^{1}H NMR spectrum, highlighting the living nature of the active species.

This overview points to the formation of an asymmetric propagating species, where the growth of a single chain occurred on one of the two metal centres, although chain transfer phenomena between the two aluminum atoms are plausible. The observation can be justified by a chelation effect between the two aluminum centres of the O-lactate propagating species in the polymerization of LA, as described by several authors.[60, 64] This chelation would explain the steric encumbrances and thus the growth of a single chain of polymer per catalyst.

The propagating species revealed to be exceptionally stable and was stored in benzene solution for several weeks at room temperature without decomposition.

The same NMR experiment was conducted with complex **2** and **3**. This time, the alcoholysis proceeded slowly even at 70 °C and about two hours were required to obtain the corresponding isopropoxy derivatives quantitatively. The ^{1}H NMR spectrum, although less clear than that discussed for complex **1**, revealed a symmetric structure of the propagating species, as clearly emerged by analysis of the aromatic region of the spectrum, in which only three signals are observed. All signals were very broad suggesting fluxional structures of the propagating species. At 70 °C, all resonances became sharp. This is coherent with the formation of two polymeric chains, one for

each metal centre, in the propagating species formed by complexes **2** and **3**.

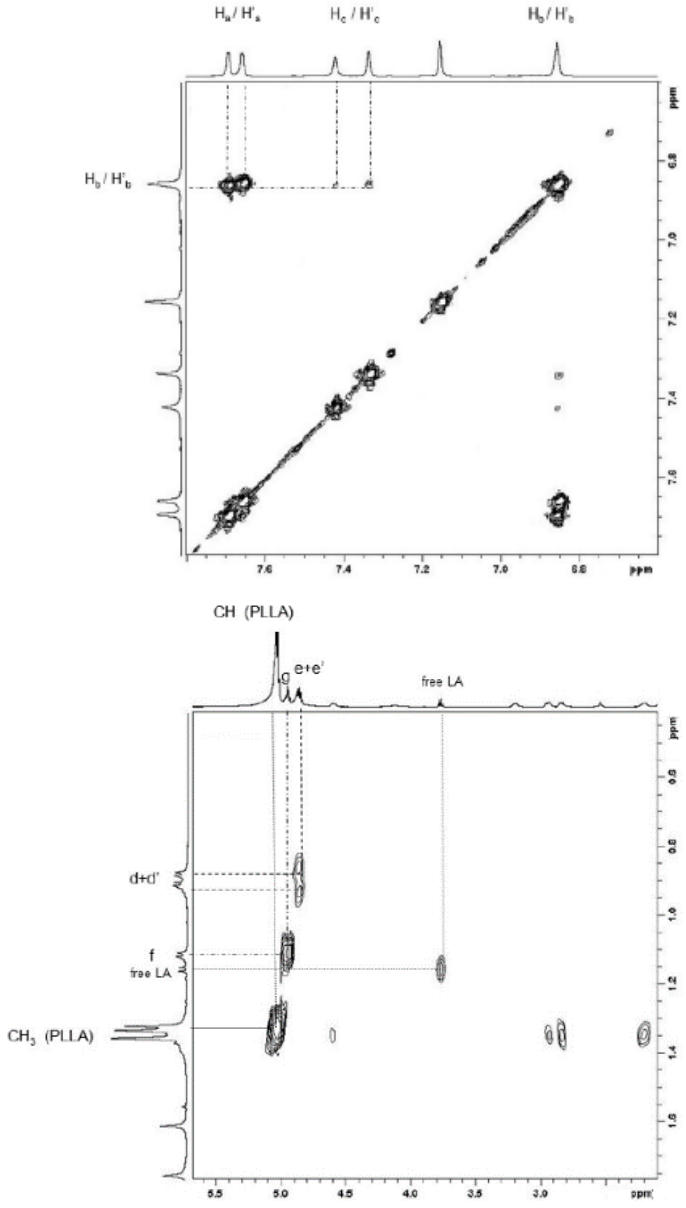

Figure 2.5. ^{1}H-^{1}H COSY spectra of the propagating species formed by complex **1** (600 MHz, C_6D_6, 298 K).

The different alcoholysis kinetics of **1** in comparison with **2** and **3** shows that the cooperation between the two metal centres of complex **1** could be fundamental both during the formation of the alkoxide derivative and during the propagation. The coordination of the alcohol at one of the acidic aluminum atoms of the bimetallic species might promote the alcoholysis of the Al-Me bonds of the proximal metal atom.

Following these evidences and the generally accepted mechanism for the ROP of lactide promoted by metal alkoxides, a mechanism for complex **1** can be hypothesized as described in Scheme 2.6.

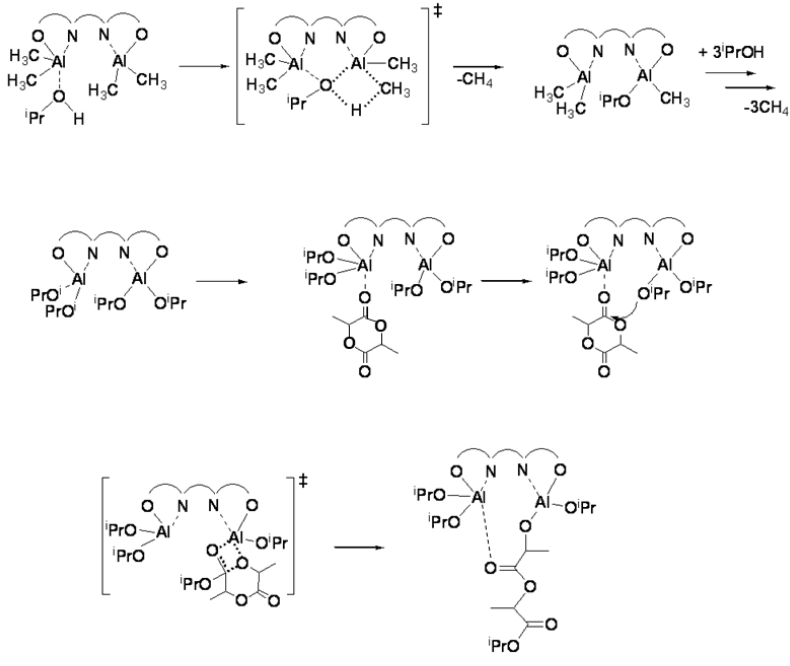

Scheme 2.6. Plausible Mechanism for the polymerization of LA Initiated by complex **1**-^{i}PrOH.

First, the hexogen alcohol coordinates to the metal and reacts exhaustively with the alkyl groups bound to the aluminum atoms of complex **1**. One of the Lewis acidic metal centres binds the incoming monomer and activates it for the attack by the metal alkoxide group of the proximal aluminum atom. The growth of the polymer chain occurs by nucleophilic attack of polymer chain at the coordinated monomer unit by shuttling between the two aluminum centres.

Kinetic study.

The NMR experiments suggested that different times are required for the initial alcoholysis of the complexes **1**-**3** and during propagation. To confirm these observations, kinetic studies were carried out for the ROP of *rac*-lactide promoted by complexes **1**-**3**, by monitoring the conversions of lactide in toluene at 70 °C by ^{1}H NMR spectroscopy at different intervals.

For complex **1**, the polymerization of *rac*-LA is a first-order reaction with instantaneous initiation (Figure 2.6).

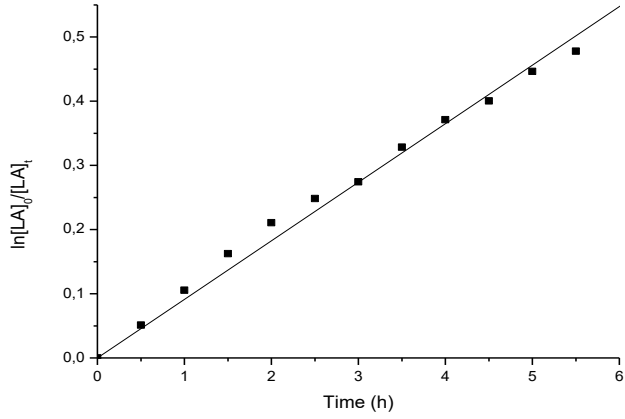

Figure 2.6. Kinetic plot for ROP of *rac*-LA promoted by **1**.
The concentrations were determined by ^{1}H NMR spectroscopy, $[LA]_0$ is the initial concentration of *rac*-LA and $[LA]_t$ the concentration at time *t*. Pseudo first-order rate constant is $k_{app} = 0.643\ h^{-1}$, R = 0.9975. Reaction conditions: [Cat] = 0.01 M; [LA]/[cat] = 100; T = 343 K; toluene-d_8 as solvent.

On the other side, the polymerization of *rac*-LA promoted by complexes **2** and **3** displayed an induction time of about 2 h (Figure 2.7). After this initiation, the polymerizations are first-order reactions in monomer concentration with k_{app} values of 0.133 h^{-1} and 0.0502 h^{-1}, respectively. The induction period is coherent with the NMR study, that showed a slow reaction between the isopropyl alcohol and the metal complexes **2** and **3**. The k_{app} values for these complexes are significantly lower than that of complex **1**. The cooperation between the two metal centres seems to have a role both in the alcoholysis reaction for the formation of the catalytically active species and during the polymerization reaction. At higher temperatures (100 °C) no induction time was observed with complex **3**, and the catalytic activity raised significantly (Figure 2.8).

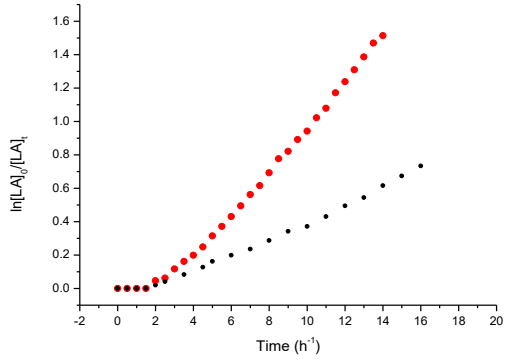

Figure 2.7. Kinetic plot for ROP of *rac*-LA promoted by **2** (red) and **3** (black).

The pseudo first-order rate constants are k_{app} (**2**) = 0.133 h^{-1} (R = 0.9983) k_{app} (**3**) = 0.0502 h^{-1} (R = 0.9972). Reaction conditions: [cat] = 0.01 M; [LA]/[cat] = 100; T = 343 K; toluene-d_8 as solvent.

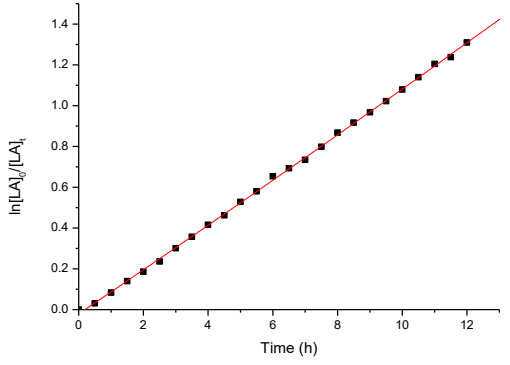

Figure 2.8. Kinetic plot for ROP of *rac*-LA promoted by **3**.

The pseudo first-order rate constant k_{app} = 0.111 h^{-1} (R = 0.9975). Reaction conditions: [**3**] = 0.01M; [LA]/[**3**] = 100; T = 373 K; toluene-d_8 as solvent.

2.3.2. ROP OF LACTONES

To verify the synergistic effects between the two metal centres in complex **1**, the polymerization studies were extended to other monomers and compared with complex **4**.

The reactivity of catalyst **1** and **4** in the ROP of the lactones: ε-CL, and *rac*-β-BL was studied (Scheme 2.7).

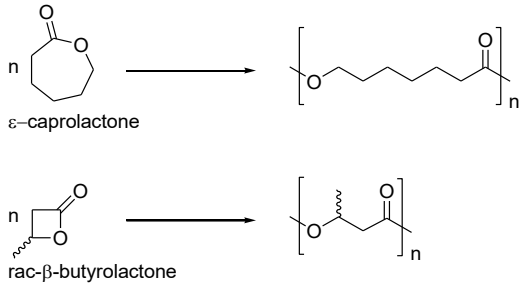

Scheme 2.7. ROP of ε-caprolactone and *rac*-β-butyrolactone.

The ROP of *rac*-β-BL was investigated with complex **1** and **4**. Despite its favourable ring strain, there are only a few examples of initiators able to promote controlled ROP of *rac*-β-BL[2a, 65] because of side termination reactions such as transesterification and chain transfer reactions.[66]

Table 2.3. Reactivity of complex **1** in the ROP of lactones.[a]

Entry	Monomer (equiv)	Time (h)	T (°C)	Yield (%)	M_{nGPC} [b] (kDa)	M_n^{th} [c] (kDa)	Đ[b]
1	β-BL (200)	20	70	64	5.2	5.5	1.07
2[d]	β-BL (200)	20	70	91	2.4	2.0[e]	1.06
3	ε-CL (500)	0.33	70	46	10.1	13.1	1.22
4	ε-CL (500)	6	25	18	7.0	5.1	1.05

[a]All reactions were carried out with 10 μmol of **1** at 70 °C, in 2 mL of toluene, [**1**]/[^{i}PrOH] = 1:4. [b]Experimental M_n (corrected using factor 0.56 for PCL and 0.54 for PHB) and Đ values were determined by GPC analysis in THF using polystyrene standards. [c]Calculated M_n^{th} = MM_{mon} x ([Mon]/[Al]) x yield. [d][**1**]/[^{i}PrOH] = 1:8. [e]Calculated $M_n = MM_{mon} \times ([Mon]/[^iPrOH]) \times conv.$

Complex **1** showed good performance allowing the conversion of 130 equivalents of *rac*-β-BL in 20 hours at 70 °C (entry 1, Table 2.3).

The cooperation between the metal centres was found to be essential also in the ROP of *rac*-β-BL since the related monometallic phenoxy-imine aluminum complex **4** was completely inactive under the same conditions.

Complex **1** was tolerant to an excess of alcohol (8 equiv. of ^{i}PrOH) promoting an "immortal" polymerization (entry 2, Table 2.3). The molecular weight of the resultant PHB decreased depending on ^{i}PrOH loading, while the polydispersity did not change. The MALDI-ToF analysis of the low molecular weight PHB sample displayed only linear chains, initiated by isopropoxy or methyl (marginally) groups (Figure 2.9). No cyclic oligomers were detectable suggesting that intramolecular transesterification reactions did not happen during polymerization.

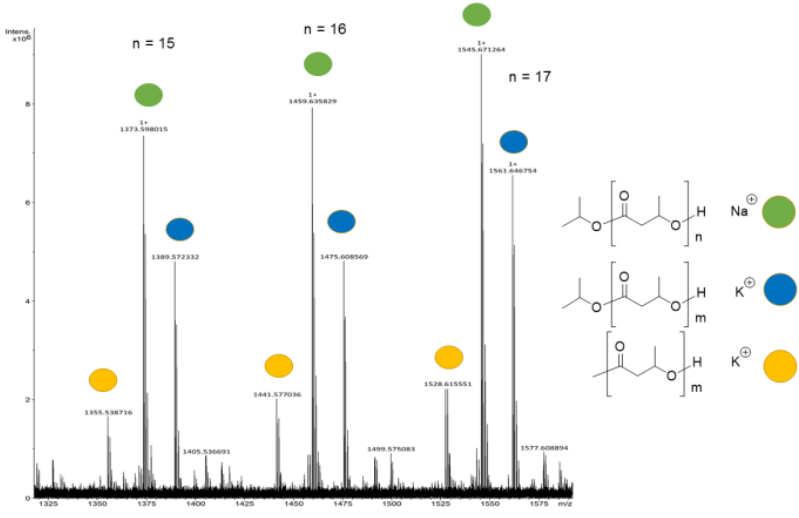

Figure 2.9. MALDI-ToF-MS spectrum of PHB synthesized in entry 2 of Table 2.3.

The ^{1}H NMR analysis showed the existence of $HOCH(CH_3)CH_2$- and $-OCH(CH_3)_2$ groups as exclusive chain end groups (Figure 2.10). No evidence of transcrotonate species from side termination reactions were detected. These findings corroborate a living polymerization following a coordination-insertion mechanism with a ring-opening of the monomer through acyl–oxygen bond cleavage.

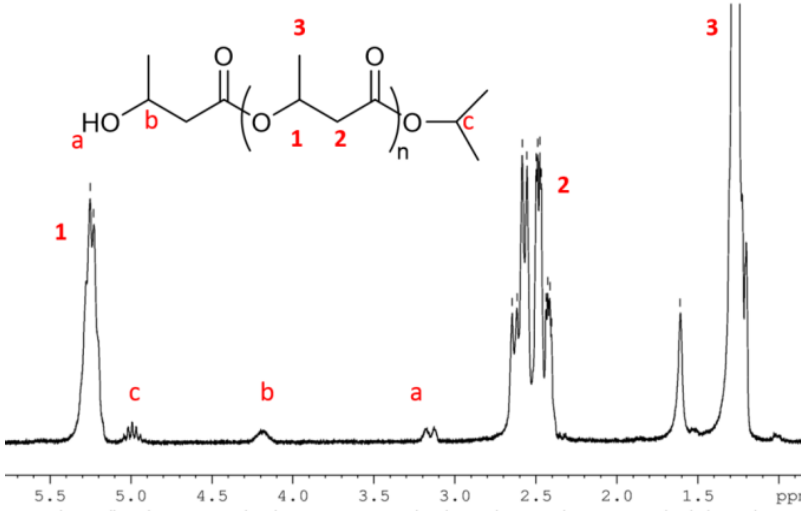

Figure 2.10. ^{1}H NMR spectrum (250 MHz, $CDCl_3$, 298 K) of a PHB produced in entry 2 of Table 2.3.

The microstructure of the obtained PHB was analysed by observation of the methylene resonances (40 ppm) in the ^{13}C NMR spectrum. The signals of the rm-, mm-, rr-, and mr- triads resulted equal in their intensity revealing an atactic PHB polymer (Figure 2.11).

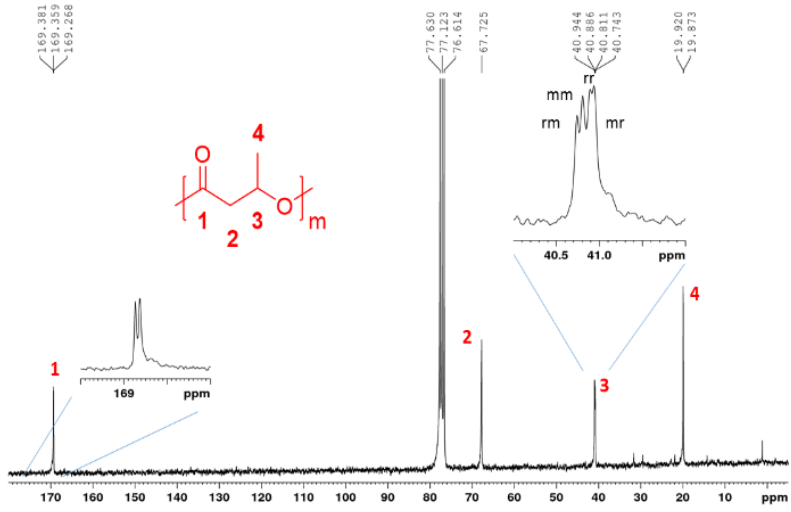

Figure 2.11. ^{13}C NMR spectrum (63 MHz, $CDCl_3$, 298 K) of the atactic PHB.

In the ROP of ε–caprolactone, complex **1** demonstrated a very high activity (entry 3, Table 2.3), higher than those of most of the phenoxy-imine aluminum complexes and as high as the most efficient aluminum complexes,[67] thus corroborating once more the synergistic effect between the two aluminum centers.[3d, 6a, 53d, 56]

Complex **1** was also tested at room temperature and showed a moderate activity (entry 4, Table 2.3).

The GPC analysis of all the obtained polymers displayed monomodal distributions of the molecular weights with narrow polydispersity indexes. The experimental molecular weights of PCLs and PHBs were lower than those obtained for PLAs, and they are in agreement with the growth of two polymeric chains per catalyst unit, one for each metal center.

NMR study of the propagating species.

To elucidate these findings and understand the difference with the polymerization of LA, NMR experiments were conducted.

A solution of complex **1** (10 µmol) with four equivalents of ^{i}PrOH in deuterated benzene at 70 °C in the presence of four equivalents of *rac*-β-BL was prepared. After 2 hours at 70 °C, the exhaustive alcoholysis of the methyl groups of complex **1** and the almost complete consumption of the monomer were observed.

The ^{1}H NMR spectrum revealed a symmetric structure of the propagating species, as clearly evidenced by the presence of only three signals in the low field region of the spectrum (Figure 2.12).

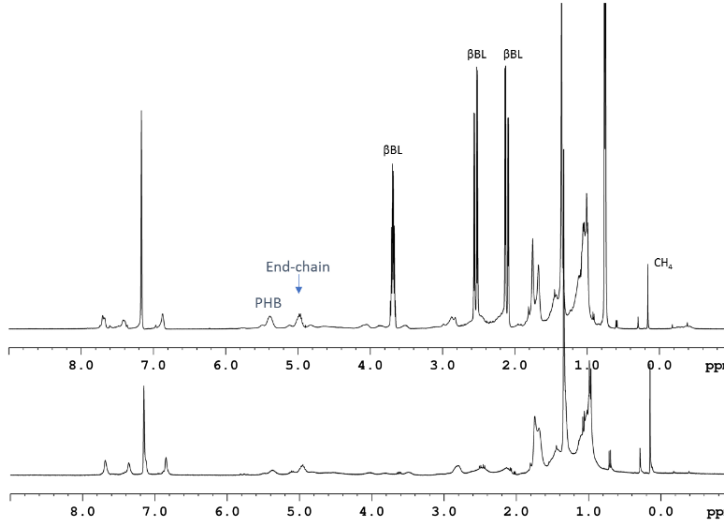

Figure 2.12. ^{1}H NMR spectrum (C_6D_6, 300 MHz, 298 K) of the propagating species of **1**-PHB.

Up: After addition of more β-BL, showing the increase of the signal of the polymer PHB.

This suggested that two polymeric chains grew independently on the two reactive aluminum centers.

On the contrary, in the ROP of LA, an asymmetric propagating species was formed from complex **1**. These different findings between the lactones and the lactide can be justified by a chelation effect between the two aluminum centres of the O-lactate propagating species in the polymerization of LA, as described by several authors.[60, 64] This chelation would explain the growth of a single chain of poly(lactic acid) per catalyst, likely due to the steric encumbrance.

Kinetic studies.

The polymerization rate of the ROP was first-order dependent on the ε-CL concentration (Figure 2.13).

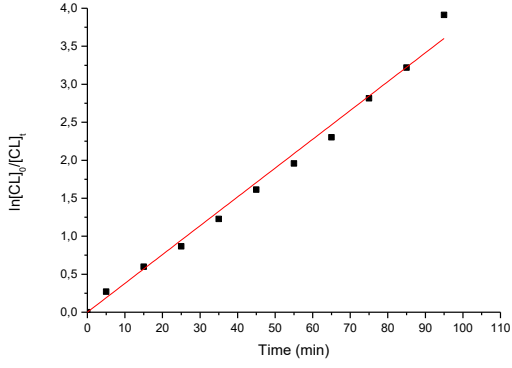

Figure 2.13. Plot of $\ln([\varepsilon\text{-CL}]_0/[\varepsilon\text{-CL}]_t)$ *vs* time depicting a reaction order of unity with respect to monomer concentration, $k_{app} = 0.379$ min^{-1} ($R^2 = 0.9960$).

Similarly, the plot of $\ln([\beta\text{-BL}]_0/[\beta\text{-BL}]_t)$ *vs* time was linear, indicating a first order reaction in concentration of monomer (Figure 2.14). The apparent kinetic constant was 0.00649 min^{-1} (0.389 h^{-1}),

slightly lower than that obtained for polymerization of *rac*-LA (0.643 h^{-1}), and about one order of magnitude lower than that obtained for the polymerization of CL.

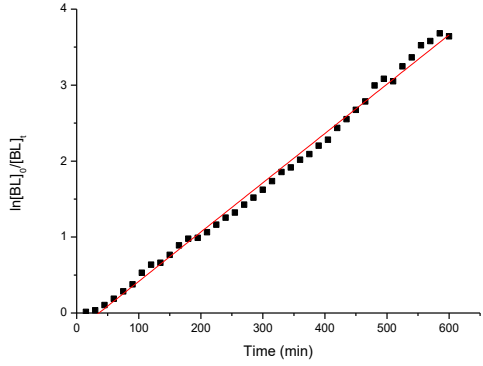

Figure 2.14. Plot of $\ln([\beta\text{-BL}]_0/[\beta\text{-BL}]_t)$ *vs* time depicting a reaction order of unity with respect to monomer concentration. $k_{app} = 0.00649$ min^{-1} ($R^2 = 0.9948$).

2.3.3. ROP OF EPOXIDES

The previously discussed data strongly support the hypothesis of cooperation between the two reactive centres of the dinuclear complex **1** favoured by the architecture of the salen ligand that forces the two coordinative pockets in proximal positions. Cooperation between two metal centres has been reported to be an important prerequisite for highly active catalysts in the ring-opening polymerization[68] and copolymerization of epoxides.[22a, 31, 32b, 32c] Thus, complexes **1**-**4** were studied in the ROP of epoxides.

Complexes **1**-**3** were tested in the ROP of cyclohexene oxide (CHO) in CH_2Cl_2 solution (Scheme 2.8). After 48 h at room temperature, 22% of the monomer was converted by complex **1** (run 1, Table 2.4)

whereas no activity was observed with complexes **2** and **3** under the same conditions.

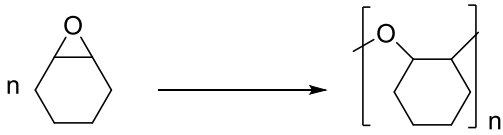

cyclohexene oxide

Scheme 2.8. Ring-opening polymerization of cyclohexene oxide.

These observations go in the direction of an essential cooperation between the two reactive centres to have catalytic activity in this kind of reaction. For complexes **2** and **3** the longer distance between the coordinative tasks does not allow any interaction between the two aluminum atoms.

Table 2.4. Polymerization of CHO.[a]

Run	Cat	[CHO]/ [Cat]	^{i}PrOH (eq)	Time (h)	Temp (°C)	Conv.[b] (%)	M_{nGPC} [c] (kDa)	M_n^{th} [d] (kDa)	[c]Đ
1[e]	**1**	250	-	48	25	22	398.7	5.4	1.43
2	**1**	250	-	0.33	25	40	256.6	9.8	1.72
3	**2**	250	-	0.33	25	40	223.7	9.8	1.77
4[e]	**1**	250	4	48	25	27	18.4	6.6	1.66
5	**1**	500	-	0.08	70	74	38.0	36.3	2.09
6	**1**	250	4	0.08	70	95	4.3	4.6	1.67
7	**1**	500	4	0.08	70	79	10.7	7.8	1.79
8	**1**	750	4	0.25	70	85	12.4	12.5	1.76
9	**1**	1000	4	30	70	85	17.1	16.7	1.70
10	**1**	500	10	0.08	70	90	5.2	4.1	1.77

[a]Reactions were performed without solvent at room temperature in an inert atmosphere workstation by using 9.0 μmol of catalyst and 4.5 mmol of CHO. [b]Conversions determined by ^{1}H NMR spectroscopy. [c]Determined by GPC, in THF *vs* polystyrene standards. [d]Calculated M_n of PCHO (in g.mol^{-1}) = 98.14 x ([CHO]/[cat]) x conversion of CHO hypothesizing the formation of a single chain for catalyst unit (runs 1-3 and 5), M_n = 98.14 x ([CHO]/[cat+^{i}PrOH]) x conversion of CHO (runs 4 and 6-10). [e]Using 2mL CH_2Cl_2.

Without solvent, the polymerization rate is much faster, 40% of monomer is converted within 20 min with complexes **1** and **2** (runs 2 and 3, Table 2.4), while still no conversion was achieved with complex **3**. Complex **2** might became active in neat conditions because of the different polarity of the reaction medium that can influence the fluxionality of the binuclear complex which means the possibility of interaction between the reactive centres. As ultimate evidence, the phenoxy–imine aluminum complex **4** was used under the same reaction conditions. This complex did not show any activity when used in the same concentration of aluminum centres and not even when its concentration was ten times higher.

In the light of these results, the polymerization is confirmed to proceed *via* a bimetallic process that is favoured by the closeness of two metallic centres. This has also been reported in a recent work in which the ROP of CHO is promoted by $[UO_2Cl_2(THF)_3]$ catalyst.[69] As already proposed in the ROP of lactide, the growth of the polymer chain might occur by nucleophilic attack of the polymer chain at the coordinated epoxide unit by shuttling between the two aluminum centers (Scheme 2.9).

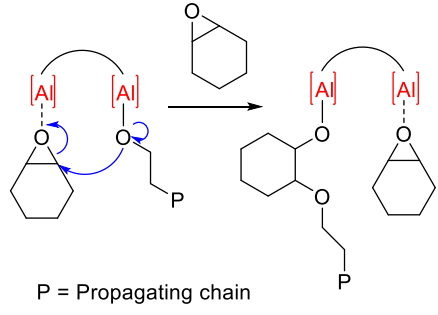

Scheme 2.9. Bimetallic pathway proposed for the ROP of CHO by complex **1**.

The obtained polyethers displayed high molecular masses with molecular weight distributions inferior to 2.0 (Table 2.4). There is a restricted number of catalysts able to produce high molecular weight polyethers,[70] such as group 4[71] and rare earth catalysts[72] and, more recently, Kerton reported aluminum amine-phenolate complexes.[73]

The divergence between the experimental and theoretical molecular weights (calculated presuming the formation of a single chain per complex) implies the partial efficiency of the initiation, probably due to the scarce nucleophilicity of the alkyl ligands.

With the addition of alcohol at room temperature, the activity did not change (27% of conversion in 48 hours) however the molar masses lessened since the hexogen alcohol is acting as a chain transfer agent (runs 1 and 4, Table 2.4). The experimental masses and the theoretical ones still did not concord perfectly, reasonably because the alcoholysis of the complex does not occur at room temperature, as discussed in the NMR study with lactide.

When the polymerization reaction was performed at 70 °C and in the absence of alcohol, the catalytic activity improved drastically, and a very good control of the molecular weights was achieved. These results suggest that the increase of the reaction temperature allows overcoming the activation energy barrier of the initiation step (run 5, Table 2.4).

At 70 °C and in the presence of alcohol, complex **1** achieved immortal polymerization of CHO producing many polymeric chains per metal initiator (entries 6–9, Table 2.4). With a higher amount of the hexogen alcohol as the chain transfer agent, the activity was further increased (entry 10, Table 2.4) and no decomposition of

complex **1** was observed. The linear relationship between the M_n and monomer/initiator ratio confirms the ability of the catalytic system **1**/^{i}PrOH to promote efficient control of the molecular masses (Figure 2.15).

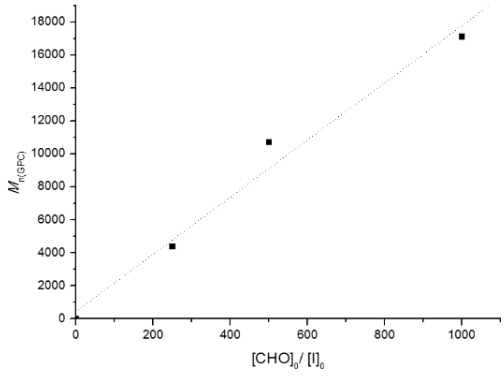

Figure 2.15. Linear relationship between M_n and the initial mole ratio $[CHO]_0/[I]_0$.

The MALDI-ToF spectrum of the PCHO polymer of run 6 of Table 2.4 showed a single series of peaks separated by a gap of 98 Da (Figure 2.16). The series shows sodium adducts of PCHO chains with hydroxyl and isopropoxide end groups (^{i}PrO-$[CHO]_n$–H·Na+).

The microstructure of the obtained poly(1,2-cyclohexeneoxide) was investigated by ^{1}H and ^{13}C NMR spectroscopy.[74] The ^{1}H NMR spectrum displayed three signals (δ 3.52, 3.39, and 3.36 ppm) attributable to syndiotactic (rr), heterotactic (mr and rm), and isotactic (mm) triads for the methine protons. Likewise, three main peaks appeared in the ^{13}C NMR spectrum for the methine carbons at

δ 80.0, 78.7, and 75.6 ppm, showing the stereoirregularity of the polymer.

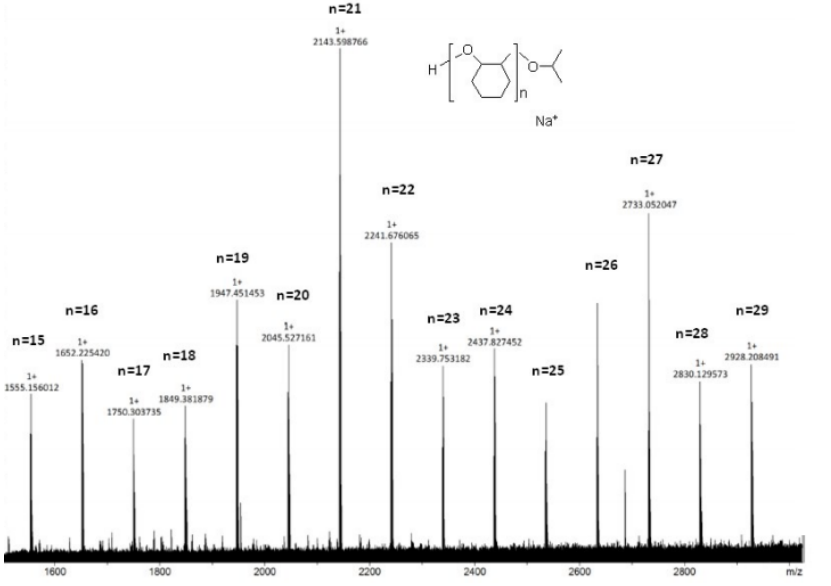

Figure 2.16. MALDI-ToF spectrum of oligomers of PCHO obtained in run 6 of Table 2.4.

The ROP of various epoxides (propylene oxide, styrene oxide and epichlorohydrin) were tested with complex **1**. Surprisingly, for all these monomers, no polymer was detected, even at 70 °C. However, these uncommon findings were also reported with the aluminum catalysts of Kerton.[73]

2.4. Copolymerizations of Cyclic Esters and Epoxides

ROP of cyclic esters is a powerful method to synthesize well-defined polyesters. However, this synthetic approach produces polyesters with a limited range of properties.[2a, 2c] Copolymerization is a solution

to expand the polymer architectures that can be obtained starting from a limited library of monomers. In addition, the mechanical properties of these copolymers can be finely tuned according to the composition and the distribution of the different monomers along the polymeric chain.

Furthermore, the copolymerization of cyclic esters with other monomers, such as cyclic carbonates[75] or epoxides,[76] allows to further play with structure-property relationships in the materials produced.

Since synergies between reactive aluminum centers[77] in multinuclear complexes often cause unexpected activities and performances in the polymerizations[53a, 53d, 78] and copolymerizations of cyclic esters,[6b, 53e, 56, 79] we extended the use of catalyst **1** to the copolymerization of diverse heterocyclic substrates.

2.4.1. COPOLYMERIZATIONS OF CYCLIC ESTERS

PLA is a thermoplastic polymer with excellent mechanical properties but poor elasticity. PCL has very good elasticity and remarkable drug permeability.[80] Isotactic PHB has excellent physical properties and gas barrier properties, close to those of polypropylene.[81]

Their copolymerizations allow to obtain materials with mediated properties in comparison to the related parent homopolymers.

Complex **1** was thus tested in the copolymerizations of the cyclic esters, given its high activity in the homopolymerizations.

The polymerizations were performed under the same conditions, in toluene at 70 °C with four equivalents of alcohol, using 200

equivalents of each monomer that were introduced simultaneously (Table 2.5).

Table 2.5. Copolymerizations of cyclic esters promoted by **1**.[a]

Entry	Monomer	Time (h)	Yield (%)	M_{nGPC} [b] (kDa)	M_n^{th} [c] (kDa)	Đ[b]
1	ε-CL/L-LA	12	100/100	17.2	12.9	1.28
2	ε-CL/β-BL	12	100/100	16.8	10.5	1.44
3	L-LA/β-BL	24	100/50	12.3	9.6	1.07

[a]All reactions were carried out with $1 \cdot 10^{-5}$ mol of **1** at 70 °C, in 2 mL of toluene, [**1**]/[^{i}PrOH]/[Mon_1]/[Mon_2] = 1:4:200:200. [b]Experimental M_n (corrected using factor 0.58 for PLA, 0.56 for PCL portions and 0.54 for PHB portions) and Đ values were determined by GPC analysis in THF using polystyrene standards. [c]Calculated M_n (in g.mol^{-1}) = MM_{Mon1} x ([Mon_1]/[Al]) x conversion of Mon_1 + MM_{Mon2} x ([Mon_2]/[Al]) x conversion of Mon_2.

2.4.1.1. PCL/PLA COPOLYMER

After 12 hours, the copolymerization between ε-CL and L-LA showed the complete consumption of both monomers (entry 1, Table 2.5). The obtained polymer showed a monomodal molecular weight distribution with a narrow polydispersity index (Đ = 1.28). The molar mass of the obtained polymer (M_n = 17.2 kDa) was higher than that of pure homopolymers on their own (maximum estimated M_n = 7.2 kDa) and in agreement with the theoretical molar masses (M_n^{th} = 12.9 kDa) for a PCL/PLA copolymer.

The ^{1}H NMR spectrum of the crude polymer is coherent with a 1:1 ratio of PLA and PCL, as the initial monomer feed ratio. In addition to the signals expected for the homodiads CL–CL and LA–LA, characteristic resonances corresponding to the CL-LA heterodiads were detected at 2.3 and 4.1 ppm (Figure 2.17).

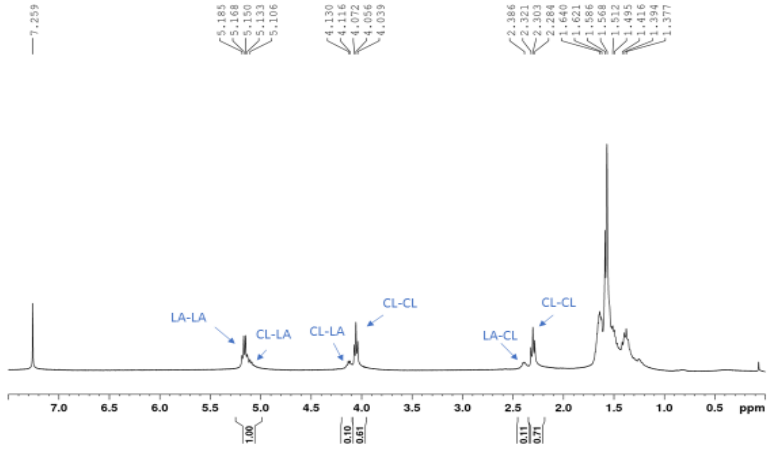

Figure 2.17. ^{1}H NMR spectrum (250 MHz, $CDCl_3$, 298 K) of ε-CL/L-LA copolymer.

The microstructure was determined by analysis of the carbonyl region (ranging from 165 to 175 ppm) in the ^{13}C NMR spectrum (Figure 2.18) and the assignments of the peaks were made according to the literature.[82] In addition to the presence of carbonyl resonances due to the homosequences CL-CL and LA-LA (at 173.7 and 169.9 ppm, respectively), additional resonances of lower intensity were observed for the CL-LA heterosequences. No peak could be observed at 170.8 ppm corresponding to sequences in which a lactyl unit, resulting from the cleavage of the lactyl–lactyl bond in the lactidyl unit, is surrounded by two CL units.

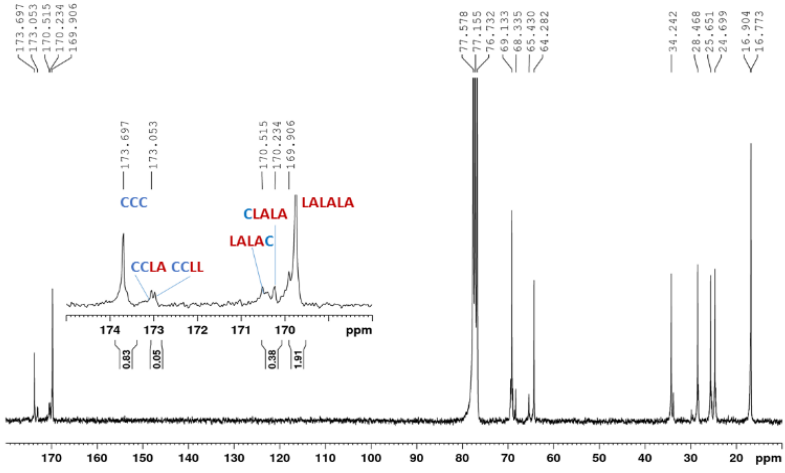

Figure 2.18. ^{13}C NMR spectrum (75 MHz, $CDCl_3$, 298 K) of ε-CL/L-LA copolymer.

The results of the thermal analysis (see Appendix 2) showed the presence of a PLLA crystalline phase having T_m = 121 °C and ΔH_m = 28.8 J/g (corresponding to a crystallinity degree of ≈ 20% [83,84] which in second DSC heating run was reduced to 10% as usual occurs in copolymers) while none thermal transitions were observed for the PCL phase. The T_g of both phases were also not observed.

The wide-angle X-ray diffraction (WAXD) analysis of the same sample showed only the typical peaks of the PLLA alpha form, confirming that only PLA phase was crystalline while the PCL phase was amorphous.

These results agree with a gradient microstructure (Scheme 2.10), in which the crystallization of the most rigid PLA phase hinders that of the more flexible PCL phase.

Scheme 2.10. Copolymer sequence with a gradient microstructure.

The copolymerization of L-lactide and ε-CL catalyzed by complex **1** in deuterated toluene was carried out at 70°C and monitored by ^{1}H NMR spectroscopy (Figure 2.19). As often observed, the rate of enchainment of lactide was faster than that of caprolactone. Thus, the L-LA incorporation was preferable although a gradual consumption of ε-CL was observed, confirming a gradient microstructure. A gradient copolymer exhibits a gradual change in composition along the polymer chain from mostly lactide monomer to mostly caprolactone monomer.

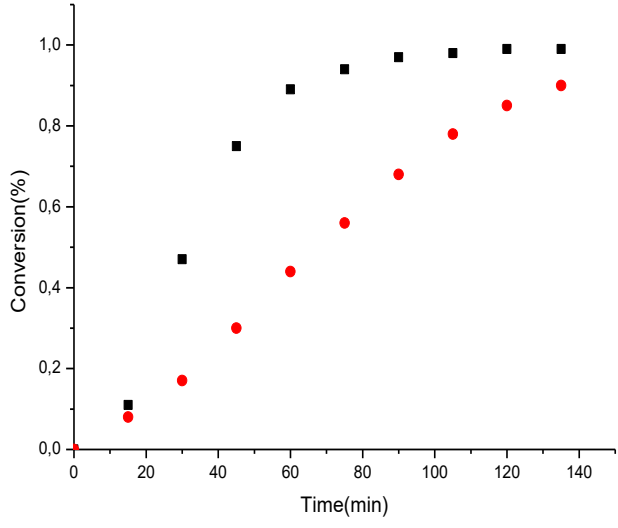

Figure 2.19. Plot of conversion *vs* time for L-LA (black solid squares) and ε-CL (red solid circles) concentration.

2.4.1.2. PCL/PHB COPOLYMER

For ε-CL and β-BL copolymerization (entry 2, Table 2.5), the complete conversions of both monomers were achieved in 12 hours and the composition of the polymer faithfully reflected the monomer feed composition (Figure 2.20).

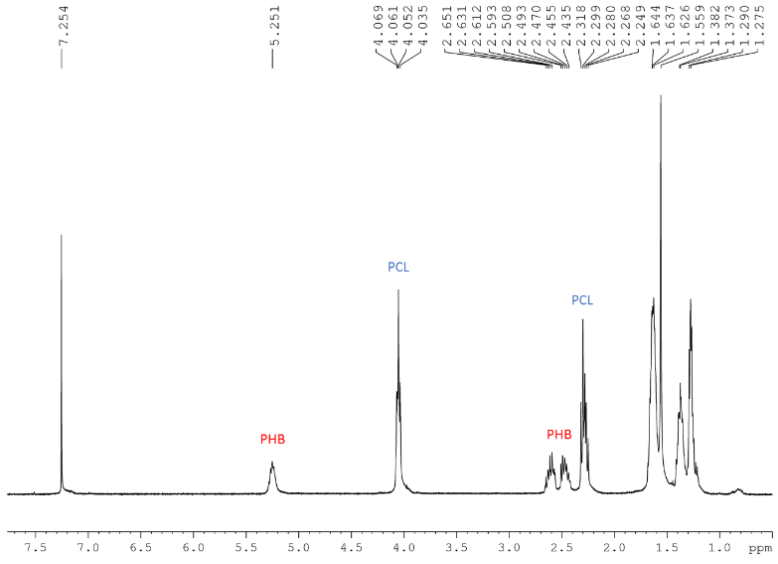

Figure 2.20. ^{1}H NMR spectrum (400 MHz, $CDCl_3$, 298 K) of poly[HB-co-CL].

In the carbonyl region of the ^{13}C NMR spectrum of the sample (Figure 2.21), in addition to the resonances of the homosequences CL-CL and BL-BL (at 173.5 and 169.4 ppm, respectively), less intense resonances were observed, attributable to the CL-BL and BL-CL heterosequences (at 172.7 and 170.3 ppm, respectively).[85]

The degree of randomness (RD) of the copolymer, calculated as reported in the literature, was 0.14.[86] When RD = 1, the HB and CL units are randomly distributed. If RD < 1, the monomers are in blocks

of each unit, and finally if RD = 0, a homopolymer mixture is produced. Thus, the RD value suggested that the monomers tend to cluster in blocks of each unit. The monomers tend to cluster in blocks of each units with an average sequence length of 18 units for BL and of 12 units for CL.

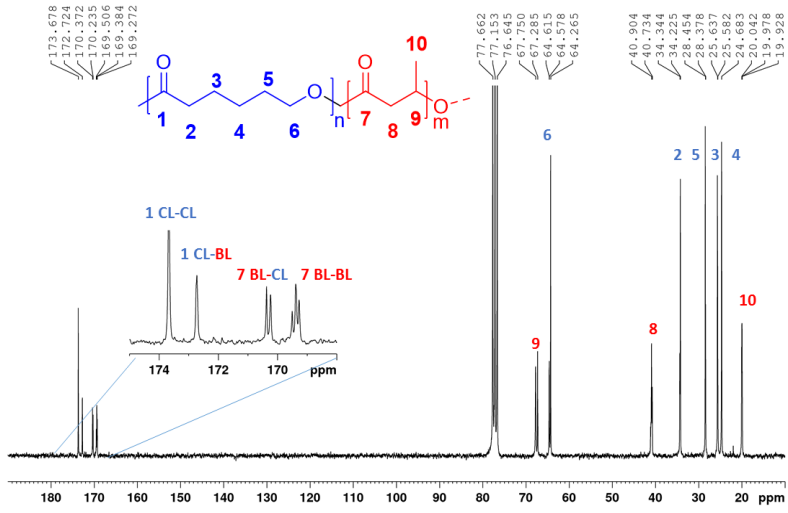

Figure 2.21. ^{13}C NMR spectrum (63 MHz, $CDCl_3$, 298 K) of poly[HB-co-CL].

The absence of thermal transitions in both the first and second DSC heating runs indicates an amorphous sample (the T_g of both phases were also not observed).

In the WAXD pattern of the sample only a large amorphous halo was observed, confirming the results of the thermal analysis.

These results are coherent with a polymer microstructure consisting of short blocks of both monomers (ε-CL and β-BL) randomly distributed along the polymer chain so that the crystallization of both phases is hindered (Scheme 2.11).

Scheme 2.11. Copolymer sequence with a blocky microstructure.

The blocky microstructure proposed for poly[HB-co-CL] was supported by kinetic measurements (Figure 2.22). After 30 min the conversion of 72% of ε-CL was observed, while the conversion of β-BL was only of 2%. After additional 15 min, the conversion of ε-CL remained unchanged (74%) while the conversion of β-BL reached 43%. After additional 30 min the almost complete conversion of ε-CL was achieved (95%) while the conversion of β-BL changed only weakly (54%).

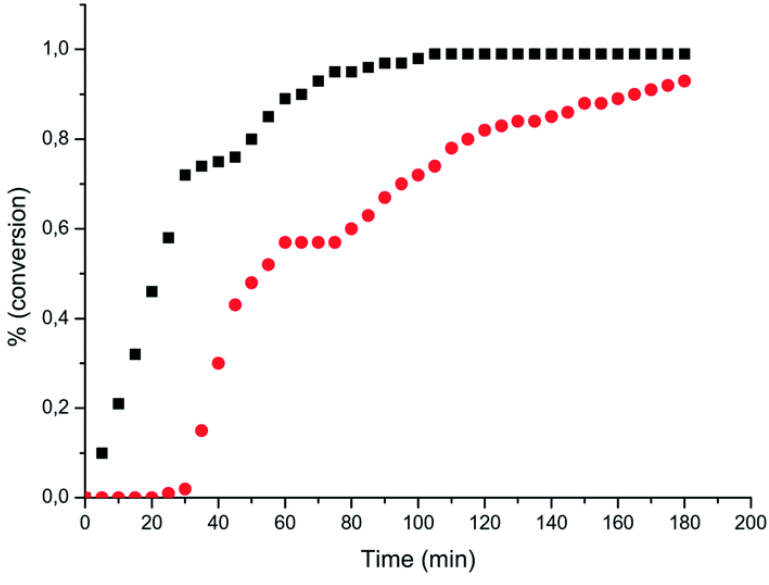

Figure 2.22. Plot of conversion *vs* time for ε-CL (black solid squares) and β-BL (red solid circles).

2.4.1.3. PHB/PLA COPOLYMER

Finally, the copolymerization of β-BL and L-LA was conducted (entry 3, Table 2.5). In the literature, the complexes that promote the ROP of both β-BL and L-LA, and that are effective in their copolymerization are rare.[87] After 12 hours, complex **1** promoted the complete conversion of L-LA while β-BL conversion was significantly lower (50%). For classical half-salen aluminum complexes, no incorporation of *rac*-β-BL during the copolymerization was achieved, even after extended polymerization times.[75b]

In the carbonylic region of the ^{13}C NMR spectrum (Figure 2.23), the resonance corresponding to LA-LA homodiads was the most intense signal, and less intense resonances were observed for the BL-LA, LA-BL and BL-BL heterosequences.

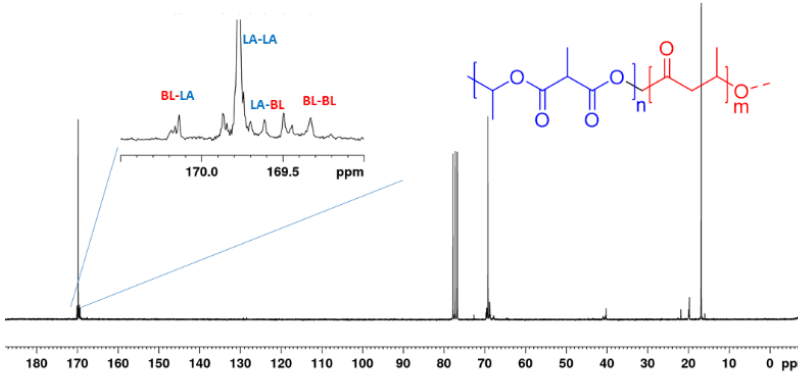

Figure 2.23. ^{13}C NMR spectrum (75 MHz, $CDCl_3$, 298 K) of poly[LA-co-HB] obtained.

The thermal analysis (see Appendix 2) of the obtained sample showed an endotherm peak centered at T = 133 °C with a melting enthalpy of 28.7 J/g. This melting transition was tentatively attributed to the PLLA phase so that the corresponding degree of crystallinity resulted in ≈ 20% (in the second DSC run it was drastically reduced to only 2%). No thermal transitions were attributed to the PHB phase. In the second DSC heating run, no endothermal or exothermal phenomena were observed while a single T_g at about 45 °C was evident. This T_g value, lower than that of the PLLA homopolymer, indicates the presence of inter-crystalline phases, in which the two homopolymers are at least partially miscible.

In the WAXD pattern of the sample, only the typical peaks of the PLLA alpha form were present, confirming that only the PLA phase is crystalline.

These results agree with a polymer tapered microstructure (Scheme 2.12) in which the most rigid PLA phase is formed and crystallized before the more flexible and stereo-irregular PHB phase, so that the PHB crystallization process is hindered. In a tapered copolymer, a first block sequence of one monomer (lactide) is connected by a short sequence of a mixture of the comonomers to a block sequence of the second monomer (butyrolactone).

Kinetic studies by ^{1}H NMR spectroscopy revealed that the rate of insertion of *rac*-β-BL into the copolymer was significantly slower than that observed for L-LA (Figure 2.24). When the conversion of L-LA reached 90% the *rac*-β-BL inserted was only about 10%.

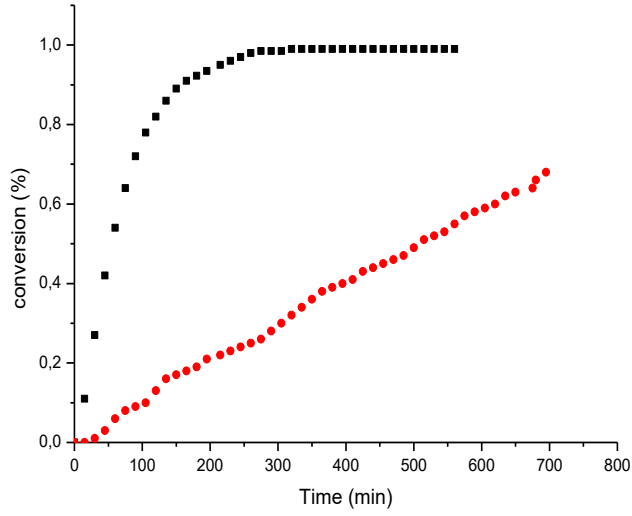

Figure 2.24. Plot of conversion *vs* time for L-LA (black solid squares) and β-BL (red solid circles) concentration.

These observations suggested that the obtained copolymer must have a tapered microstructure, where the monomer composition varied from all lactydic-units to all BL units along the polymer chain.

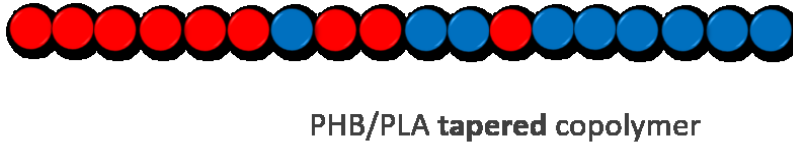

Scheme 2.12. Copolymer sequence with a tapered microstructure.

2.4.2. COPOLYMERIZATIONS OF CYCLOHEXENE OXIDE WITH CYCLIC ESTERS

Complex **1** showed a high activity for the homopolymerization of cyclohexene oxide (CHO). At 70 °C, in the absence of solvent,

complex **1** was able to convert 500 equivalents of CHO in only 5 min.

To extend our study, the copolymerization of CHO with structurally distinct cyclic esters was explored.

The copolymerization of ε-CL and CHO was initially conducted in toluene at 70 °C. After 30 minutes, the conversion of ε-CL was of 33% while CHO did not react. It seems that the reactivity of ε-CL was not influenced by the presence of CHO, diversely, the presence of the cyclic ester inhibited completely the reactivity of complex **1** towards the epoxide.

The homopolymerization of CHO follows a bimetallic pathway, the cooperation between the two metal centers is influenced by the fluxionality of the ligand skeleton so by the polarity of the reaction medium. The same polymerization reaction was repeated in neat, still, no conversion of the epoxide was observed. PCL was isolated as unique product even after prolonged reaction times (24 h). Analogous results were obtained with other cyclic esters. Even though complex **1** is active in the ROP of all these heterocycles, there is no evidence of incorporation of CHO either in the polyester, i.e., no ether linkages, or as a separate polyether.

Diblock copolymers, poly(ether)-co-(ester), were successfully obtained by sequential polymerization of first CHO and then the cyclic ester (Figure 2.25). The synthesis of the first block was performed at 70 °C for 3h, for the second block the reaction time was chosen depending on the reactivity of the respective cyclic ester.

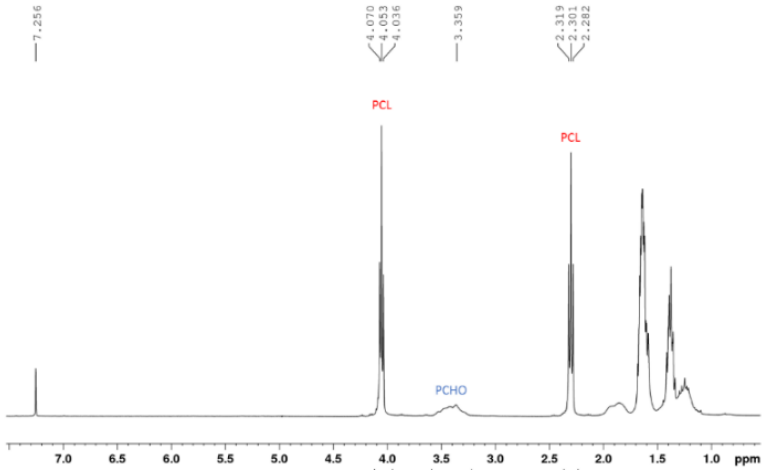

Figure 2.25. ^{1}H NMR spectrum (400 MHz, $CDCl_3$, 298 K) of co-polymer of CHO and ε-CL.

The copolymers were characterized by ^{1}H and ^{13}C NMR spectroscopy and GPC analysis.

Table 2.6. Sequential copolymerization of CHO with cyclic esters promoted by **1**.[a]

Entry	Monomer (equiv)	Time (h)	Yield (%)	M_{nGPC} [b] (kDa)	M_n [th c] (kDa)	Đ[b]
1	ε-CL	72	93	11.1	10.0	1.97
2	L-LA	21	100	11.0	11.9	1.57
3	β-BL	48	100	3.2	8.7	1.08

[a]All reactions were carried out with 1.10^{-5} mol of **1** at 70 °C, in 2 mL of toluene, [**1**]/[^{i}PrOH]]/[CHO] = 1:4:200 for 3 hours, then 200 equivalents of lactone were added. [b]Experimental M_n (corrected using factor 0.58 for PLA, 0.56 for PCL portions and 0.54 for PHB portions) and Đ values were determined by GPC analysis in THF using polystyrene standards. [c]Calculated M_n (in g.mol^{-1}) = [MM_{CHO} x ([CHO]/[^{i}PrOH]) x conversion of CHO + MM_{mon2} x ([Mon_2]/[^{i}PrOH]) x conversion of Mon_2].

GPC showed monomodal distributions for all the copolymers; this is a clear indication that the samples were block copolymers and not mechanical mixtures of homopolymers. As expected, the molar masses evaluated by GPC increased with the growth of the second block and, in all cases, they agreed with the expected values. For example, for the PCHO-b-PLA and PCHO-b-PCL copolymers, the molar masses increase from 6.7 kDa (Đ = 1.51) or 7.4 kDa (Đ = 1.52) for the PCHO blocks to 11.0 kDa (Đ = 1.57) and 11.1 kDa (Đ = 1.97) respectively, for the diblock copolymers with unimodal distributions. As expected, in the ^{1}H NMR spectrum, the signals of the copolymer were observed (see Figure 2.25 for PCHO-b-PCL and Figure 2.26 for PCHO-b-PLA).

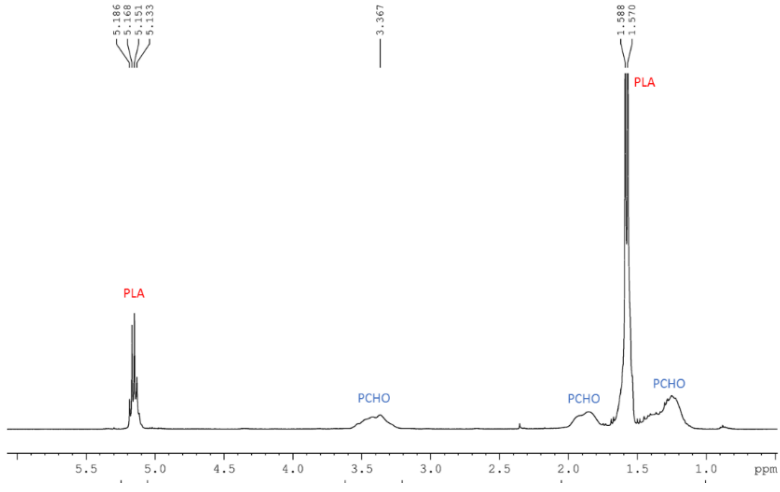

Figure 2.26. ^{1}H NMR spectrum (250 MHz, $CDCl_3$, 298 K) of co-polymer of CHO and L-LA.

This conclusion was confirmed by the 2D DOSY NMR experiments which provided diffusion coefficients of molecules related to the hydrodynamic radius and molecular weight. DOSY NMR

experiments of the PCHO-b-PCL copolymer showed that the signals of the first PCHO block and those of the second PHB block lay at the same diffusion coefficient, and therefore belonged to the same polymeric chains, thus confirming the diblock nature of the obtained samples (Figure 2.27).

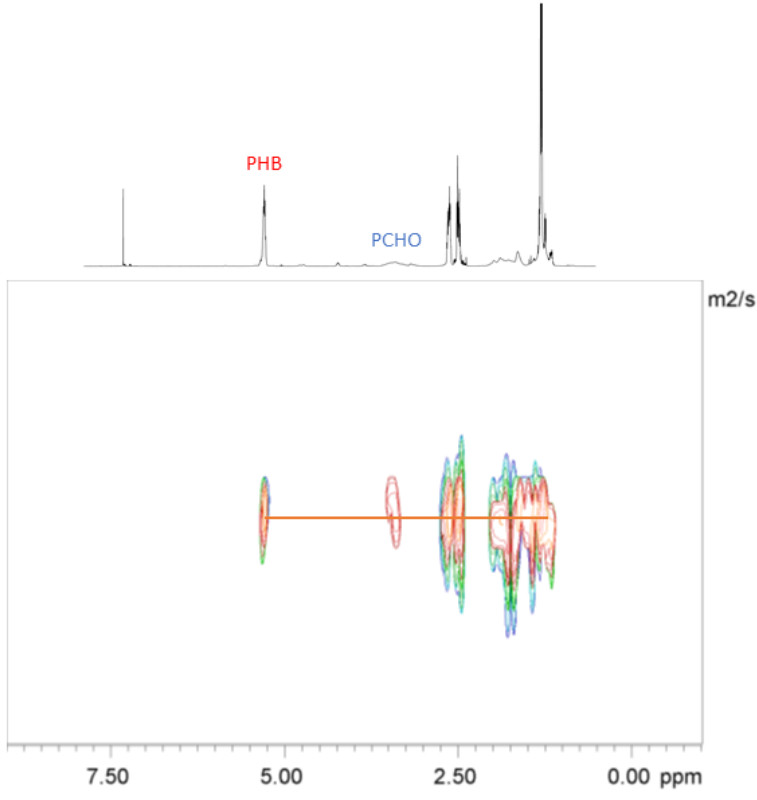

Figure 2.27. ^{1}H DOSY spectrum (600 MHz, $CDCl_3$, 298K) of the co-polymer from Table 2.6, Entry 3.

CONCLUSIONS OF CHAPTER 2

Dinuclear aluminum complexes supported by salen-type frameworks were synthesized and tested in the ring-opening polymerization of *rac*- and L-lactide, ε-caprolactone, *rac*-β-butyrolactone and cyclohexene oxide.

All complexes, activated by isopropyl alcohol, promoted controlled homopolymerization of lactide. However, the activities varied with the distance between the two metal centres. The complex in which the aluminum centres are proximal (**1**) revealed to be much more active than the complexes in which longer alkyl bridges hinder interaction between the reactive aluminum centres (**2-3**).

In addition, complex **1** was the only one able to produce isotactic PLA from *rac*-lactide.

The synergistic interaction between the two metal centres has a role in both the alcoholysis reaction and the propagation steps.

NMR studies of the structure of the active species **1**-PLA demonstrated the growth of only one polymer chain on a single aluminum centre when the two reactive centres are proximal, probably because of a chelation effect of lactate between the aluminum atoms.

The cooperation was even more evident in the ROP of cyclohexene oxide and butyrolactone where complex **1** was the only active.

These evidences prove that the cooperation between the metal reactive centres in a multinuclear species can be induced by an opportune ligand design.

Seeing the high activity of complex **1** in the ROP, co-polymerization reactions were also performed.

The co-polymerizations with different couples of cyclic esters produced co-polyesters ranging from gradient to blocky microstructures, determined by the kinetics of the reactions.

In the co-polymerization of cyclic esters with cyclohexene oxide, a drastic chemoselectivity emerged, since only the homopolyesters could be produced when both monomers were present simultaneously in the reaction medium. Polyether-co-ester were obtained by sequential addition of the monomers.

Given the high reactivity of complex **1** towards cyclohexene oxide and considering the vast potential of the ROCOP between epoxides and cyclic anhydrides to broaden the structure of the produced polymers, in the next chapter, the focus will be on the reactivity of this series of complexes in this catalysis.

CHAPTER 3. ROCOP OF EPOXIDES WITH CYCLIC ANHYDRIDES BY BIMETALLIC AND MONOMETALLIC ALUMINUM COMPLEXES.

3.1. INTRODUCTION

While a plethora of catalysts is described in the ROP, a far narrower range is known for the ROCOP. In recent studies, intramolecular bimetallic synergistic effects were frequently invoked in the ROCOP of epoxides with cyclic anhydrides.[4, 32a, 33, 88,5] Notable contributes are the homo- and hetero- bimetallic complexes of magnesium and zinc reported by Williams and the bimetallic complexes of nickel, cobalt and zinc reported by Ko.[89]

A few examples of catalysts have been reported able to perform both the ring-opening polymerization of cyclic esters and the ring-opening copolymerization of epoxides with anhydrides or CO_2.[90] Williams[91] and Rieger[92] recently reported systems that allowed a shift between the two catalytic cycles and produced block copolymers via chemoselective polymerization from a complex mixture of monomers.

In this chapter, the catalytic behaviour of our series of aluminum complexes in the ROCOP was studied to verify the possibility of a bimetallic mechanism, as reported in the ROP in the previous chapter. First, the copolymerizations of cyclohexene oxide (CHO) and limonene oxide (LO) with succinic (SA) and phthalic (PA) anhydrides were conducted. The effects of different co-catalysts and reaction conditions were studied.

3.2. EFFECT OF THE MONOMERS, CO-CATALYSTS AND SOLVENT

Initially, the copolymerizations of cyclohexene oxide (CHO) with cyclic anhydrides, such as succinic and phthalic anhydrides, were conducted at 110 °C with a ratio of [CHO]:[anhydride]:[Cat] = 250:250:1 (Scheme 3.1). The chosen reaction conditions are the ones already reported by Duchateau with pentacoordinate (Salen)AlCl catalysts.[29]

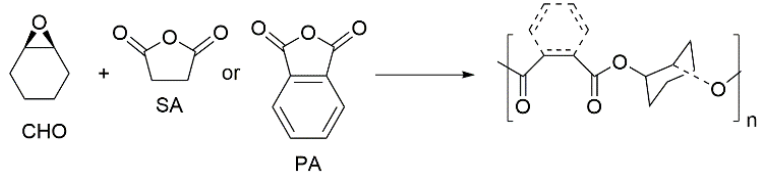

Scheme 3.1. Ring-Opening Co-Polymerization of CHO with succinic anhydride (SA) or phthalic anhydride (PA).

The polymers were characterized by ^{1}H NMR, GPC and MALDI-ToF-MS analyses. The composition of the obtained polymers was estimated by ^{1}H NMR analysis, by comparing the integrals of the signals of epoxide/anhydride sequences with those of ether linkages from sequential enchainment of epoxides (see Appendix 3).

Usually, NMR spectra do not allow a good estimation because of the overlapping of the polyether signals with the signals of chain end groups of the polyester in $CDCl_3$. Interestingly, the use of a high resolution ^{1}H NMR analysis allowed a faultless separation of the resonances enabling the precise determination of the ratio of the two sequences (Figure 3.1). Thus, the microstructural analyses of all polymers were performed in $CDCl_3$ by using a 600 MHz

spectrometer and allowed to evaluate the selectivity of the ROCOP process.

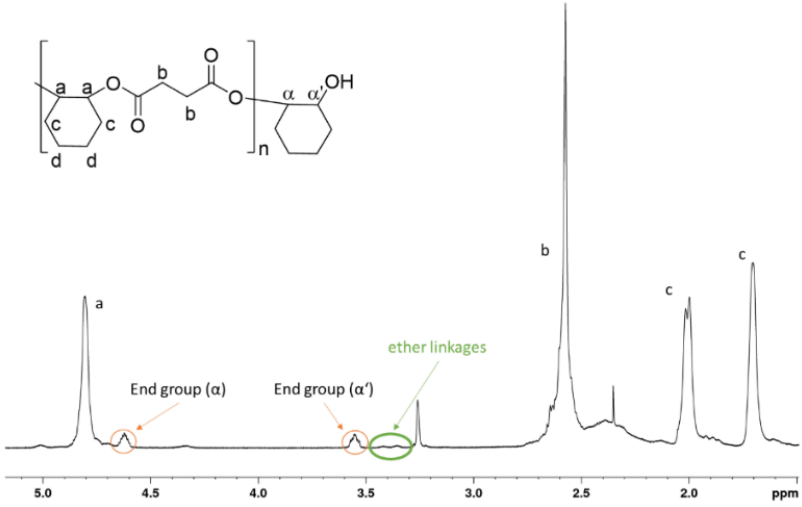

Figure 3.1. ^{1}H NMR spectrum (600 MHz, $CDCl_3$) of the CHO/SA copolymer.

3.2.1. COPOLYMERIZATION OF CYCLOHEXENE OXIDE WITH ANHYDRIDES

At 110 °C, complex **1** (see Appendix 1 for the structure of the complexes) revealed to be a very active catalyst. The almost quantitative conversion of CHO was achieved in less than 1 hour producing a poly(ester-co-ether) with 54% of ester linkages (entry 1, Table 3.1). Performing the reaction in toluene, the activity decreased because of the reduced concentration of the monomer (entry 2, Table 3.1). At the same time, a discrete increment of the selectivity was observed (63% of ester linkages), since the CHO homopolymerization in toluene solution is slower, as previously reported (Chapter 2.3.3).

Table 3.1. Ring-Opening co-Polymerization of CHO with anhydrides promoted by **1**.[a]

Entry	**1**/ DMAP (equiv)	anhydride	solvent	time (min)	CHO conv. (%)[b]	anhydride conv. (%)[b]	ester (%)[b]	M_{nGPC} (kDa)[c]	Đ[c]
1	1:0	SA	bulk	50	94	57	54	5.51	1.56
2	1:0	SA	toluene	300	100	61	63	5.34	1.43
3	1:1	SA	bulk	50	84	73	94	1.78	1.18
4	1:2	SA	bulk	50	79	69	97	1.98	1.16
5	1:2	SA	toluene	240	84	86	>99	1.81	1.19
6	1:8	SA	toluene	180	87	89	>99	1.45	1.19
7	1:2	MA	toluene	300	66	23	45	0.75	2.20
8	1:2	PA	toluene	240	85	76	98	3.56	1.06
9	0:2	SA	toluene	50	2	-	99	-	-
10	1:2	SA	toluene	50	29	26	99	-	-

[a]Reaction conditions: [**1**] = 1.10^{-5} mol; [**1**]/[CHO]/[anhydride] = 1:250:250; T = 110 °C. [b]Determined by ^{1}H NMR spectroscopy of crude reaction mixture. [c]Mn_{GPC} and Đ were determined by GPC, in THF *vs* polystyrene standards.

The addition of a nucleophilic cocatalyst has been reported to boost both the activity and the selectivity in the ROCOP of epoxides and cyclic anhydrides promoted by porphyrinato and salophen chromium catalysts,[26] and also in the reaction of epoxides with CO_2.[93] Common cocatalysts include ammonium or phosphonium salts, or Lewis bases such as DMAP, 4-(N,N-dimethylamino)pyridine. It is proposed that the Lewis base or the anion coordinates to the metal centre, thus labilizing the initiating group or the propagating chain, and accelerating the polymerization.

With complex **1**, the addition of one equivalent of DMAP clearly improved the anhydride conversion and therefore the ester content (up to 94%) in the resulting polymer (entry 3, Table 3.1). With a double amount of co-catalyst, the activity remained the same while the selectivity slightly increased to reach 97% (entry 4, Table 3.1).[94]

Conducting the reaction in toluene and with two equivalents of DMAP, a perfectly alternate polyester was obtained: the ester linkages content was found to be > 99% in the ^{1}H NMR spectrum.
With 8 equivalents of DMAP, the perfect selectivity of the process was preserved, and the activity significantly increased (entry 6, Table 3.1). A blank experiment was conducted in the presence of DMAP alone and afforded polymeric products, but the conversions were significantly lower than with the catalytic system **1**/DMAP (entries 9 and 10 of Table 3.1).
Interestingly, complex **1** revealed activities much higher than those reported in the literature for monometallic penta-coordinate salen aluminum complexes.[29] In terms of turnover frequencies (TOF calculated on catalyst concentration), complex **1** showed TOF up to 220 h^{-1} and 74 h^{-1}, in bulk and in solution, respectively (entries 3 and 6 of Table 3.1). Under the same reaction conditions, the reported monometallic penta-coordinate salen aluminum complexes showed activities in the ranges 25 h^{-1}< TOF < 100 h^{-1} and 15 h^{-1} < TOF < 50 h^{-1}, for reactions in bulk and in solution respectively, depending on the structure of the ligand-diimine backbone.[29]
The GPC analysis of all polymers displayed monomodal distributions with narrow polydispersity (Đ < 1.2 for polymers obtained in the presence of cocatalyst), indicating a controlled behaviour of the ROCOP. The molar masses (M_n) measured by GPC (without any calibration correction) were coherent with the values calculated by evaluation of chain-end groups performed by NMR, and they were always lower than the theoretical ones expected for a living system.

Many authors observed this discrepancy and they often attributed this to the presence of protic impurity traces, such as diacid resulting from hydrolyzed anhydride and/or trace of water, that can act as chain transfer agents (CTAs).[95] On the other hand, the catalytic system is stable in the presence of protic species in the polymerization medium.

The MALDI-ToF-MS spectrum of the crude product obtained by catalyst **1** in bulk without the addition of cocatalyst (entry 1, Table 3.1, Figure 3.2), showed two major distributions, one having a slightly higher CHO than SA content coherently with the NMR evaluation.

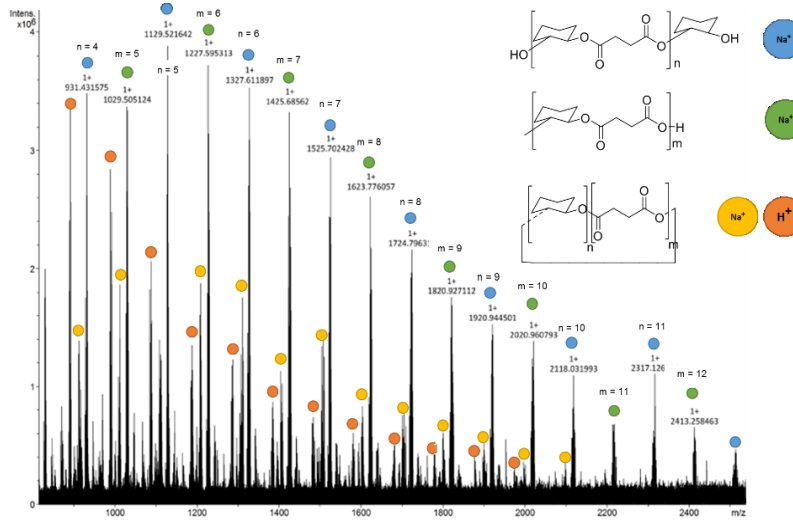

Figure 3.2. MALDI-ToF spectrum CHO/SA polyester (entry 1, Table 3.1).

One series corresponds to linear polymer chains with a methyl and an hydroxyl end group while the other describes α,ω-hydroxy-terminated chains, probably due to nucleophilic attack of the methyl

group of the catalyst and of water present in traces, respectively. Cyclic products can also be observed, revealing that intramolecular transesterification side reactions occurred during the polymerization. The MALDI-ToF-MS spectra of the polymers obtained in the presence of DMAP (entry 6, Table 3.1) showed two distinct distributions, both corresponding to linear polymer chains with sequences of [CHO+SA] repeating units, coherently with perfectly alternate structures containing more than 99% of ester linkages (Figure 3.3). Cyclic products were not detected anymore. End group determination revealed exclusively DMAP end-capped chains. Initiation by methyl groups of the catalyst cannot be excluded since the polymer chains initiated by DMAP are intrinsically charged and they can totally overrule the originally uncharged chains in the MALDI-ToF-MS spectra. This suggest switterionic chain structures, $DMAP^{+}$-$[SA+CHO]_n^{-}$ as proposed by Duchateau.[29]

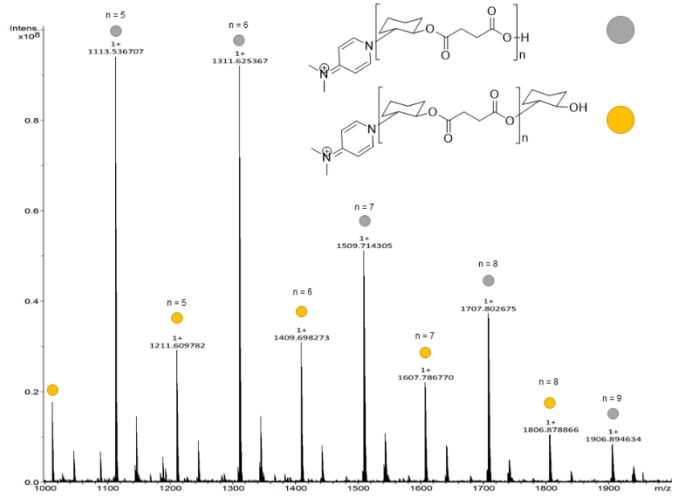

Figure 3.3. MALDI-ToF-MS spectrum of SA/CHO copolymer synthesized in entry 6 of Table 3.1.

The study was extended to different anhydrides, under the same conditions optimized for CHO/SA copolymerization. Phthalic (PA) and maleic (MA) anhydrides are particularly interesting since the polyesters obtained have a backbone containing respectively aromatic or unsaturated repeating units; especially since aromatic polyesters cannot be obtained by ROP but confer good mechanical properties. For the CHO/PA copolymerization the activity was similar than with SA, however the selectivity was not perfect (entry 8 of Table 3.1). The copolymerization of CHO with maleic anhydride (MA) showed low conversion and poor selectivity (entry 7 of Table 3.1). As already discussed, the molecular weights of the obtained polymers were lower than the expected ones.

3.2.2. Effect of the cocatalyst

Nucleophilic cocatalysts have an important role during the epoxide/anhydride copolymerization, not only in terms of activity but also of selectivity.[29] Therefore, the performance of several cocatalysts were examined in the ROCOP of CHO/PA since complex **1** showed a good activity but the selectivity was not perfect.

DMAP: 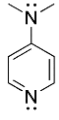

TBABr: 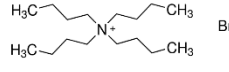

PPNCl: 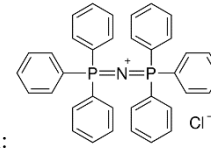

Scheme 3.2. Types of nucleophilic cocatalysts investigated.

Herein the effect of different types of nucleophilic cocatalysts was studied, including several ammonium salts and the (bis(triphenylphosphine)iminium) salt (Scheme 3.2). The ionic

cocatalysts have a poor solubility in toluene so the reaction conditions were changed, and the polymerizations were conducted in CH_2Cl_2 at 50 °C (Table 3.2).

Table 3.2. Copolymerization of CHO/PA in CH_2Cl_2 catalyzed by **1** with different co-catalysts.[a]

Entry	Cocat (equiv)	CHO conv. (%)[b]	Ester (%)[b]	$M_{n\text{GPC}}$ (kDa)[c]	Đ[c]
1	DMAP (2)	20	71	1.76	1.09
2	DMAP (8)	40	97	2.88	1.16
3	PPNCl (2)	21	89	1.67	1.22
4	PPNCl (4)	25	95	4.49	1.14
5	PPNCl (8)	61	>99	2.45	1.40
6	TBABr (2)	30	90	2.88	1.12
7	TBABr (4)	35	>99	3.00	1.17
8	TBABr (8)	46	>99	2.89	1.17
9	TBACl (2)	21	81	1.99	1.08
10	TBAI (2)	16	76	1.68	1.07
11	PPh_3 (2)	16	76	1.63	1.08

[a]All reactions were carried out with 10 μmol of **1** at 50 °C, in 1 mL of dichloromethane, [**1**]/[CHO]/[anhydride] = 1:250:250. [b]Determined by ^{1}H NMR after 20 h. [c]Experimental M_n and Đ values were determined by GPC analysis in THF using polystyrene standards.

With all the different cocatalysts, the conversions of CHO were around 20% after 20 hours (entries 1, 3, 6 and 9-11 of Table 3.2). Significant effects were instead observed on the selectivity of the ROCOP towards polyester formation.

In methylene dichloride, DMAP was less selective than in toluene (entry 1, Table 3.2). Although the temperature was changed too, the decrease in selectivity seems to be more caused by the nature of the

solvent rather than the different temperature. In fact, previous studies performed by Coates[27] and Duchateau[29] showed that hydrocarbon solvents have beneficial effects on the selectivity of the catalytic process.

PPNCl and TBABr cocatalysts resulted to be the most selective ones, since the polymers produced possess about 90% of ester linkages (entries 3 and 6 of Table 3.2). Among the ammonium salts, TBAX (X = Cl, Br, I), the bromide salt, a good compromise between nucleophilicity and basicity, gave the highest selectivity (entries 6 *vs* 9-10 of Table 3.2). Among the two chloride salts PPNCl and TBACl, the bulky (bis(triphenylphosphine)iminium) salt resulted more selective (entries 3 and 9 of Table 3.2), reasonably because the nucleophilicity of the chloride anion is stronger since it depends on the nature of the associated cation since in methylene chloride ions exist in the form of ion pairs linked electrostatically. A perfect selectivity was possible increasing the equivalents of the cocatalyst TBABr up to 4 (entry 7 of Table 3.2). To achieve this good result with PPNCl, 8 equivalents were required (entries 5 and 8 of Table 3.2), whereas even with 8 equivalents of DMAP, the selectivity was lower (entry 2 of Table 3.2). Poor activity and selectivity were obtained with PPh_3 as cocatalyst (entry 11 of Table 3.2).

The selection of the optimal cocatalyst seems to depend on the polarity of the reaction medium. Ionic cocatalysts are more efficient in polar solvents, while neutral ones are the best choice when less polar solvents are used.

To confirm this hypothesis, the most efficient cocatalysts in methylene chloride, TBABr and PPNCl, were tested in toluene.

Table 3.3. Copolymerization CHO/PA in toluene solution catalyzed by **1** with different cocatalysts.[a]

Entry	Cocat	CHO conv (%)[b]	Ester (%)[b]	$M_{n\text{GPC}}$ (kDa)[c]	Đ[c]
1	TBABr	30	76	2.05	1.09
2	PPNCl	54	64	2.34	1.09
3	PPh_3	42	76	2.13	1.08
4[d]	TBABr	91	91	3.38	1.11
5[d]	PPNCl	91	75	4.27	1.15
6[d]	DMAP	81	98	4.33	1.10

[a]All reactions were carried out with 10 μmol of **1** at 110°C, in 1 mL of toluene, [**1**]/[cocatalyst]/[CHO]/[PA] = 1:2:250:250. [b]Determined by ^{1}H NMR after 5 h. [c]Experimental M_n and Đ values were determined by GPC analysis in THF using polystyrene standards. [d]Cocatalyst dissolved in 0.1 mL of CH_2Cl_2.

In toluene, the activities and selectivities of TBABr and PPNCl shrinked, probably because of their low solubility (entries 1 and 2 of Table 3.3). The neutral cocatalyst PPh_3 resulted a poor cocatalyst in toluene solution as well. To avoid spurious effects due to the different solubility of cocatalysts, additional polymerizations were performed dissolving the ionic cocatalysts in the minimum amount of CH_2Cl_2 and adding the resulting solution in the reaction medium (toluene). Not surprisingly, in toluene solution, ionic cocatalysts were less selective than the neutral DMAP (entries 4-6 of Table 3.3). In conclusion, the non-ionic cocatalysts, such as DMAP, are more selective in apolar media while ionic cocatalysts are more efficient in polar solvents such as methylene chloride.

3.2.3. COPOLYMERIZATION OF LIMONENE OXIDE WITH PHTHALIC ANHYDRIDE

In the last few years, the interest towards renewable feedstocks as substrates in polymer science for the production of sustainable materials deepened. Limonene oxide (LO) is an available bio-based and non-food resource. As substrate, it has been used for reaction with CO_2 for the synthesis of cyclic carbonates or polycarbonates. [96] However, LO has been surprisingly under-investigated in the copolymerization with anhydrides.[30, 38, 97]

The reactivity of the commercially available LO monomer, the mixture of *cis* and *trans* (R)-limonene oxide, was studied in the ROCOP with phthalic anhydride, considering the structural analogies of LO with CHO (Scheme 3.3).

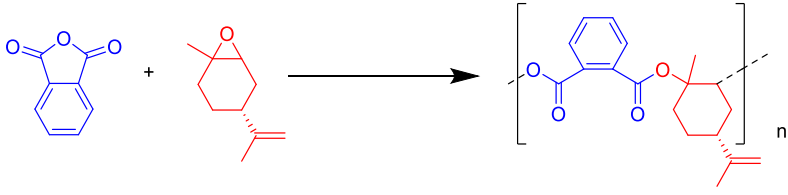

Scheme 3.3. Synthesis of polyesters from limonene oxide (LO) and phthalic anhydride (PA).

Complex **1**/ DMAP showed a very high activity in bulk allowing an almost quantitative conversion of the monomers in two hours (entry 1, Table 3.4). As expected, in toluene solution, the activity decreased drastically because of dilution effects, as already observed for the CHO copolymerization (entry 3, Table 3.4).

Table 3.4. Ring-Opening co-Polymerization of LO with PA promoted by **1** and **4**.[a]

Entry	Cat	LO conv (%)[c]	Time (h)	M_{nGPC} (kDa)[d]	Đ[d]	T_g (°C)
1	**1**	72	2	3.75	1.15	52.9
2	**4**	91	2	4.36	1.15	83.7
3[b]	**1**	56	5	2.30	1.10	-

[a] Reaction conditions: [LO]:[PA]:[cat]:[DMAP] = 250:250:1:2; T = 130 °C. [b] 1 mL of toluene. [c] Determined by ^{1}H NMR spectroscopy. [d] M_{nGPC} and Đ were determined by GPC, in THF *vs* polystyrene standards.

Interestingly, complex **1** displayed higher activities in comparison to the related monometallic penta-coordinate salen aluminum complex, for which less than 30% of conversion was achieved and no isolable polymer was obtained in solution.[98]

The ^{1}H NMR analysis of the copolymers obtained showed the absence of ether linkages, thus perfectly alternated copolymers were obtained, as expected because of the bulky nature of LO.

The microstructure elucidated by the ^{13}C NMR analysis showed atactic polymers, coherently with the achiral structure of the catalyst (Figure 3.4).

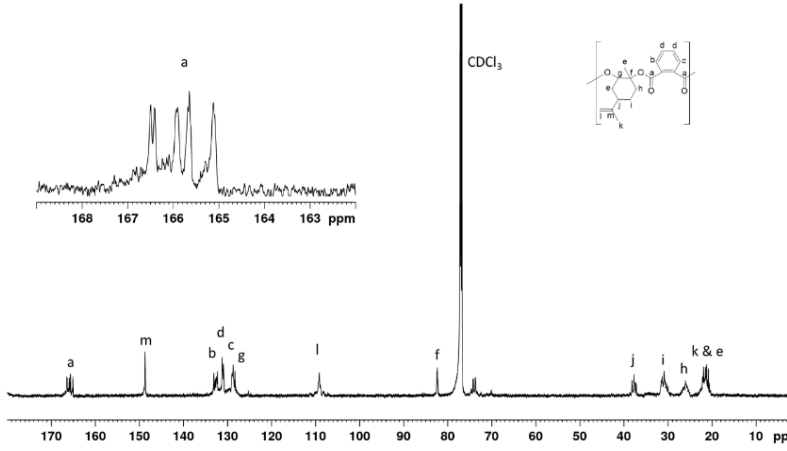

Figure 3.4. ^{13}C NMR spectrum of polyester LO/PA catalyzed by **1**.

As already observed in the ROCOP of CHO/SA, the molecular weights obtained were systematically lower than the theoretical ones for a living catalyst system, reasonably because of protic impurities present in the polymerization medium. Nonetheless, complex **1** was able to exert good control on the polymerization. The evolution of molecular weights of the polyesters plotted against the PA conversion (Figure 3.5) displayed a linear correlation while the molecular weight distributions remained narrow ($Đ < 1.22$).

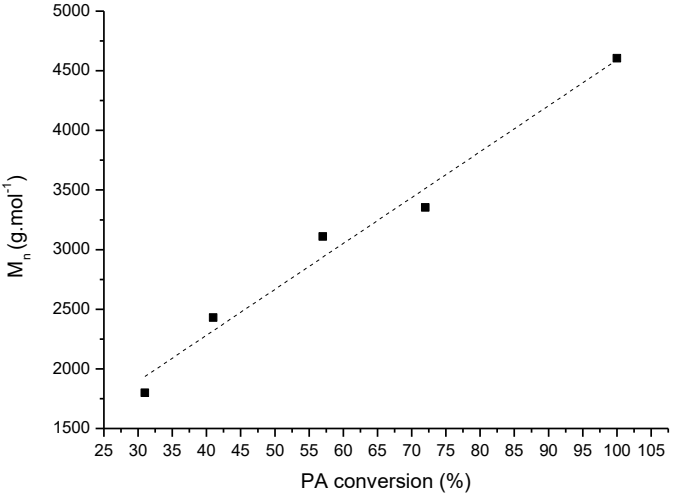

Figure 3.5. Linear dependence of M_n *vs* conversion of PA for ROCOP catalysed by complex **1** (R = 0.974).
Polymerization conditions: [**1**]:[DMAP]:[PA]:[LO]=1:2:250:250, T = 130°C, toluene solution.

The MALDI-ToF-MS spectrum of the crude product obtained by **1**/DMAP (entry 1, Table 3.4) showed two distinct series of peaks. Each series exhibited a *m/z* interval of 300 between the consecutive peaks, corresponding to a [LO + PA] repeating unit, showing a perfectly alternating structure. The two distributions correspond to DMAP end-capped chains, hydroxyl functionalized, consisting of n PA and (n + 1) LO units and n [PA+ LO] units, respectively (Figure 3.6).

Additionally, a copolymerization experiment of LO with succinic anhydride (SA) was performed in toluene. After 5 h a conversion of 37% of LO was achieved. The molar masses of the obtained polyester were quite low (M_n = 700) with a polydispersity of 1.58.

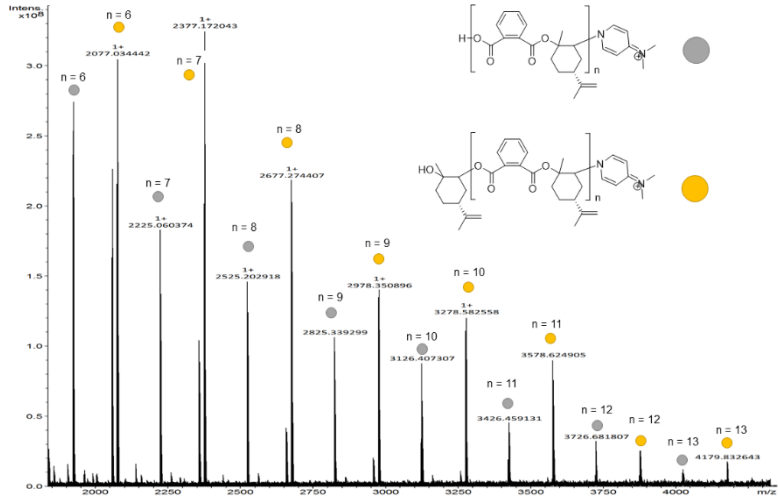

Figure 3.6. MALDI-ToF spectrum of LO/PA copolymer obtained by **1**/DMAP (entry 3 of Table 3.4).

3.3. MECHANISM AND KINETICS: BIMETALLIC *VS* MONOMETALLIC

3.3.1. COMPARISON OF THE CATALYSTS ACTIVITY

Bimetallic complex **1** showed a catalytic activity higher than that achieved with the penta-coordinate monometallic aluminum complexes bearing analogous ligands reported in the literature.[29]

To find out the role of a possible cooperation between aluminum centres, the catalytic behaviour of complex **1** was compared with those of the bimetallic complex **2** and the related monometallic one **4.** In complex **2**, the presence of a long alkyl chain between the imine functionalities inhibits the interaction between the reactive centres. Complex **4** reproduces the coordinative environment of each aluminum centre of the dinuclear complexes **1** and **2**.

All complexes were tested in the ROCOP of CHO/SA, in the same molar concentration (Table 3.5). The reactions were performed in toluene with two equivalents of DMAP, the optimized conditions found in the paragraph 3.2.1.

Table 3.5. Comparison of activity among complexes **1**-**4** in the ROCOP of CHO/SA.[a]

Entry	Cat	CHO conv. (%)[b]	SA conv. (%)[b]	Ester (%)[b]	$M_{n\text{GPC}}$ (kDa)[c]	Đ[c]
1	**1**	28	29	>99	1.96	1.15
2	**4**	26	24	>99	1.17	1.14
3	**2**	57	55	>99	1.96	1.33

[a]Polymerization conditions: [cat]:[DMAP]:[SA]:[CHO] = 1:2:250:250, T = 110°C, toluene 1 ml, time = 50 min. [b] Determined by ^{1}H NMR spectroscopy. [c] $M_{n\text{GPC}}$ and Đ were determined by GPC, in THF *vs* polystyrene standards.

Surprisingly, complexes **1** and **4** resulted having a similar activity (entries 1 and 2, Table 3.5). It suggests that this time for the bimetallic complex **1** a single aluminum centre is involved in the catalytic process without cooperation between the metal centres, although chain transfer phenomena between the two aluminum atoms are still plausible. Reasonably, the simultaneous growth of two chains on complex **1** is not permitted because of excessive steric encumbrance.

Coherently, a doubled activity (CHO conversion of 57% after 50 min) was achieved with complex **2** (entry 3, Table 3.5). In this case, the longer distance between the aluminum atoms allows the growth of two polymeric chains, one for each metal centre. The two reactive centres are acting independently. Analogous results were obtained by complexes **1** and **4** in the LO/PA copolymerization (Table 3.4).

These findings suggest that no cooperation between the adjacent aluminum centres is at stake in the ROCOP for any of these systems. To have more insight in the copolymerization mechanism promoted by complex **1**, kinetics of the reaction was plotted: succinic anhydride conversion *vs* reaction time (Figure 3.7). The ^{1}H NMR data showed a linear dependence signifying a zero-order dependence of the reaction rate on SA concentration. Thus, the rate of polymerization is independent of the concentration of succinic anhydride, suggesting that the rate-determining step of the copolymerization is the insertion of the epoxide on the carboxylate intermediate to regenerate the metal alkoxide intermediate, as already reported by several authors.[88, 99]

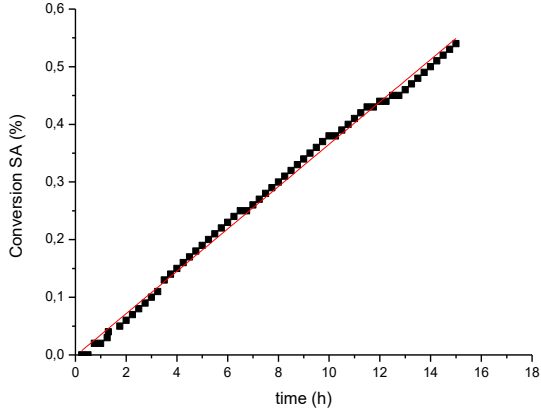

Figure 3.7. Linear dependence of the SA conversion *vs* time (**R^2** = 0.9959).

In the mechanism generally accepted for this catalysis, the initiation step proceeds by ring-opening of the epoxide by an initiation group that can be, or the labile group bound to the metal catalyst or the nucleophilic cocatalyst. The resulting metal-alkoxide intermediate

then reacts with the anhydride to produce a metal-carboxylate intermediate. The propagation steps consist in iterative and alternate insertions of these two monomers.

The lower coordination number of these complexes, in which the reactive aluminum centre is tetra-coordinate, in comparison to the traditional penta-coordinate complexes could favour both the coordination of the nucleophilic cocatalyst and the incoming epoxide monomer at the same reactive centre.

Since the rate determining step is the insertion of the epoxide on the carboxylate intermediate, the presence of a Lewis base/ nucleophilic cocatalyst has a crucial role, since its coordination to the central metal ion will change the acidity of the reactive centre and can improve the lability of the carboxylate intermediate.

3.3.2. NMR STUDY OF THE REACTION

To have more insights about the mechanism, NMR monitoring of the reaction was conducted. After the addition of 1 equivalent of DMAP into a benzene solution of complex **1**, the spectrum of the resulting mixture revealed to be a simple overlap of the spectra of the two starting compounds. The same result was obtained after subsequent addition of 1 equivalent of CHO into the solution (Figure 3.8). The symmetry of **1** was still preserved and the signals of DMAP and CHO were coincident with those of the compounds alone. This could suggest rapid exchange phenomena between the coordinated DMAP and CHO at the metal centres and the free ones. This was confirmed by the NOESY spectrum of the sample in which no correlation peaks between complex **1** and both CHO or DMAP were observable.

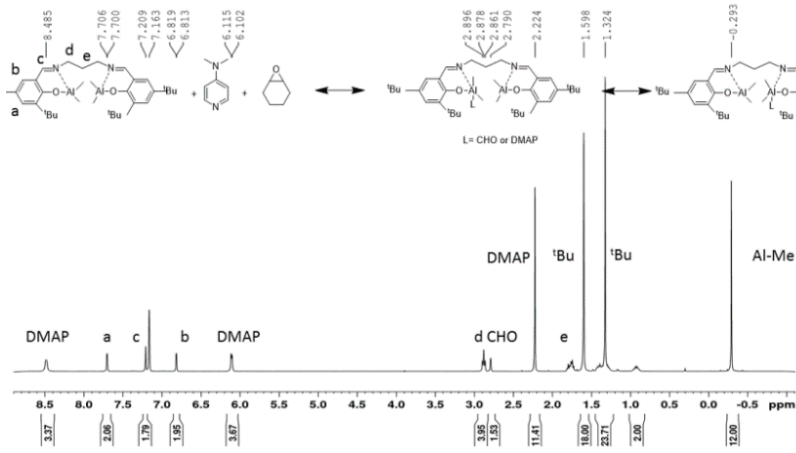

Figure 3.8. ^{1}H NMR spectrum (400 MHz, 25 °C, C_6D_6) of a sample containing complex **1**, DMAP and CHO in 1:1:1 ratio.

After heating the reaction mixture at 70 °C for 12 h, a second set of sharp resonances appeared, close to the initial peaks of the starting species (Figure 3.9).

Probably, the formed species could consist of complex **1** in which an aluminum centre bound a CHO molecule opened by DMAP. [100] The high symmetry of the produced species can be a consequence of a rapid flip of the opened CHO unit between the two aluminum centres. Thus, it is possible to conclude that the attack of CHO occurred by DMAP and no cooperation between the two metal centres is evident.

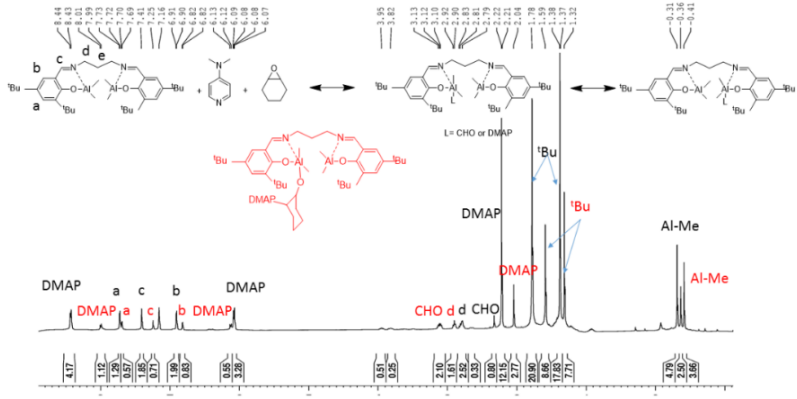

Figure 3.9. ^{1}H NMR spectrum (400 MHz, 25 °C, C_6D_6) of a sample containing complex **1**, DMAP and CHO in 1:1:1 ratio after heating at 70 °C.

In conclusion, it seems that the mechanisms are different for these catalysts in the homopolymerization of CHO *vs* in the co-polymerization of CHO with SA.

For the homopolymerization of CHO, a bimetallic coordination-insertion mechanism was proposed in which one of the Lewis acidic metal centres binds the incoming monomer and activates it for the nucleophilic attack by the growing polymer chain bound to the second aluminum atom (Chapter 2). On the other hand, a monometallic pathway is suggested in the ROCOP reaction.

The high activity showed for all our tetra-coordinate complexes in comparison to the related penta-coordinate aluminum complexes suggests that the lower coordination of the reactive aluminum centres could have a role in promoting the reaction rate.

3.4. COMBINING ROP & ROCOP

Recently, Williams reported the chemoselective synthesis of copolymers of defined compositions from a mixture of monomers promoted by bimetallic zinc complexes[88] as well as a commercial chromium catalyst.[91f] The polymerization selectivity depends on the nature of the functionality at the growing polymer chain bound to the metal center.[91c, 101]

Rieger described the switching process between ROP of β-butyrolactone (β-BL) and CHO/CO_2 ROCOP triggered by the presence of the gaseous monomer in the reaction medium.[92]

The bimetallic aluminum complex **1** supported by a salen ligand showed high activity both in the ROP of cyclic esters and in the ROCOP of epoxides with cyclic anhydrides.

Copolymerization is a powerful tool to extend the variety of polymer architectures that can be obtained.

In an attempt to combine both catalytic cycles, the co-polymerization of CHO with SA was performed, in the presence of ε-caprolactone (ε-CL). After 5 hours, poly(cyclohexene succinate) was the unique product while the polymerization of ε-CL was completely inhibited. No evidence of incorporation of the cyclic ester in the growing chain was observed, even after extended reaction times.

These observations are coherent with the literature[88, 91c] and justified by the rapid insertion of SA into the aluminum alkoxide bond, coupled with the inability of the resulting carboxylate intermediate to initiate the ROP of the cyclic lactone.

Analogous results were obtained by the combination of CHO and SA with the other cyclic esters (L-LA and β-BL).

The polyesters obtained from all these copolymerization reactions have perfectly alternated microstructures with no evidence of the presence of polyether sequences. This is surprising since the ROCOP is often reported to be selective only in the presence of a nucleophilic co-catalyst. This suggested that, in the catalytic mixture investigated, the cyclic ester might act as a co-catalyst.

Performing the same experiment with less equivalents of anhydride (50 equivalents), a diblock copolymer poly(cyclohexene succinate)-co-PCL was obtained (entry 1, Table 3.6), confirming the hypothesis that the insertion of the cyclic ester is possible on the alkoxylate-aluminum bond of the growing chain (Scheme 3.4). The DOSY experiment confirmed the diblock structure of the copolymer poly(cyclohexene succinate)-co-PCL (Figure 3.10).

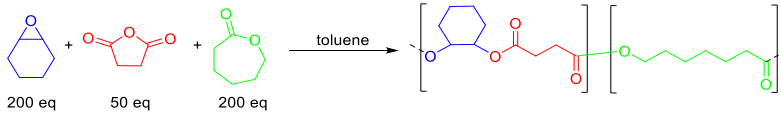

Scheme 3.4. Copolymerization from a mixture of monomers.

Analogous results were obtained when the monomer couple CHO/SA was used in combination with L-lactide and β-butyrolactone (Table 3.6).

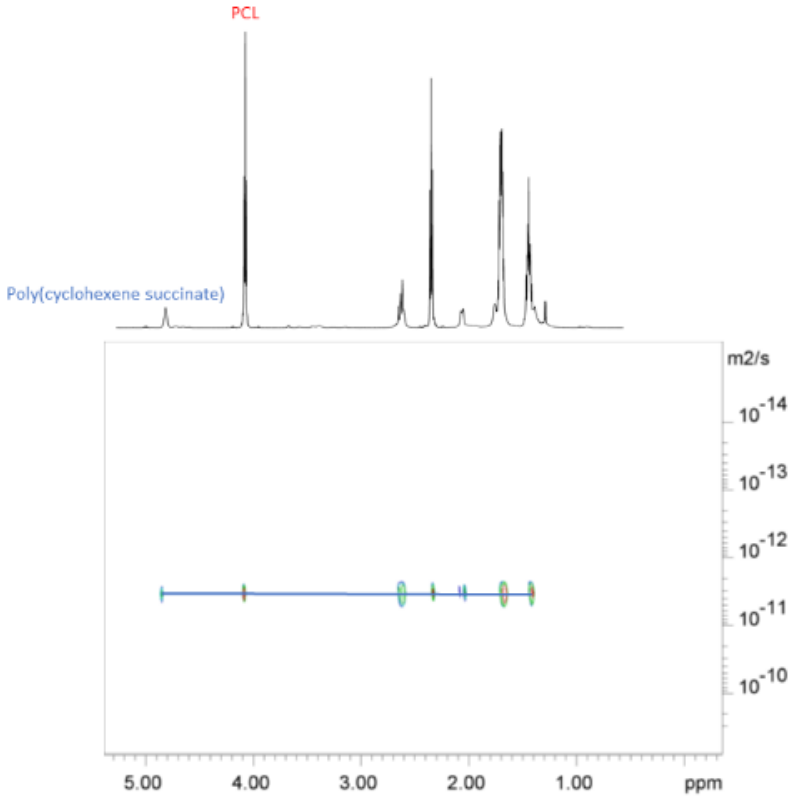

Figure 3.10. ^{1}H DOSY spectrum (600 MHz, $CDCl_3$, 298 K) of the ter-polymer from Table 3.6, Entry 1.

Table 3.6. Copolymerizations of CHO/SA with cyclic esters promoted by **1**.[a]

Entry	Monomer (equiv)	Time (h)	Yield (%)	M_{nGPC} [b] (kDa)	M_n^{th} [c] (kDa)	Đ[b]
1	ε-CL	4	100	13.3	10.2	1.42
2	L-LA	23	97	9.2	9.5	1.71
3	β-BL	23	100	4.6	6.8	1.29

[a]All reactions were carried out with 1.10^{-5} mol of **1** at 110 °C, in 2 mL of toluene, [**1**]/[^{i}PrOH]/[CHO]/[SA] = 1:4:200:50 and 200 equivalents of lactone. [b]Experimental M_n (corrected using factor 0.58 for PLA, 0.56 for PCL portions and 0.54 for PHB portions) and Đ were determined by GPC, in THF *vs* polystyrene standards. [c]Calculated M_n.

These experiments underline the different roles that monomers can play in the reaction medium, the anhydride acts as a switch to trigger the copolymerization CHO/SA over the ROP of the cyclic ester to produce the first block, at the same time the cyclic ester serves as cocatalyst to ensure the selectivity of the ROCOP.

CONCLUSIONS OF CHAPTER 3

Bimetallic phenoxy-imine aluminum complexes are effective catalysts in ring-opening copolymerization of cyclohexene oxide with several cyclic anhydrides. Nice results were also obtained in the ROCOP of the less reactive but renewable, limonene oxide with phthalic anhydride.

The study of the effects of different cocatalysts and reaction solvents, revealed that non-ionic cocatalysts, such as DMAP, are more selective in apolar media while ionic cocatalysts are more efficient in polar solvents, such as methylene chloride.

The comparison of the catalytic behaviour of the dinuclear complexes bearing the aluminum reactive centres at different distances (**1**-**2**) as well as of their mononuclear counterpart (**4**) suggests that the copolymerization follows a monometallic pathway, differently from what was observed in the homopolymerization of CHO.

The higher activity of these complexes in comparison to the related penta-coordinate aluminum complexes suggests that a lower coordination of the reactive aluminum centres helps to promote the reaction rate.

This work puts in evidence that tetracoordinate aluminum complexes represent more efficient and less synthetically expensive alternatives to traditional salen analogues for the copolymerization of epoxides and cyclic anhydrides.

The bimetallic aluminum complex **1** supported by a salen ligand showed high activity both in the ROP of cyclic esters and in the

ROCOP of epoxides with cyclic anhydrides. Combining both catalytic processes is an interesting challenge because of the opportunities to modify and improve upon the polymer properties. With a monomer feedstock comprising cyclohexene oxide, succinic anhydride and a cyclic ester, combined in opportune proportions, terpolymerization was indeed achieved producing a block poly(cyclohexene succinate)-co-polyester. Interestingly, the portion of copolymer obtained by copolymerization of CHO and SA showed a perfectly alternate structure suggesting that, during the production of the first block, the cyclic ester acted as a co-catalyst.

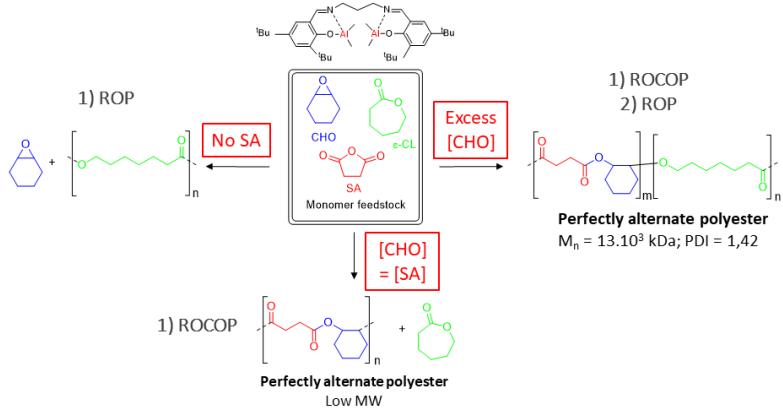

Scheme 3.5. Combining ROP & ROCOP.

In these reactions, a dual role of the involved monomers emerged. The succinic anhydride switches the catalyst from the ROCOP of epoxide with anhydride to the ROP of cyclic esters while the cyclic ester acts as cocatalyst favouring the production of perfectly alternated polyester (Scheme 3.5).

CHAPTER 4. HIGHLY SELECTIVE CATALYSTS FOR ROCOP OF EPOXIDES WITH CYCLIC ANHYDRIDES BY TAILORED LIGAND DESIGN.

4.1. INTRODUCTION

In the previous chapter, bimetallic aluminum complexes supported by salen ligands and the related monometallic one demonstrated high activity for the ROCOP of cyclohexene oxide and limonene oxide with phthalic and succinic anhydrides.

The experimental evidences supported the hypothesis of a monometallic mechanism in which no cooperation between metal centres was involved, and at the same time all complexes resulted highly active. We speculated that the lower coordination of the reactive aluminum centres could allow for coordination of sterically more demanding substrates with a positive effect in promoting the reaction rate.

Following the previous findings, tetra-coordinate monometallic aluminum complexes supported by bidentate monoanionic ligands of phenoxide-type such as phenoxy-imine, phenoxy-amine and phenoxy-thioether ligands were investigated in the copolymerization of epoxides with cyclic anhydrides.

Although these complexes have been widely investigated in the ROP of cyclic esters,[60, 102] no study has ever been reported regarding the copolymerization of epoxides with cyclic anhydrides.

The effects of the steric and electronic environment of the metal centre on the activity and selectivity are explored.

4.2. Effect of the Catalyst Structure on the Catalytic Behaviour

4.2.1. Simple phenoxy-based aluminum complexes synthesis

Complex **4** is the simple hemi-salen complex with a n-propyl chain on the imine nitrogen, as described previously. For complexes **5a-e**, the ligands have a phenyl substituent on the imine moiety, granting an easy modification of the steric and electronic properties of the ancillary ligand by introducing different substituents on the *ortho* and/or *para* positions of the aromatic ring.

Afterwards, the nature of the neutral donor bound to the metal centre was modified by substituting the imine nitrogen donor with a less Lewis basic amine nitrogen for complex **6** or with the softer sulphur atom for complex **7** (Scheme 4.1).

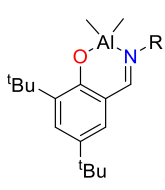

(4) R = *n*-propyl
(5a) R = Ph
(5b) R = 2,6-diisopropylphenyl
(5c) R = 2,6-dimethylphenyl
(5d) R = 4-methoxyphenyl
(5e) R = C_6F_5

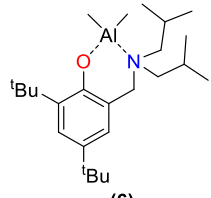

(6)

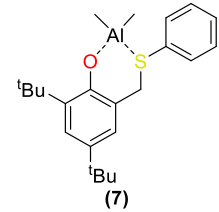

(7)

Scheme 4.1. Phenoxy-based aluminum complexes **4**-**7**.

The pro-ligands were synthesized according to published procedures.[60, 102b] All the related aluminum-alkyl complexes were obtained, in quantitative yields, by direct reaction between the

opportune pro-ligand with one equivalent of $AlMe_3$. The identity of all these simple phenoxy-based complexes was established by ^1H, and ^{13}C NMR spectroscopy, and 2D ^1H-^1H COSY. Complexes **5a-c** and **7** are reported in the literature.[103]

Diagnostic resonances in the protonic spectra are sharp singlets in the high-field region (between $\delta = -0.13$ and -0.29 ppm) assigned to the equivalent protons of the two Al–Me groups and integrating for 6 protons (see Complex **4** in Figure 4.1).

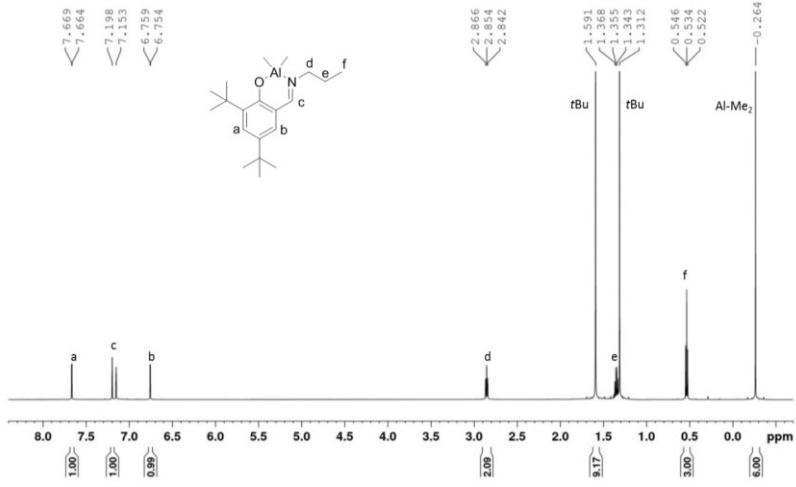

Figure 4.1. ^1H NMR (400 MHz, C_6D_6) of complex phenoxy-imine n-propyl **4**.

4.2.2. COPOLYMERIZATION OF CYCLOHEXENE OXIDE WITH SUCCINIC ANHYDRIDE

Initially, the copolymerization of cyclohexene oxide (CHO) and succinic anhydride (SA) was carried out employing the complexes under different reaction conditions: at 110 °C, in neat or in toluene solution, with an [epoxide]:[anhydride]:[catalyst] ratio of 125:125:1,

and one equivalent of 4-(N,N-dimethylamino)pyridine (DMAP) as cocatalyst.

The polymers were characterized by ^{1}H NMR, GPC and MALDI-ToF-MS analyses. The copolymer composition was estimated by ^{1}H NMR analysis performed in $CDCl_3$ by using a 600 MHz spectrometer, by comparing the integrals of the signals of epoxide/anhydride sequences with those of epoxide homosequences, as explained previously.

Under the explored reaction conditions, all complexes resulted active. In neat, complex **4** was able to convert 60 equivalents of CHO in less than 1 hour. The polymer obtained was a poly(ester-ether) with 89% of ester functionalities (entry 1, Table 4.1).

Table 4.1. Ring-Opening Co-Polymerization of CHO with SA promoted by complexes **4-7** in the absence of solvent.[a]

Entry	Cat	Conv SA (%)[b]	Ester (%)[b]	TOF (h^{-1})[c]	Mn_{GPC} (kDa)[d]	Đ[d]
1	**4**	44	89	66	2.43	1.18
2	**5a**	69	97	104	1.85	1.19
3	**5b**	94	82	141	1.62	1.23
4	**5c**	60	73	90	1.86	1.23
5	**5d**	56	84	84	1.42	1.17
6	**5e**	54	88	81	1.43	1.15
7	**6**	40	73	60	1.88	1.23
8	**7**	43	42	65	1.45	1.16

[a]Reaction conditions: cat = $2 \cdot 10^{-5}$ mol, [SA]:[CHO]:[Al]:[DMAP] = 125:125:1:1, T = 110 °C, time = 50 min. [b]Determined by ^{1}H NMR spectroscopy. [c]Calculated from SA conversion. [d]Molecular weight data M_{nGPC} and Đ were determined by GPC, in THF *vs* polystyrene standards.

Complexes **5a-e**, bearing a phenyl group on the imine donor, showed higher activities than that of complex **4** (entries 2-5 *vs* entry 1, Table

4.1). However, the presence of electron-withdrawing fluorine atoms on the phenyl ring (complex **5e**) reduced the catalytic activity in comparison to complex **5a** (entry 6 *vs* entry 2, Table 4.1). For complexes **6** and **7**, in which softer neutral donors were introduced, a decrease of both activity and selectivity occurred (entries 7-8, Table 4.1).

Subsequently, the same set of polymerizations were performed in toluene solution. In these conditions, the selectivity will be discussed more finely. The results of polymerizations performed in toluene are reported in Table 4.2.

Table 4.2. Ring-Opening co-Polymerization of CHO with SA promoted by complexes **4-7** in toluene solution.[a]

Entry	Cat	Conv SA (%)[b]	Ester (%)[b]	TOF (h^{-1})[c]	Mn_{GPC} (kDa)[d]	Đ[d]
1	**4**	94	>99	42	1.57	1.17
2	**5a**	91	>99	36	1.91	1.20
3	**5b**	87	94	36	1.81	1.22
4	**5c**	87	95	30	1.82	1.26
5	**5d**	100	>99	41	1.85	1.23
6	**5e**	62	>99	31	3.75	1.12
7	**6**	85	90	27	1.97	1.27
8	**7**	86	97	33	1.62	1.16
9[e]	**5a**	91	>99	105	3.85	1.20
10[e]	**5d**	91	>99	103	4.09	1.24
11	**1b**	80	>99	-	2.31	1.30

[a]Reaction conditions: cat = $2 \cdot 10^{-5}$ mol, [SA]:[CHO]:[Al]:[DMAP] = 125:125:1:1, T = 110 °C, toluene 1 mL, time = 5 h. [b]Determined by ^{1}H NMR spectroscopy. [c]Calculated from SA conversion after 50 min. [c]Molecular weight data M_{nGPC} (kDa) and Đ were determined by GPC, in THF *vs* polystyrene standards. [e][Al] = $1 \cdot 10^{-5}$ mol [SA]:[CHO]:[Al]:[DMAP] = 250:250:1:2.

As expected, the activities lessened because of the reduced concentration of the monomer. The activities were substantially similar in toluene solution (TOF were calculated on SA conversions after 50 min).

Meanwhile, a discrete increment of the selectivity was observed for all catalysts, and complexes **4**, **5d** and **5e** revealed to be able to produce polyesters with rigorously alternate structures.

Complexes with a phenyl ring on the imine donor showed higher activities than that of complex **4** as evidenced by the turnover frequencies (TOF). When electron donating substituents are in the *ortho* positions of the phenyl ring (complexes **5b-c**), lower selectivity was observed in comparison with the less encumbered complexes **4**, **5a** and **5d-e** (entries 3 and 4 *vs* 1, 2, 5, Table 4.2). Otherwise, with electron withdrawing fluorine atoms, we observed a reduced catalytic activity while the selectivity was preserved. As previously observed in bulk, complexes **6** and **7**, bearing softer neutral donors, were the less efficient, in terms of both activity and selectivity (entries 7-8).

An electronic effect clearly appeared: electron-withdrawing substituents attached to the phenoxy donors afforded less active reactive centres, presumably because of enhanced metal electrophilicity (compare entries 2 and 6, Table 4.2). This is in sharp contrast with the effects generally reported in the ROP of cyclic esters promoted by phenoxy-imine aluminum complexes: the presence of electron-withdrawing substituents typically promotes higher polymerization activities than their counterparts bearing unsubstituted phenoxide rings.[102d, 102e] Reasonably, in the

copolymerization of epoxides with anhydrides, the increase of the Lewis acidity of the reactive metal centre reduces the nucleophilicity of the alkoxide intermediate during the propagation steps. This effect was previously observed for salen aluminum complexes.[104]

A steric effect was also evidenced: the presence of substituents on the *ortho* positions of the phenyl group of the imine portion had detrimental consequences on the selectivity. The less encumbered imine complexes **4**, **5a**, **5d** and **5e** provided perfectly alternate polyesters, i.e. no ether linkages were observed. Whereas complexes with alkyl groups on the *ortho* positions of the phenoxide rings or with amine and sulphur as neutral donors, produced polymers with a small percentage of ether linkages.

The most selective catalysts, **5a** and **5d**, were used to optimize the reaction conditions. With a reduced catalyst loading and increased amount of DMAP (2 equivalents), a significant increase of the activity was observed (entries 9 and 10, Table 4.2). In these conditions, the turnover frequencies for complexes **5a** and **5d**, calculated after 50 min, were 105 and 103 h^{-1} respectively.

The GPC analysis of produced polymers displayed monomodal distributions with narrow polydispersities ($Đ \leq 1.3$), indicating a controlled behaviour of the ROCOP reaction. However, the number average molecular weight (M_n) values measured by GPC (without any calibration correction) were always lower than the theoretical expected ones for a living system. This is often explained as a consequence of the presence of protic impurities, such as diacid resulting from hydrolyzed anhydride and/or trace water, that can act as chain transfer agents (CTAs).[105]

The MALDI-ToF-MS spectra of the polymers obtained (entry 10, Table 4.2) showed two distinct distributions, both corresponding to DMAP end-capped chains consisting in sequences of [CHO+SA] repeating units, coherently with perfectly alternating structures with more than 99% of ester linkages (Figure 4.2).[106]

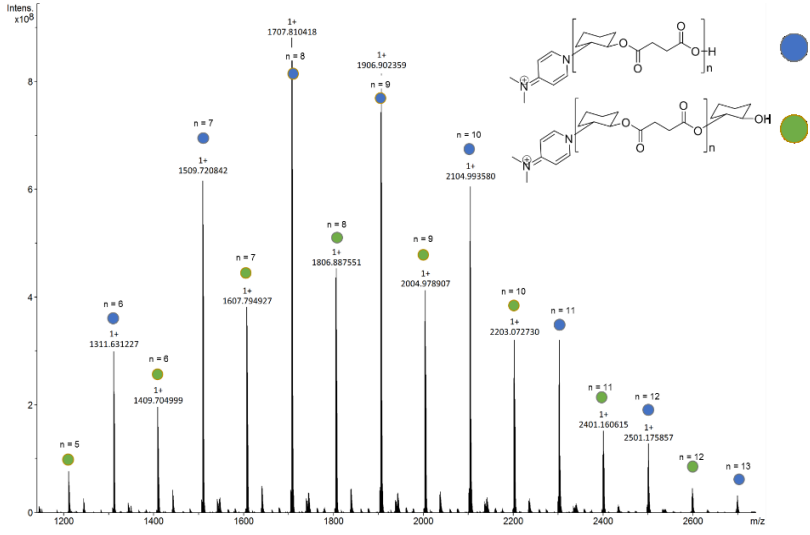

Figure 4.2. MALDI-ToF-MS spectrum of SA-CHO copolymer synthesized in entry 10 of Table 4.2.

4.2.3. COPOLYMERIZATION OF LIMONENE OXIDE WITH PHTHALIC ANHYDRIDE

LO/PA copolymerizations were performed in toluene solution by using the commercially available monomer: the mixture of *cis* and *trans* R-limonene oxide (Table 4.3).

Complex **4** converted 90% of both monomers after 17 hours. The reactivity scale was conserved as for CHO/SA copolymerization, where phenoxy-imine complexes **5a**, **5b** and **5d** showed the highest

activities. All the complexes showed good activities as previously discussed for CHO/SA copolymerization.

The ^{1}H NMR analysis confirmed that perfectly alternate copolymers were obtained, as expected because of the bulky nature of LO. The ^{13}C NMR analysis revealed an atactic polymer, coherently with the achiral structure of the catalysts.

As already observed, the molecular masses of the obtained polymers were lower than the theoretical values for a living catalyst system, although the polydispersities were narrow (Đ ≤ 1.2).

Table 4.3. Ring Opening co-Polymerization of LO with PA promoted by aluminum complexes **4-7**.[a]

Entry	Cat	Time (h)	LO conv. (%)[b]	M_{nGPC} (kDa)[c]	Đ[c]	Tg (°C)
1	**4**	17	91	2.02	1.18	34.2
2	**5a**	8	51	2.23	1.07	27.3
3	**5b**	8	69	2.75	1.10	42.9
4	**5c**	17	76	3.20	1.08	39.5
5	**5d**	8	78	2.34	1.09	32.8
6	**6**	17	80	2.62	1.10	40.7
7	**7**	17	87	2.53	1.10	30.2

[a]Reaction conditions: cat = $2 \cdot 10^{-5}$ mol, [PA]:[LO]:[cat]:[DMAP] = 125:125:1:1, T = 130 °C, toluene 1 mL. [b]Determined by ^{1}H NMR spectroscopy of crude reaction mixture. [c]Molecular weight data M_{nGPC} (kDa) and Đ were determined by GPC, in THF *vs* polystyrene standards.

The MALDI-ToF-MS spectrum of the LO/PA copolymer obtained by complex **4** (entry 1, Table 4.3) showed two distinct series of peaks. Each series exhibited a *m/z* interval of 300 between the consecutive peaks, corresponding to a [LO + PA] repeating unit, in agreement with a perfectly alternating structure (Figure 4.3).

The thermal analysis showed glass transition temperatures lower than 43°C, coherently with the low molecular weights.

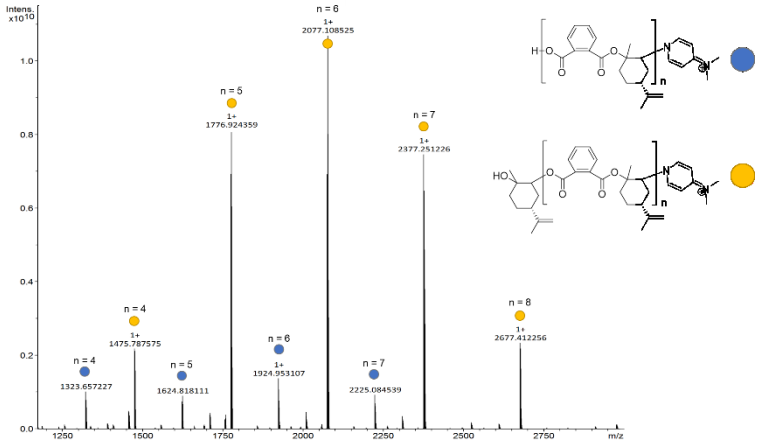

Figure 4.3. MALDI-ToF-MS spectrum of LO/PA copolymer synthesized by **4** (entry 1, Table 4.3).

4.3. MECHANISM STUDY

According to the mechanism generally accepted for the epoxide/anhydride copolymerization, the initiation step is the ring-opening of the epoxide by an initiating group which can be the labile group bound to the metal catalyst or a Lewis base/nucleophilic cocatalyst. The next step is the insertion of the anhydride into the resulting metal alkoxide intermediate to produce a metal carboxylate intermediate. The propagation consists in alternate insertions of the two monomers.

The cocatalyst has a crucial role also during the propagation, since its coordination to the metal centre can modulate the acidity of the reactive centre and increase the lability of the growing chain, the alkoxylate and/or carboxylate intermediates.

Recently, meticulous mechanistic studies concerning the alternating copolymerization of epoxides and cyclic anhydrides using a (salophen)AlCl and iminium salt catalytic system have been described by Tolman and Coates.[107] The authors proposed a mechanism involving two catalytic cycles wherein the alternating copolymerization proceeds via anionic 6-coordinate intermediates formed by combinations of (salph)AlX and [PPN]X (X = alkoxide or carboxylate). Albeit these elegant studies clearly enlighten several mechanistic aspects of the copolymerization process, they are tailored for a specific catalytic system.

To have more insights about the mechanism with the tetra-coordinate aluminum complexes, different experiments were performed and monitored by NMR analysis since a different mechanism could be at stake.

First, complex **4** (0.05 M in 0.5 mL of C_6D_6) was mixed with 1 equivalent of CHO. After 1 hour at room temperature, no reaction was observed and neither upon heating at 70 °C for 5 h. This was coherent with the fact that complex **4** was not able to promote the polymerization of cyclohexene oxide (Chapter 2).

Then, a new experiment was performed by adding one equivalent of DMAP into the solution of **4** and CHO. After 1 hour at room temperature the spectrum of the solution revealed to be a simple overlap of the spectra of the starting compounds. The resonances of DMAP and CHO, both in the ^{1}H and ^{13}C NMR spectra, were coincident with those of the two compounds alone which suggests the absence of interaction with the metal centre (Figure 4.4).

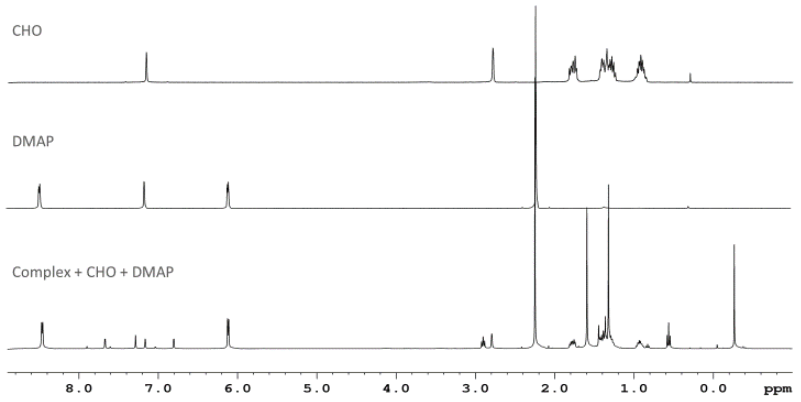

Figure 4.4. ^{1}H NMR spectrum (400 MHz, C_6D_6, 298 K) of complex **4**, CHO and DMAP.

After heating the sample at 70 °C for 5 hours, the formation of a new species (**1a**) was observed (Figure 4.5). In the aromatic region of the ^{1}H NMR spectrum, three peaks, with equal intensity and integrating for one proton, appeared close to the initial three peaks of the starting complex **4**, illustrating the formation of a new phenoxy-imine aluminum complex. In the high-field region of the spectrum, a singlet integrating for 1.5 protons (at - 0.05 ppm) appeared and should be relative to hydrogen atoms of methyl groups bound to the aluminum. Additionally, the presence of a singlet at 0.15 ppm, from the release of methane, showed the partial hydrolysis of the aluminum-methyl bonds by the adventitious traces of water present or occurring into the sample. The formation of this species was followed by NMR. After 12 hours the reaction was complete and the signals of the starting complex vanished almost completely (< 5%).[108]

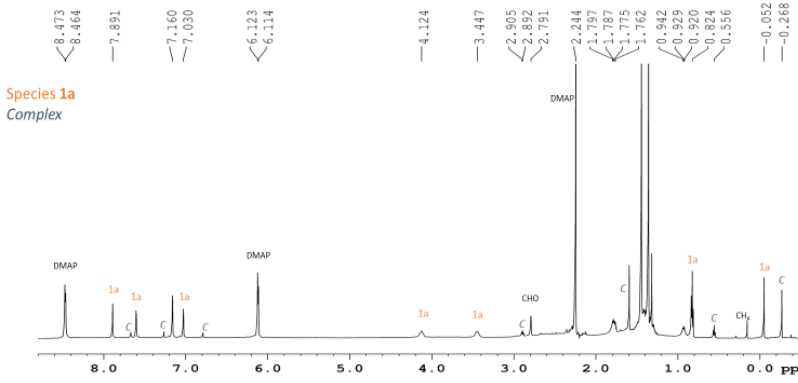

Figure 4.5. ^{1}H NMR spectrum (600 MHz, C_6D_6, 298 K) of species **1a**, in the presence of CHO and DMAP.

After additional 6 hours at 70 °C, the ^{1}H NMR spectrum revealed the formation of another species (**1b)** and, after prolonged reaction time (5 days at 70 °C), the quantitative conversion of species **1a** into species **1b** occurred (Figure 4.6).

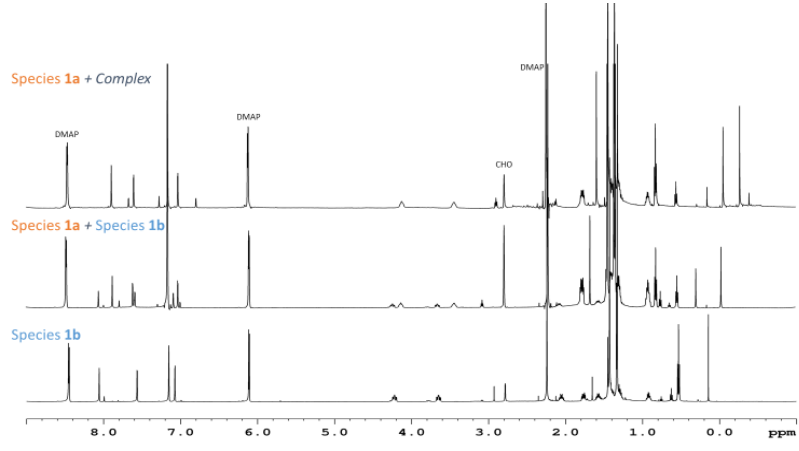

Figure 4.6. ^{1}H NMR spectrum (600 MHz, C_6D_6, 298 K) of the evolution of complex **1**, CHO and DMAP after heating at 70 °C.

Again, the CHO and DMAP appeared as free species, not bound at the metal centre. The ^{1}H NMR spectrum of species **1b** revealed to be

very simple (Figures 4.7) and the full NMR assignment was solved thanks to 1D and 2D homo- and hetero-nuclear NMR experiments (^{1}H-^{1}H COSY, and ^{1}H- ^{13}C HSQC).

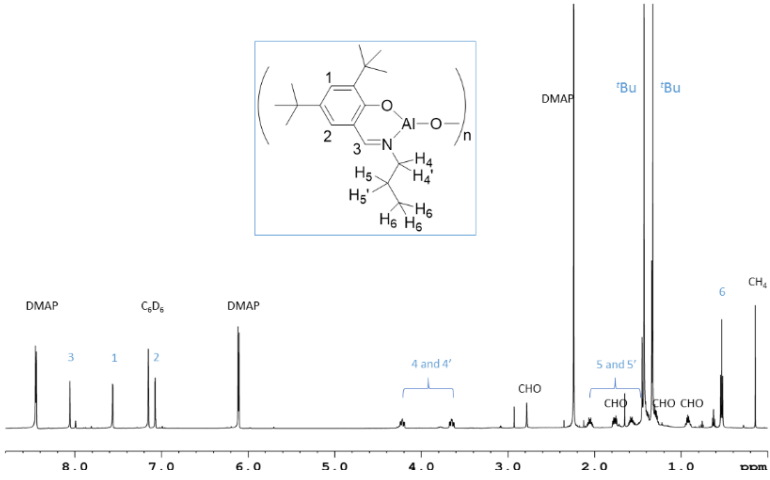

Figure 4.7. ^{1}H NMR (600 MHz, C_6D_6 298 K) of the species **1b.**

In the high-field region of the ^{1}H NMR spectrum, no signals attributable to the methyl groups bound to the aluminum were present, suggesting a complete hydrolysis. Consistently, a signal corresponding to methane was observed at 0.16 ppm. In the aliphatic region, in addition to the signals of free DMAP and CHO, and ^{t}Bu groups, the methyl protons of the n-propyl group (H_6) were easily identified as triplet at δ = 0.53 ppm (Figure 4.7). A set of four multiplets, for the four diasterotopic methylene protons of the n-propyl group were also recognizable ($H_{4,4'}$ and $H_{5,5'}$). The attribution of the n-propyl group was confirmed by 2D COSY and HSQC spectra (Figure 4.8).

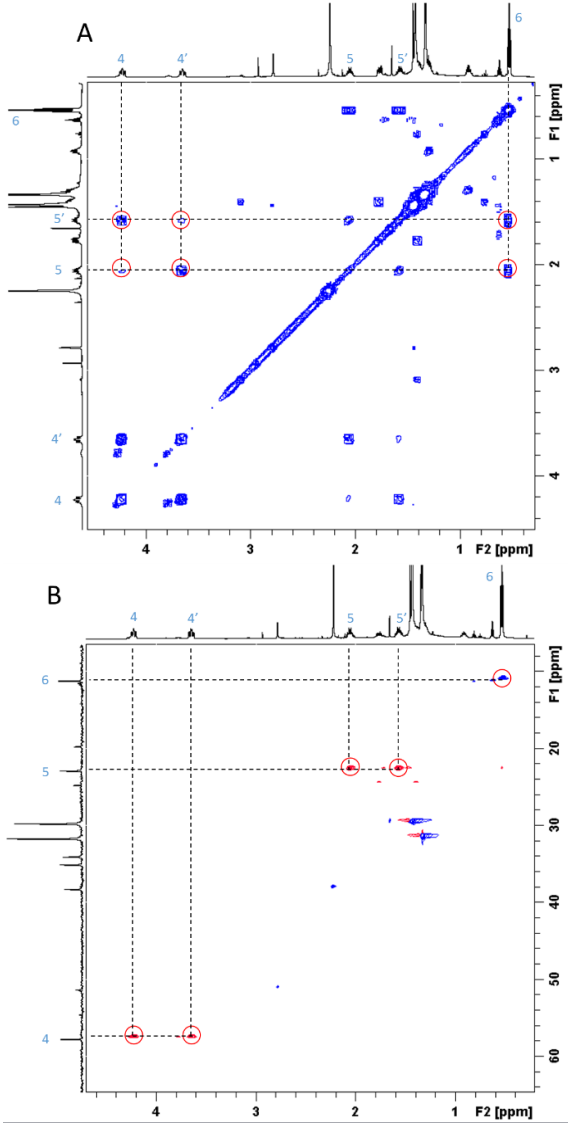

Figure 4.8. A) A section of the ^{1}H COSY NMR spectrum of **1b** (600 MHz, C_6D_6 298 K) and B) a section of HSQC NMR spectrum of **1b** (600 MHz, C_6D_6, 298 K).

In the low field region of the protonic spectrum, two doublets for the aromatic protons and a singlet for the imine proton were observed.

All the spectral data lead to the hypothesis of a rigid multinuclear (dimeric or tetrameric) structure of the type $(L\text{-}AlO)_n$ (n = 2 or 4) in which the aluminum centres are linked via oxygen bridges. Reasonably, this species resulted from the hydrolysis of aluminum-alkyl bonds of the complex **4** by adventitious traces of water. The species demonstrated to be extremely stable and was heated at 80 °C for several days without any decomposition or any reactivity with the CHO present in the solution.

The monomers used, although purified by conventional techniques, might contain traces of water due to their high hydrophilicity, thus it is legitimate to suppose that species **1b** could also be formed in the reaction medium.

Bimetallic aluminum species of the type (salen)Al μ-oxo dimers[109] have been reported by different authors as efficient catalysts for asymmetric Michael additions[110] and for the production of cyclic carbonates from the reaction of CO_2 and epoxides.[111]

Species **1b** was tested in the copolymerization of CHO/SA. One equivalent of succinic anhydride was added into the J-Young containing the solution of species **1b**, the unreacted CHO and DMAP. After 1 hour at 80 °C, species **1b** was still observed, no evolution was observed also in the presence of the anhydride. Reasonably, the concentration of the monomers is a crucial parameter for the formation of the active species because of the high stability of species **1b**.

Coherently, after the addition of five equivalents of SA and five of CHO, ^1H NMR analysis demonstrated a quick and distinctive evolution of the species **1b** upon heating at 70 °C, consisting of the

disappearance of the rigid multinuclear structure, and the progressive consumption of both monomers.

This new species was maintained during all the polymerization process and showed a structure coherent with a phenoxy-imine aluminum complex (Figure 4.9). Interestingly, the aromatic resonances attributable to the free DMAP disappeared during the copolymerization reaction, a clear evidence of the initiation step promoted by the co-catalyst. A brown precipitate is observed in C_6D_6, attributable to the resulting zwitterionic polymer chain initiated by DMAP as confirmed by ^1H NMR in CD_2Cl_2 of the precipitate.

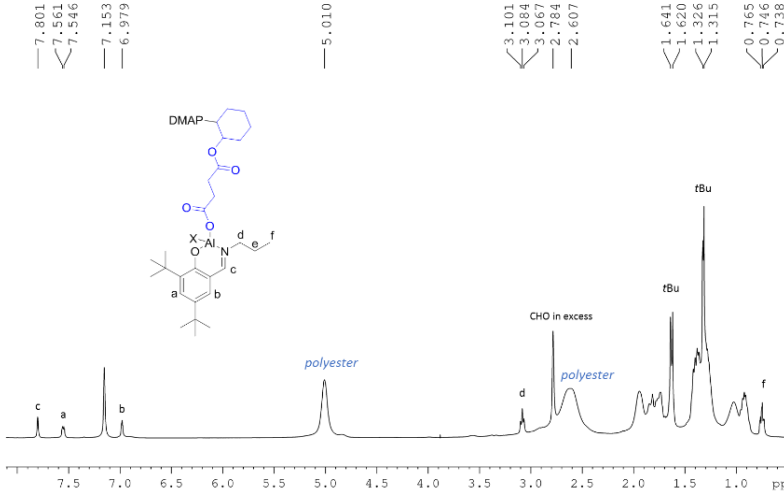

Figure 4.9. ^1H NMR spectrum (400 MHz, C_6D_6, 298 K) from [**1b**]:[DMAP]:[CHO]:[SA] = 1:1:6:6.

Kinetics studies of this copolymerization (at 70 °C in C_6D_6) showed an induction period (about 50 minutes), probably a consequence of the initial inertia of the multinuclear species **1b** that slowly converted

to the propagating species (Figure 4.10). After this time, the polymerization rate was first-order dependent on CHO concentration (with a $k_{app} = 1.66x10^{-3}$ min^{-1} and $R^2 = 0.990$) as previously observed.

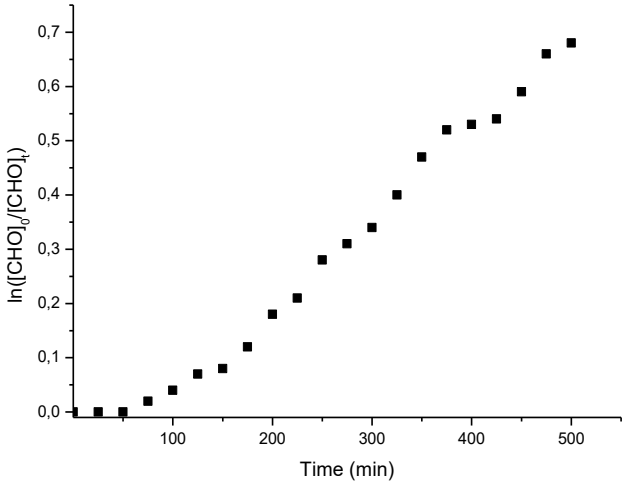

Figure 4.10. Plot of $ln([CHO]_0/[CHO]_t)$ *vs* time.

Kinetics studies were repeated under reaction conditions analogous to those described in Table 4.2 for the copolymerization reaction: at 100°C and in deuterated toluene solution. This time no induction period was detected (Figure 4.11).

The inertia of the species **1b** can be easily overcome adjusting the reaction conditions chosen for the polymerization reactions, i.e. in the presence of high concentration of the monomers and at high temperature.

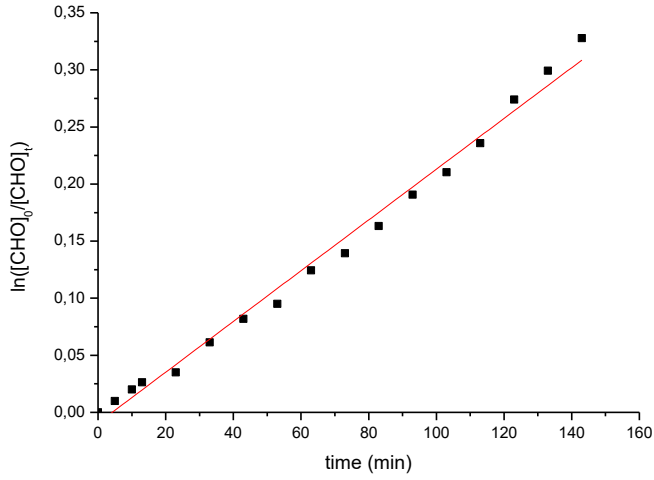

Figure 4.11. Plot of $\ln([CHO]_0/[CHO]_t)$ *vs* time describes a reaction order of unity with respect to monomer concentration, $k_{app} = 2.22 \times 10^{-3}$ min^{-1} ($R^2 = 0.990$).

The copolymers obtained by these experiments were characterized by MALDI-ToF analysis (Figure 4.12). They showed DMAP end-capped chains with a rigorously alternated structure, as previously described for the samples obtained by the polymerization reactions reported in Table 4.2.

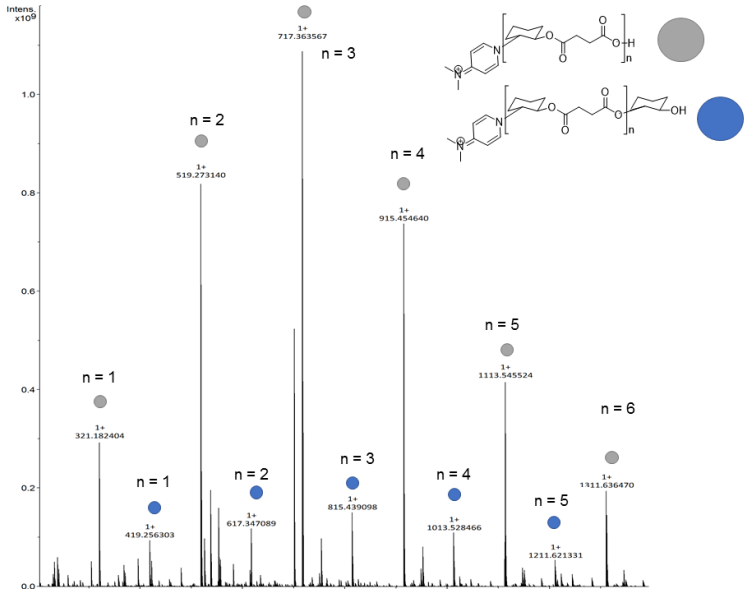

Figure 4.12. MALDI-ToF-MS spectrum of CHO/SA copolymer synthesized during kinetic experiment.

Under the reaction conditions used for the ROCOP, the species derived from the hydrolysis, must evolve towards the formation of a monometallic propagating species bearing a growing chain produced after the nucleophilic attack of DMAP on an epoxide unit in the initiation step.

To confirm the structure of species **1b**, and have more insights about the hydrolysis times, **1b** was directly synthesized by adding the opportune amount of deuterated water to a benzene solution of complex **4.** Initially, by adding sub-stoichiometric equivalents of D_2O to a solution of complex **4** in deuterated benzene, species **1a** was formed. The structure of the species **1a** was not completely elucidated. The high symmetry of this species and the anomalous ratio between the signals of protons of the ligand moiety and the

signals of the methyl groups bound to aluminum (1:1.5) suggested the formation of a multinuclear species, in agreement with the low steric encumbrance offered by the ancillary ligand and the propensity of aluminum to maximize its coordination number. Linear and/or cyclic oligomeric species, consisting of alternating aluminum and oxygen atoms, could be formed, as previously observed for products obtained by an incomplete hydrolysis of aluminum trialkyl species.[112]

After the addition of one equivalent of D_2O, within only 10 min at 70 °C, **1a** was quantitatively converted into the species **1b**. The ^1H NMR spectrum (Figure 4.13) was identical to that obtained by the previously described experiment and showed the presence of a triplet for the deuterated methane (CH_3D). This confirmed the nature of the species **1b** and that DMAP and/or CHO did not have an active role in the production of the latter. Moreover, this experiment suggested that the hydrolysis of the aluminum-alkyl bonds is fast.

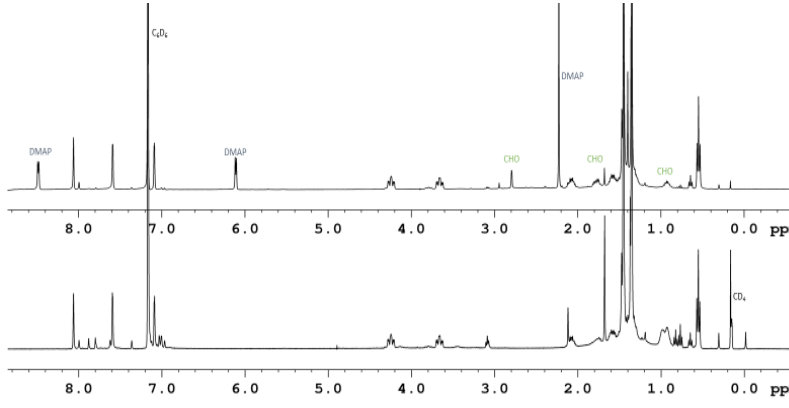

Figure 4.13. ^1H NMR spectrum (600 MHz, C_6D_6, 298 K) of species **1b.** Up: From heating in the presence of CHO and DMAP. Down: From hydrolysis with D_2O.

The structure proposed for **1b** was also addressed through pulsed gradient spin-echo (PGSE) NMR spectroscopy. The PGSE method assesses translational motion of the analyte in solution through determination of the diffusion coefficient, inversely proportionated to its molecular mass. It is used successfully for characterizing supramolecular structures in solution. The diffusion coefficient of **1b** was determined by the 2D version of the PGSE experiment (DOSY, Diffusion Ordered SpectroscopY) in C_6D_6 solution, using the ligand (0.3 equivalents) as internal standard. The diffusion coefficients of both species have been evaluated. The diffusion coefficient of the ligand (D_L = 2.13e-11 m^2/s (error = 4e-13)) was about the double of that evaluated for **1b** (D_{1b} = 1.08e-11 m^2/s (error = 7e-14)). Since the other parameters are identical, the size of the corresponding species can be compared based on their diffusion coefficients (D) and the molecular masses in solution (m) were simply estimated using Graham's law of diffusion: $D = K(T/m)^{1/2}$, where the constant K depends on geometric factors, including the area over which the diffusion is occurring. By assuming a constant temperature and that K is the same for both species in solution, the molecular mass of **1b** (m_{1b}) was easily obtained by the following equation: $D_L/D_{1b} = (m_{1b}/m_L)^{1/2}$. The great agreement between the molecular mass $m_{\mathbf{1b}}$ and the value calculated for the tetramer $(L\text{-}AlO)_4$ supported the hypothesis that **1b** could be a discrete tetrameric species.

The ESI analysis of **1b** did not show a peak corresponding to the molecular ion. However, several fragments with a *m/z* ratio higher than that corresponding to a dimer of the type $(L\text{-}AlO)_2$ were

detected. This is in line with the formation of a tetramer, as suggested by the DOSY experiment.

To confirm the role of this species in the polymerization process, species **1b** obtained from this hydrolysis experiment was tested as catalyst in the ROCOP of CHO/SA under the same reaction conditions described for the experiments reported in Table 4.2 showing a similar behaviour (compare entries 11 and 1, Table 4.2).

All these data seem to suggest the following picture: traces of water in the polymerization medium can hydrolyse the Al-Me bonds and form a multi-nuclear species. This, under catalytic conditions, evolves into a propagating species of lower nuclearity with a structure coherent with a phenoxy-imine aluminum complex.

4.4. Design of Bifunctional Catalysts

4.4.1. Introduction

Our tetra-coordinate monometallic aluminum complexes supported by bidentate monoanionic phenoxy-imine ligands are able to promote the ring-opening co-polymerization of epoxide with anhydride in a perfectly alternate manner thanks to the addition of a nucleophilic co-catalyst, DMAP (dimethylaminopyridine).

The examples of catalysts that are selective without any addition of cocatalyst are rare in the ROCOP between anhydride and epoxide. The first one was the BDI-Zn catalyst by Coates.[24] Subsequently, Williams described a series of homo- and heterobimetallic complexes of magnesium and zinc showing high activity and selectivity in the ROCOP of cyclohexene oxide and phthalic anhydride without co-catalyst.[32a] In all cases, they are bimetallic

species or it is supposed that the propagating species is bimetallic. Bifunctional catalysts contain both a Lewis acid (the metal centre) and a nucleophilic species.

They have been diffusely reported for the reaction between epoxide and carbon dioxide whereas only few examples have been described in the ROCOP between epoxide and anhydride.

Nozaki pioneered this new generation of catalysts in the CO_2/epoxide reaction in 2006 using a cobalt(III) complex with a piperidinium arm to obtain poly(propylene carbonate) with a good activity and selectivity.[113] In 2015, North and Belokon developed bifunctional aluminum(salen) catalysts with quaternary ammonium groups attached to the aromatic rings that showed good activity in cyclic carbonate formation.[114] Lee and co-workers reported a bifunctional (salen)Co(III) complex tethering four quaternary ammonium salts which is highly active in CO_2/epoxide copolymerizations.[115]

In the ROCOP, the same author recently reported cobalt-salen complexes with attached quaternary ammonium groups[116] that revealed to be selective for the copolymerization of propylene oxide and phthalic anhydride.

Kleij and co-workers recently described aminotriphenolate cobalt complexes containing two cis ligating DMAP.[97a] The reversible coordination of one of these ligands provided thus a coordinative unsaturated Co(III) aminotriphenolate complex and one free DMAP, as a sort of “intrinsic bicomponent system“ that showed a moderate activity for the copolymerization of cyclohexene oxide and phthalic anhydride.

On the bases of these results, we selected Schiff base ligands bearing an additional neutral donor pendant arm which it was envisaged might simulate the role of the cocatalyst.

4.4.2. SYNTHESIS OF COMPLEXES BEARING AN ADDITIONAL DONOR

A series of potentially tridentate salicylaldimine ligands each bearing a pendant N or P donor arm attached to the imine nitrogen were prepared (Scheme 4.2).

The first objective was to investigate the effect of the presence of a pyridine-type pendant arm on a phenoxy-imine [ON]-ligand platform, in terms of denticity of the chelating ligand. Variable substituents, on the *ortho*-and/or *para*-positions of the phenoxide ring, were introduced to modulate the steric and electronic properties of the ligand (complexes **8a-d**). Subsequently, the nature of the additional donor was modified introducing an amine or a phosphine pendant arm (complexes **9** and **10**).

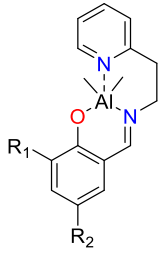

(8a) $R_1 = R_2 = {}^tBu$
(8b) $R_1 = H$, $R_2 = OMe$
(8c) $R_1 = R_2 = F$
(8d) $R_1 = R_2 = NO_2$

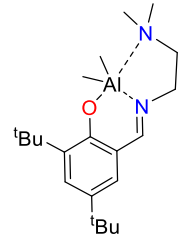

(9)

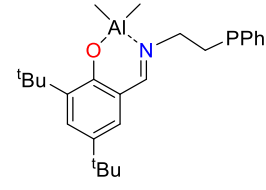

(10)

Scheme 4.2. Phenoxy-imine bifunctional aluminum complexes **8-10**.

All the pro-ligands were obtained, in almost quantitative yields, by condensation between the corresponding benzaldehyde and amine reagents, at reflux in ethanol for several hours, as previously reported in literature.[117] The aluminum dialkyl complexes were synthesized by reacting the respective pro-ligand with one equivalent of the aluminum precursor $AlMe_3$.[117a] After mixing of the reagents for two hours at room temperature, the resonances of the ligands appeared shifted respect to those of the free species and the signal relative to the -OH proton disappeared. Diagnostic resonances in the protonic spectra are sharp singlets in the high-field region assigned to the equivalent protons of the two Al–Me groups and integrating for 6 protons (Figure 4.14).

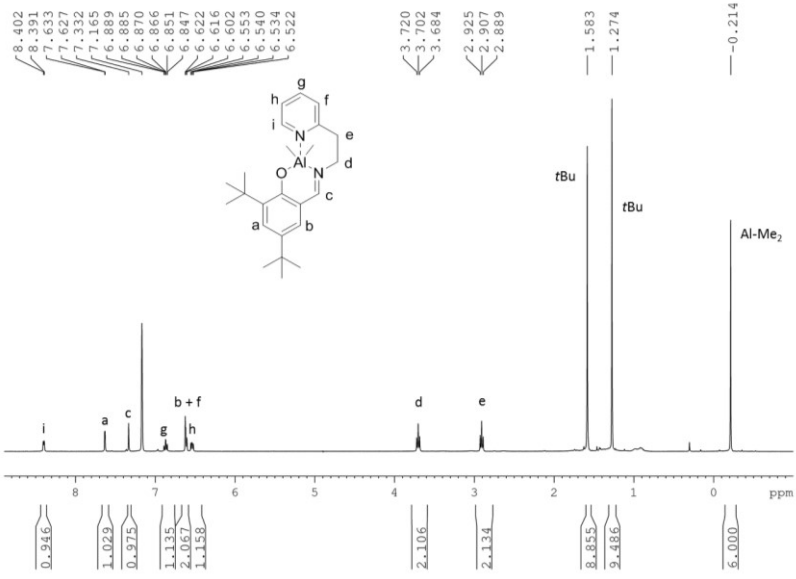

Figure 4.14. ^1H NMR spectrum (400 MHz, C_6D_6) of complex **8a**.

The obtained complexes were fully characterized by multinuclear NMR spectroscopy, including 2D experiments ^{1}H-^{1}H COSY and NOESY.

Complex **9** has been already reported in literature.[117a] The crystal structure of complex **9** showed that the ligand pendant arm donor is bound to the aluminum centre in the solid state. To get information also on the structure in solution, we performed NOESY experiments at room temperature in C_6D_6 solution, which confirmed the possible coordination of the additional amine to the Al centre since we observed the interaction between the methyls on the aluminum centre and the methyls on the amine additional donor (Figure 4.15).

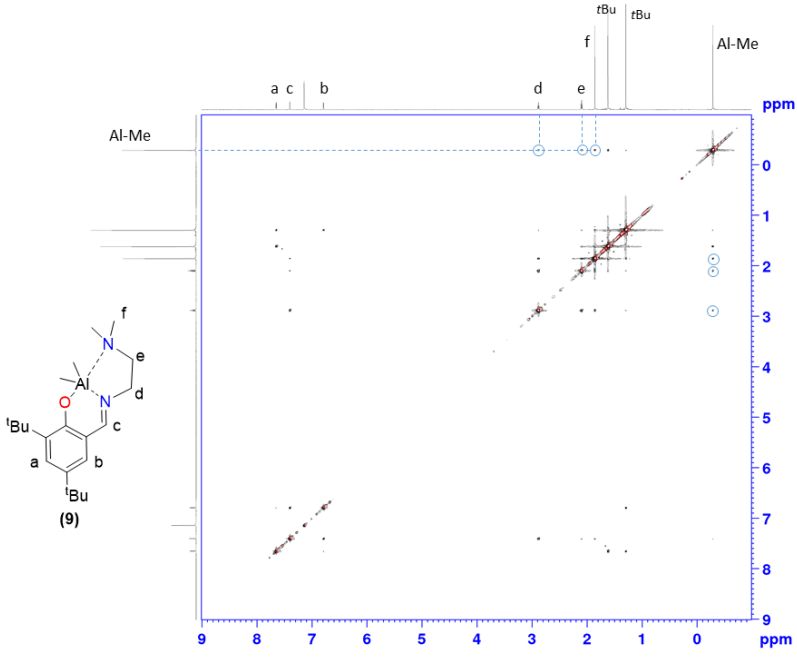

Figure 4.15. NOESY spectrum (400 MHz, C_6D_6) of complex **8a**.

The same interaction was preserved also at higher temperature (50 °C) and in the presence of one equivalent of cyclohexene oxide (CHO) and one equivalent of succinic anhydride (SA) (Figure 4.16).

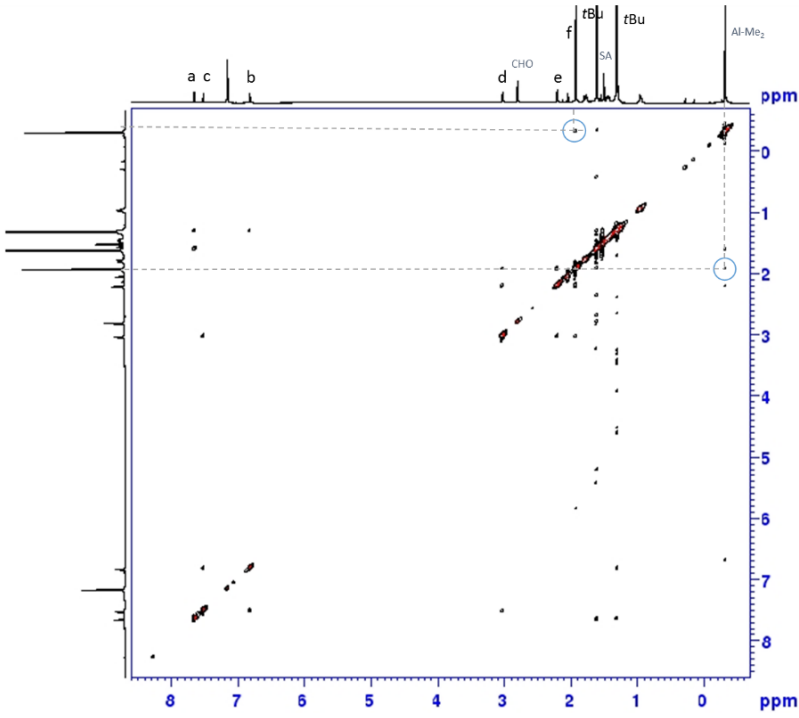

Figure 4.16. NOESY spectrum (600 MHz, C_6D_6, 323K) of complex **9** in the presence of CHO and SA.

Complex **8a** was not reported in the literature, but the solid-state structure of an analogous complex bearing a methylene pyridine-type pendant arm is described as weakly coordinated.[117a] The structure of complex **8a** in solution was studied by ^1H-^1H NOESY at room temperature in C_6D_6. Under these conditions, the ligand seems to be able to act as a tridentate ligand, binding to the aluminum via the

oxygen, the imino and the pyridine nitrogen atom. The same is observed for complex **8b**.

In complexes **8c** and **8d,** a strong interaction is observed with the pyridine pendant arm by NOESY, reasonably because of the more Lewis acidic metal centre.

For complex **10**, an analogous complex bearing a methylene pendant arm with the softer phosphine donor is reported non bounding in the solid state.[117a] The ^{31}P NMR spectra of complex **10** showed a unique singlet at -20 ppm. The NOESY experiment, performed at room temperature, revealed only a very weak interaction with the metal centre that is completely lost at temperature slightly higher (50 °C).

4.4.3. STUDY OF THE REACTIVITY

4.4.3.1. EFFECT OF THE SUBSTITUENTS ON THE PHENOXIDE RING

Complexes **8a-d** were tested as catalysts in the copolymerization of cyclohexene oxide with succinic anhydride to investigate their catalytic activity and selectivity towards polyester formation. All obtained polymers have been characterized by ^{1}H NMR (600 MHz) spectroscopy, GPC and MALDI-ToF-MS analyses.

The polymerizations were performed at 110 °C, with an [epoxide]:[anhydride]:[catalyst] ratio of 250:250:1 (Table 4.4).

Initially, the catalytic behaviour of complex **8a** was compared with that of the previously reported bicomponent system formed by complex **4** and one equivalent of a nucleophilic co-catalyst (dimethylaminopyridine, DMAP). In the absence of solvent, the two systems, **8a** and **4**/DMAP, showed comparable activity. The turnover

frequencies (TOF), calculated on SA conversion, were 67 h^{-1} and 80 h^{-1}, respectively. A lower selectivity was observed for the complex **8a** producing a poly(ester-co-ether) with 53% of ester functionalities (entries 1 and 2 of Table 4.4).

Subsequently, the polymerizations were conducted in toluene solution (entries 3-5 of Table 4.4). Under these conditions, the achieved activities were significantly lower, especially in the case of complex **8a** (TOF 13 h^{-1}, entry 3 of Table 4.4). Importantly, complex **8a** resulted able to produce a rigorously alternate polyester in the absence of a hexogen cocatalyst, demonstrating that it can act as an efficient bifunctional catalyst.

Table 4.4. Ring Opening co-Polymerization of CHO with SA promoted by complexes **8a-d** and **4**.[a]

Entry	Cat	^{i}PrOH (equiv)	t (h)	Conv. SA (%)[c]	Ester (%)[c]	TOF (h^{-1})[d]	M_{nGPC} (kDa)[e]	Đ[e]
1[b]	**8a**	-	2	54	53	68	2.7	1.44
2[b]	**4**/DMAP	-	1	32	88	80	1.3	1.37
3	**8a**	-	4	21	>99	13	nd	nd
4	**8a**	-	24	100	>99	-	3.2	1.44
5	**4**/DMAP	-	1	25	>99	63	1.2	1.47
6	**8a**/DMAP	-	1	24	>99	60	2.3	1.35
7	**8a**	2	5	40	>99	20	2.3	1.47
8	**8b**	2	5	50	>99	25	2.6	1.30
9	**8c**	2	5	57	80	29	1.2	1.50
10	**8d**	2	4	47	47	29	1.3	1.31

[a]Reaction conditions: [Al] = 10^{-5} mol, [SA]:[CHO]:[Al] = 250:250:1, T = 110 °C, toluene 1 mL. [b]No solvent [c]Determined by ^{1}H NMR spectroscopy. [d]Calculated from SA conversion. [e]Molecular weight data M_{nGPC} and Đ were determined by GPC, in THF *vs* polystyrene standards.

The lower activity observed for complex **8a** could be a consequence of the scarce nucleophilicity of the methyl groups on the aluminum in the initiation steps. In the presence of one equivalent of DMAP, the activity of complex **8a** was drastically enhanced (entry 6), being thus quite similar to the catalytic system **4**/DMAP (entry 5).

The MALDI–ToF MS spectra of the polymer obtained by **8a** (entry 4, Table 4.4) confirmed this hypothesis (Figure 4.17). It showed the presence of two major distinct distributions, both corresponding to linear polymer chains consisting in sequences of [CHO+SA] repeating units, coherently with a perfectly alternating structure. Both series describe α,ω-hydroxy-terminated chains, probably produced by nucleophilic attack of water present in traces, in the polymerization medium. No methyl groups are detected as chain end groups. This observation suggests that the metal acts as Lewis acid centre that coordinates the monomer (CHO) and activates it for the nucleophilic attack by the water.

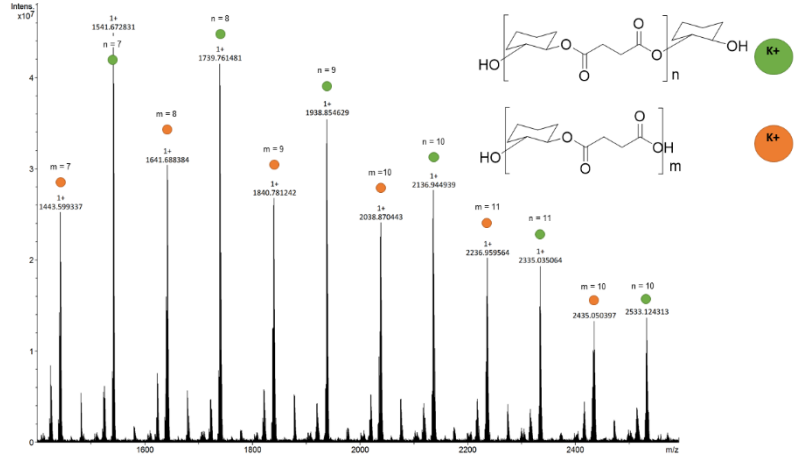

Figure 4.17. MALDI-ToF-MS spectrum of SA-CHO copolymer synthesized in entry 3 of Table 4.4.

To favour the initiation step, two equivalents of isopropanol, a hexogen nucleophile species, was added.

As expected, entry 7 showed a slightly increased activity (compare entry 7 *vs* entry 3. TOFs: 20 h^{-1} *vs.* 13 h^{-1}), while the selectivity of the catalytic system was preserved.

The MALDI–ToF MS spectrum of the polymer obtained by **8a**/ ^{i}PrOH (entry 7, Table 4.4) revealed that the polymer chains were end-capped by one isopropyl –$OCH(CH_3)_2$ and a hydroxyl -OH group (Figure 4.18). This suggested that the initiation occurred by ring opening of the monomer by isopropanol and the termination by hydrolysis of the growing chain.

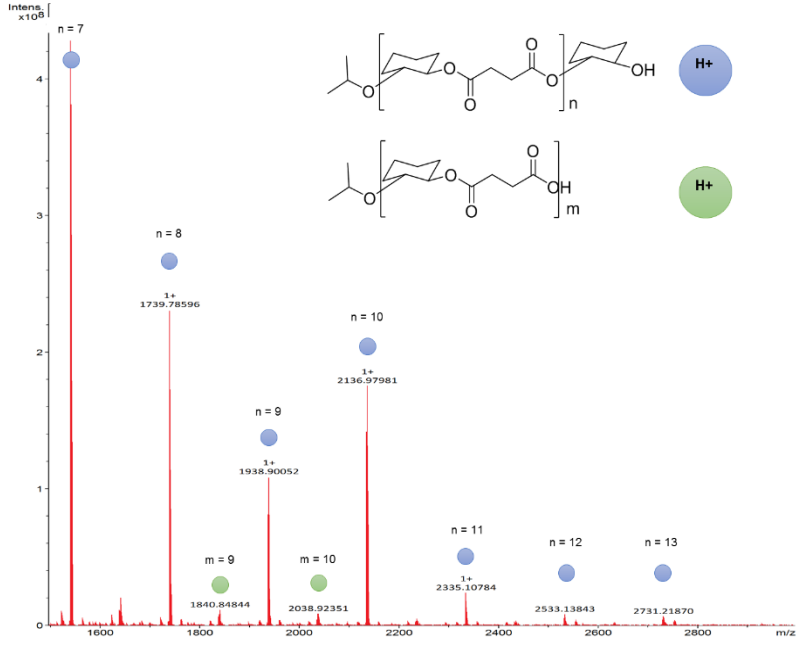

Figure 4.18. MALDI-ToF-MS spectrum of polyester CHO/SA obtained by **1a** in the presence of ^{i}PrOH.

Two main mechanisms for the initiation can be proposed.

In the first case, the initiation reaction involves coordination of the monomer at the Lewis acidic metal centre of an alkoxide derivate produced by alcoholysis of complex **8a.** The epoxide is activated for the nucleophilic attack by the isopropoxide ligand bound to the metal. This leads to ring-opening of the epoxide and generation of a new metal–alkoxide bond (Scheme 4.3, A).

Alternatively, it could act simply as a nucleophilic species in substitution of the water, as previously discussed: the epoxide is activated *via* the coordination to the metal centre of the complex, and the initiation reaction occurs by nucleophilic attack by the free alcohol to form a ring-opened adduct (Scheme 4.3, B).

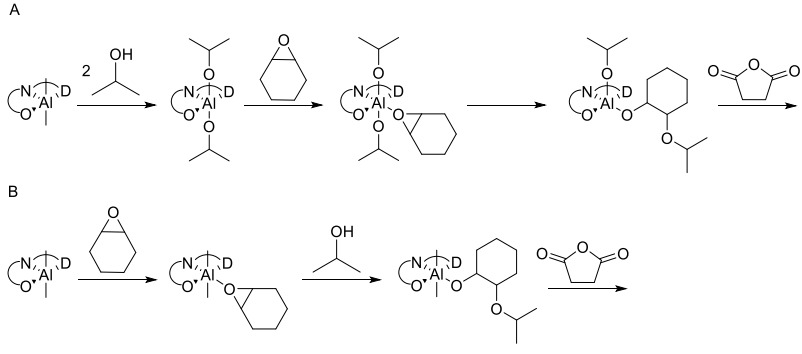

Scheme 4.3. Proposed initiation routes for **8a**/^{i}PrOH. A) First, alcoholysis and then activation and ring-opening of the epoxide. B) First, activation of the epoxide and then external attack by the alcohol. D is an additional donor thanks to a pendant arm.

To have more clear ideas about the role of the alcohol in the initiation steps, alcoholysis experiments of complex **8a** were performed and monitored by ^{1}H NMR.

Initially, the hydrolysis of complex **8a** (20 μmol) with two equivalents of ^{i}PrOH in deuterated toluene at 100 °C was performed. The NMR analysis demonstrated that the almost complete alcoholysis of methyl groups of complex **8a** occurred within 24 hours so the formation of the related isopropoxide derivative is too slow in comparison to the polymerization times. The ^{1}H NMR spectra revealed multiple products and no one species could be isolated and fully characterized, even increasing the amount of alcohol and the reaction time up to more than one day. In particular, methyl groups bound to the aluminum centre were still observed after 4h at 100 °C. Consequently, the LAl-($O^{i}Pr$)$_2$ complex cannot be formed in the reaction medium before the beginning of the polymerization since at 4h a usual 20% of conversion of both monomers is observed.

On the bases of these results, the mechanism B involving the external attack by the alcohol is more plausible (Scheme 4.3, B).

Thus, considering the beneficial presence of the alcohol as initiator, the latter reaction conditions were used to study the influence of the structure of ancillary ligand on the activity and selectivity of catalyst.

To study the influence of the Lewis acidity of the reactive centre on the activity of these complexes, electron-donating (complex **8b**) or electron-withdrawing (complexes **8c**-**d**) substituents were introduced in the *ortho* and/or *para* positions of the aromatic ring.

While the activity was substantially the same, a significant difference was observed in terms of selectivity.

Introducing a methoxy substituent, a strong electron-donating group, on the *para* position of the aryl ring, a perfect selectivity was obtained (entry 8, Table 4.4).

With electron-withdrawing substituents a significant loss of selectivity was observed, the percentage of ester linkages decreased up to 47% of in the case of complex **8d** with nitro substituents (entries 9 and 10, Table 4.4). The stronger Lewis acidity of the complexes is detrimental to the selectivity, probably because the pendant arm is thus strongly coordinated and might compete with the incoming monomer.

All the obtained polymers displayed monomodal distributions of the molecular weights with moderately narrow polydispersity indexes (Đ < 1.5).

4.4.3.2. Effect of the structure of the additional pendant arm

To further extend the potential of this bifunctional system, the pendant arm was modified, with the phenoxide ring having the same substituents. The nature of the pendant arm was changed from a pyridine to an amine or a phosphine pendant arm (complexes **9** and **10**).

Table 4.5. Ring Opening co-Polymerization of CHO with SA promoted by complexes **8-10**.[a]

Entry	Cat	t (h)	Conv SA[b] (%)	Ester[b] (%)	M_{nGPC}[c] (kDa)	Đ[c]
1	**8a**	5	40	>99	2.3	1.47
2	**9**	4	51	92	3.2	1.73
3	**10**	4	51	94	3.4	1.37

[a]Reaction conditions: [Al] = 10^{-5} mol, [SA]:[CHO]:[Al]:[^{i}PrOH] = 250:250:1:2, T = 110 °C, toluene 1 mL. [b]Determined by ^{1}H NMR spectroscopy. [c]Molecular weight data M_{nGPC} and Đ were determined by GPC, in THF *vs* polystyrene standards.

As already discussed for the effect of the substituents on the phenoxide ring, the activity was substantially independent of the nature of the neutral donor (compare SA conversions of entries of Table 4.5) while a slight decrease was observed in terms of selectivity both with the amine and phosphine neutral donors.

CONCLUSIONS OF CHAPTER 4

A study of the effects of the structure of the phenoxy-imine dimethyl-aluminum complexes on the activity and the selectivity has revealed several important aspects: high activities are favoured by electron-donating substituents attached to the phenoxy-donor although when large substituents are in *ortho* positions the selectivity is compromised. With electron withdrawing substituents such as fluorine atoms a perfect selectivity is observed but the activity is significantly reduced.

Mechanistic studies performed on this class of complexes suggested the initial formation of multinuclear species produced by hydrolysis of the methyl-aluminum bonds by adventitious traces of water present in the monomers.

In the presence of more than one equivalent of both monomers, or under catalytic reaction conditions, these species converted in the propagating one.

A clear role of DMAP in the initiation step emerged by the NMR studies as well as by the MALDI-ToF-MS analysis of the obtained polymers showing that the first event is the opening of an epoxide unit by the nucleophilic attack of DMAP.

Afterwards, complexes with an additional pendant arm to incorporate the co-catalyst structure directly in the ligand were tested in the ROCOP of epoxide and cyclic anhydride.

From the data collected emerged that complexes **8a** and **8b** were able to promote a perfect selectivity in the ROCOP of CHO/SA with no addition of an external co-catalyst, thus revealing successful

bifunctional catalysts. They both have a pyridine pendant arm with electron donating substituents on the phenoxide ring.

The approach described herein appears promising and the catalytic design can be easily modified, optimizing further the structure of the ligand or changing the nature of the metal centre.

CONCLUDING REMARKS.

The objective of the research described in this PhD thesis was the exploration of the possibility of synergistic interaction within dinuclear salen aluminum catalysts in the ring-opening polymerization of cyclic esters and in the ring-opening copolymerization of epoxides with cyclic anhydrides.

We reported the synthesis and characterization of bimetallic salen aluminum complexes **1**-**3**, in which the ligands have been designed to feature two coordinative pockets at varying distances from one another thanks to the variable alkyl backbone between the imine functionalities. In the same scope, the related hemi-salen monometallic complex **4** has been synthesized.

All complexes were tested in the ROP of several heterocyclic substrates. In the ROP of lactide and ε-caprolactone, the bimetallic complex **1** in which the two reactive centres are in proximal positions demonstrated the best activity (Scheme 1). Strikingly, in the ROP of *rac*-β-butyrolactone and cyclohexene oxide, complex **1** was the only one active.

Additionally, in the ROP of *rac*-lactide, complex **1** resulted the only one able to produce isotactic enriched PLA.

All these data suggest the existence of strong cooperative phenomena between the two vicinal metal centres in complex **1**, that are operative during the ROP of cyclic esters and epoxides. A bimetallic mechanism for the ring-opening polymerization was thus proposed (Chapter 2).

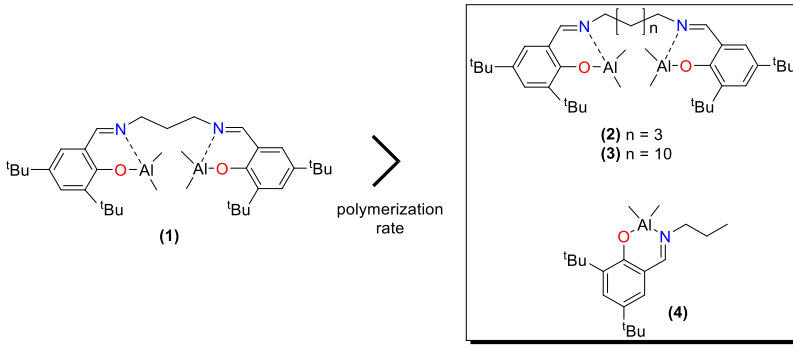

Scheme 1. Reactivities of the complexes in the ROP of *rac*-lactide.

Afterwards, the same complexes, in combination with a nucleophilic co-catalyst, were found to be highly active in the ROCOP of epoxides with cyclic anhydrides.
Interestingly, complex **1** revealed to be able to switch between the distinct polymerization cycles producing block copolyesters from ROCOP of cyclohexene oxide and succinic anhydride, followed by ROP of the cyclic ester.

From the copolymerization studies emerged that the monometallic complex **4** and the bimetallic complex **1** have the same catalytic behaviour, in terms of both activity and selectivity. This suggested a monometallic pathway with our class of complexes in the ROCOP.
The higher activity of our complexes in comparison to the related penta-coordinate aluminum complexes reported in the literature,[29] suggests that a lower coordination of the aluminum centre could help to promote the copolymerization rate (Chapter 3).

A study of the structure-performance relationship, both in terms of activity and selectivity, of tetra-coordinate phenoxy-based

monometallic catalysts, in combination with DMAP as cocatalyst, in the ROCOP of epoxides with cyclic anhydrides showed that phenoxy-imine complexes resulted the most efficient, with higher activities favoured by electron-donating substituents attached to the phenoxy-donor although when large substituents are in *ortho* positions the selectivity is compromised. This work put in evidence that phenoxy-imine aluminum complexes represent an efficient and readily available class of catalysts for the ROCOP.

Finally, bifunctional catalysts in which, in addition to the Lewis acid metal centre a nucleophilic portion was present, were synthetized. A pendant arm bearing an additional neutral donor was introduced with the aim to incorporate the co-catalyst directly in the structure of the ligand. Complexes bearing a pyridine pendant arm and with electron-donating substituents on the phenoxide ring (Scheme 2) performed best, giving a perfect selectivity without addition of an external cocatalyst. We were thus able to replace a bicomponent system catalyst/cocatalyst to a successful bifunctional catalyst (Chapter 4).

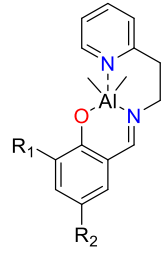

(8a) $R_1 = R_2 = {}^tBu$
(8b) $R_1 = H$, $R_2 = OMe$

Scheme 2. Bifunctional complexes bearing a pyridine-type pendant arm.

Visiting Period at IRCP (Institut de Recherche de Chimie Paris, France) under the supervision of Prof. C. M. Thomas.

CHAPTER 5. SYNTHESIS AND CHARACTERIZATION OF IRON, COBALT AND ZINC CATALYSTS FOR THE STEREOSELECTIVE RING OPENING POLYMERIZATION OF *RAC*-LACTIDE.

During my PhD, I carried out a visiting research period at the Organometallic Chemistry and Polymerization Catalysis group at IRCP (Institut de Recherche de Chimie Paris, France).

5.1. INTRODUCTION

PLA is a promising polymer, sparkling the interest of researchers from both academia and industry. Several synthetic approaches can be used for the production of PLA, but the most interesting one is the ring-opening polymerization (ROP) of lactide *via* a coordination-insertion mechanism.[1b, 2a]

Lactide exists in different enantiomeric forms: the pure enantiomers, (*S,S*)-Lactide (L-Lactide) and (*R,R*)-Lactide (D-Lactide), the racemic mixture, *rac*-Lactide, (D-Lactide and L-Lactide 50:50 mixture) and *meso*-Lactide (*R,S*)-Lactide.

When pure D- or L-lactide is polymerized, optically pure poly(D-lactide) and poly(L-lactide) respectively are obtained as isotactic polymers.

The obtained PLA from *rac*-lactide can possess diverse microstructures depending on the stereoselectivity of the process. If

there is no control of the enchainment of monomers, the PLA is atactic. If all the asymmetric carbons have the same configuration, the PLA is isotactic. If the system perfectly alternates the insertion of D- and L-lactide, the PLA obtained is heterotactic.
Stereoselectivity is crucial in the ROP of *rac*-lactide, since it will determine its mechanical properties.
Atactic PLA is amorphous with a T_g around 50-60 °C; whereas isotactic PLLA is semi-crystalline with a T_m of 180°C.

Stereocomplexation results from stereoselective interaction between two complementing stereoregular polymers, that interlock and form a new composite, demonstrating altered physical properties in comparison to the parent polymer.
Enantiopure PLAs can form stereocomplexes due to the strong interaction between L- and D-lactic acid sequences. Poly(L-lactic acid) and poly(D-lactic acid) can form a stereocomplex melting at 230 °C, which is about 50 °C higher than the homochiral crystals of the enantiopure semi-crystalline homopolymers, increasing the range of potential applications of such material.[84]

Based on previous work in the Thomas research group with tripodal ligands,[118] new achiral zinc, cobalt and iron catalysts supported by tripodal monophenoxide ligands have been synthesized, characterized and then tested in the ROP of *rac*-lactide.

5.2. SYNTHESIS AND CHARACTERIZATION OF THE METAL COMPLEXES

The pro-ligands (Scheme 5.1) were prepared in a straightforward manner by reductive amination and Mannich-type reaction, with good to excellent yields.[119] Such ligand architecture allows for steric and electronic variations on the different donor fragment. All compounds were obtained as colourless or yellowish powders and characterized by NMR and high-resolution mass spectrometry.

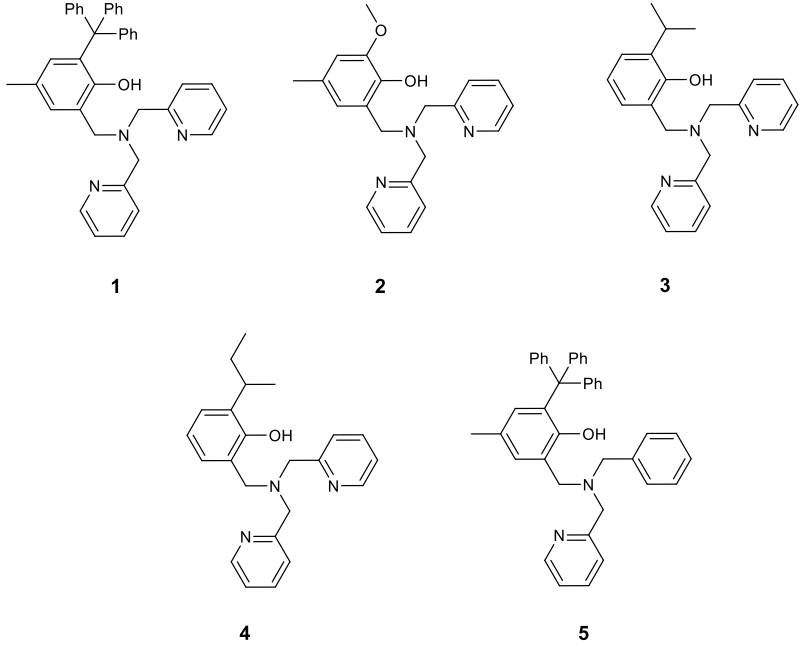

Scheme 5.1. Pro-ligands **1**-**5**.

The synthesis of pro-ligand $(N_3O)^tH$ (**1**) is done in two steps (Scheme 5.2). First the synthesis of 4-methyl-2-tritylphenol is conducted by reaction of sodium 4-methylphenolate (synthesized *in situ* by adding sodium) with trityl chloride according to the literature.[120] The

product undergoes a Mannich-type reaction with di-(2-picolyl)amine to obtain pro-ligand **1** in good yield (total yield 56%).

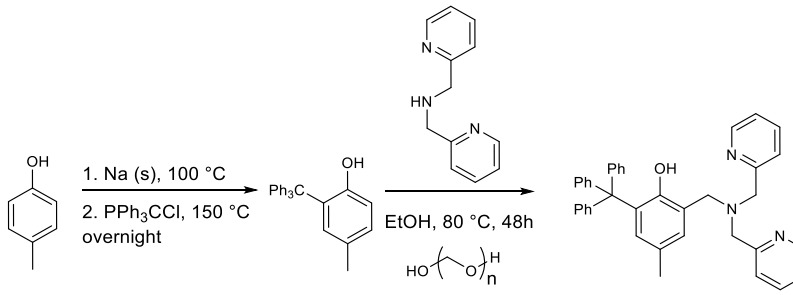

Scheme 5.2. Synthesis of pro-ligand $(N_3O)^tH$ **1**.

The ^1H NMR spectrum of pro-ligand **1** can be found in Figure 5.1.

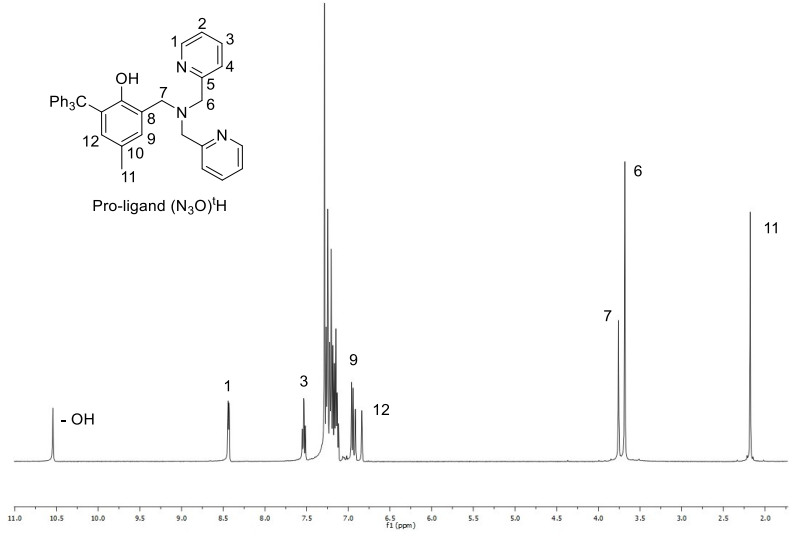

Figure 5.1. ^1H NMR spectrum (400MHz, $CDCl_3$) of pro-ligand **1**.

Pro-ligand **5** $(N_2O)^tH$ is synthesized in two steps (Scheme 5.3). N-benzyl-(2-picolyl)amine is not commercial and is synthesized from (2-picolyl)amine and benzaldehyde by reductive amination. After

purification, the product is used for the second step, Mannich-type reaction with 4-methyl-2- tritylphenol, to obtain pro-ligand **5** with a 45% total yield.

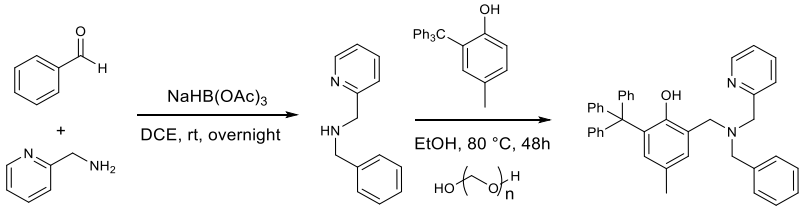

Scheme 5.3. Synthesis of pro-ligand **5**.

The ^{1}H NMR spectrum of pro-ligand **5** can be found in Figure 5.2.

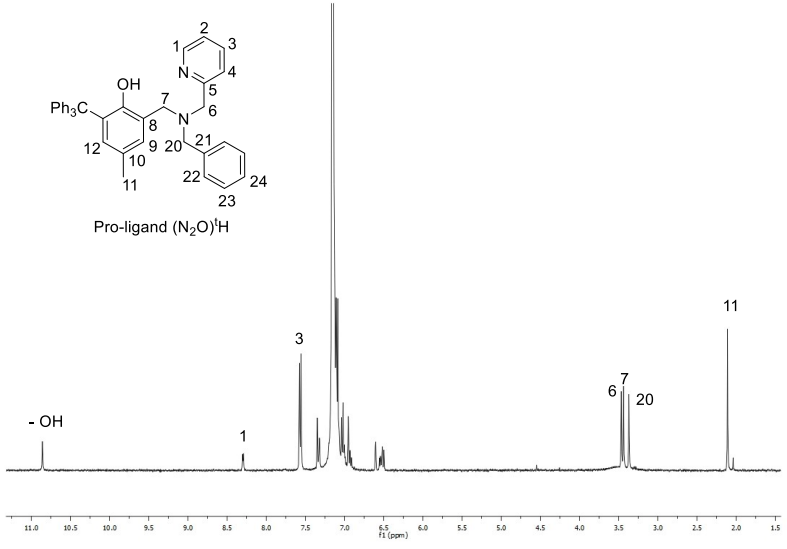

Figure 5.2. ^{1}H NMR spectrum (400MHz, $CDCl_3$) of pro-ligand **5**.

The pro-ligands were reacted with one equivalent of zinc, cobalt and iron bis-amide derivatives to give the corresponding complexes $LM[N(SiMe_3)_2]$ in good yields (34-94%).[121] The solvent was

removed *in vacuo* and the residues were washed with pentane to afford the desired complexes (Scheme 5.4).

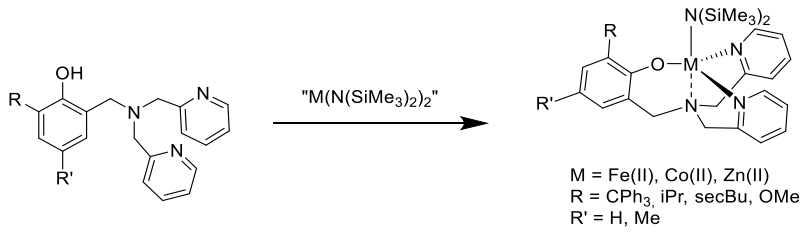

Scheme 5.4. Synthesis of the metal amido complexes.

The iron amido complex $(N_3O)^tFe[N(SiMe_3)_2]$ was also synthesized through the corresponding chloride precursor *via* a three-step salt metathesis route (Scheme 5.5). The iron chloride complex $(N_3O)^tFeCl$ was obtained in dichloromethane by adding iron (II) chloride to a solution of sodium phenolate generated *in situ* with NaH (yield 55%). The structure of the iron chloride complex was confirmed by mass spectroscopy and single crystal X-ray diffraction analysis.

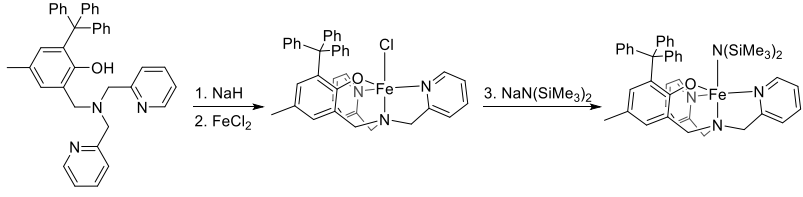

Scheme 5.5. Synthesis of the iron amido complex via a three-step reaction.

All complexes were characterized by mass spectroscopy, elemental analysis, single X-ray diffraction studies for some of them, and NMR spectroscopy for zinc complexes.

5.3. ROP OF *RAC*-LACTIDE

The reactivity of these new catalysts based on divalent metals was studied in the polymerization of *rac*-lactide.

All the amido complexes revealed to be highly active for the controlled ROP of *rac*-lactide under mild conditions (RT in toluene solution at [lactide] = 1M and one equivalent of isopropanol).

The influence of the metal centre on the microstructures of the produced PLAs, with the complexes having the same ligands was studied in detail. Subsequently, the effect of the ligands substituents on the microstructure was examined. Finally, the effect of the reaction conditions on the catalytic reactivity was investigated.

The produced polymers were characterized by NMR spectroscopy, DSC and X-ray diffraction.

5.4. MICROSTRUCTURE OF THE PLAS OBTAINED

NMR spectroscopy allows to evaluate PLA microstructure.[122] Proton resonances of distinct methine carbons can be solved through homonuclear decoupling ^{1}H NMR experiments. With PLA, this results in a spectrum displaying distinct peaks corresponding to sequences of four consecutive methine carbons, known as a tetrad.

A sequence of carbons of the same configuration is designated with an *m, meso* linkage, while an opposite configuration is known as a *racemic* linkage, labeled *r*. Eight arrangements are possible for a sequence of four carbon atoms. However, PLA from *rac*-lactide only displays five of these resonances due to the dimeric nature of the monomer (in the absence of epimerization). With each insertion of

one monomer, two stereocenters of the same configuration are created; therefore, resonances corresponding to the *rrr*, *rrm*, and *mrr*-tetrads cannot be observed (Scheme 5.6).

The relative ratio of the tetrad sequences is determined by the ability of the initiator to control *racemic* [*r*-diad] and *meso* [*m*-diad] linkage between each lactide unit.

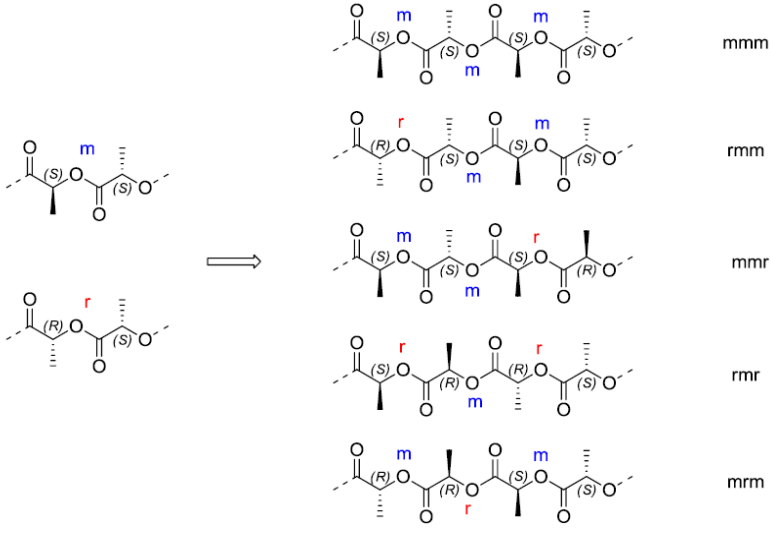

Scheme 5.6. Tetrad sequences from polymerization of *rac*-lactide.

The methine region of ^{1}H NMR spectra and of the homonuclear decoupled of a PLA sample produced by the iron amido complex $(N_3O)^{t}Fe[N(SiMe_3)_2]$ are shown in Figure 5.3 and 5.4. Only one major peak is observed in the homonuclear decoupled spectra, the *mmm*-tetrad, revealing an isotactic PLA.

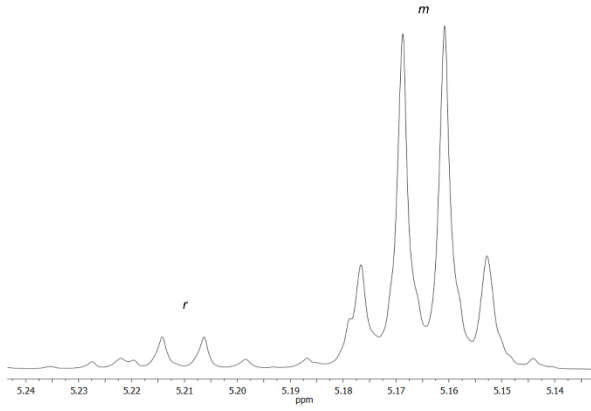

Figure 5.3. Methine region of the ^{1}H NMR spectrum (900 MHz, $CDCl_3$) of a PLA sample. Observation of dyads [*m*] and [*r*].

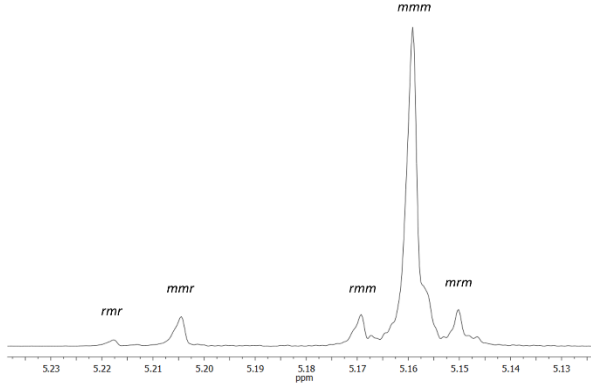

Figure 5.4. Methine region of the homodecoupled ^{1}H NMR spectrum (900 MHz, $CDCl_3$) of a PLA sample. Observation of tetrads.

In addition to information about tacticity, NMR spectroscopy provides insights into the polymerization mechanism since two types of mechanisms of stereocontrol can operate. An enantiomorphic site control mechanism takes place when the asymmetric environment of the catalyst reacts with the monomer selectively.

In a chain-end control mechanism, the stereochemistry of the last inserted lactide unit in the growing polymer chain dictates the stereoselection of the next monomer insertion.

These two mechanisms produce polymers that can be distinguished by NMR spectroscopy due to distinct stereochemical errors. In a site control mechanism, errors are immediately corrected whereas the mistake is propagated if the chain-end dictates the following insertion. The tetrad distribution is therefore different in PLAs formed from *rac*-LA under these different mechanisms.

Statistical analysis of the tetrad distribution in the decoupled ^{1}H NMR spectrum is used to differentiate these two processes. In a site-control process, the selectivity is defined in terms of α, defined as the probability that a given enantiomer of the catalyst will react preferentially with one enantiomer of *rac*-LA. Chain-end control is defined in terms of probability of a *meso* (P_m) or *racemic* (P_r) linkage. By comparing these predicted values to the observed spectrum, the mechanism of stereocontrol and the degree of selectivity in the polymerization may be determined.[123]

In a chain-end mechanism, Bernoullian statistics can be used to define relationships between tetrad probabilities and P_m (Table 5.1).

Table 5.1. *n*-ades probabilities based on Bernoullian statistics for PLA from *rac*-LA in terms of P_m.

n-ades	Probability				
Dyads	[*m*]	[*r*]			
	$(P_m+1)/2$	$(1-P_m)/2$			
Triads	[*mm*]	[*mr*]	[*rm*]		
	P_m	$(1-P_m)/2$	$(1-P_m)/2$		
Tetrads	[*mmm*]	[*mrm*]	[*mmr*]	[*rmm*]	[*rmr*]
	$P_m\,(P_m+1)/2$	$(1-P_m)/2$	$P_m\,(1-P_m)/2$	$P_m\,(1-P_m)/2$	$(1-P_m)^2/2$

High resolution NMR spectroscopy at 900 MHz revealed to be a powerful tool to investigate PLA microstructures from stereosensitive resonances. The resonances of the decoupled ^{1}H NMR spectrum of the PLA sample (Figure 5.4) fit to the theoretical intensities expected for a Bernoulli trial process with a P_m of 0.82 (Table 5.2). From tetrad information, a Bernoulli model can be postulated, demonstrating a chain-end control mechanism.

Table 5.2. Bernoulli model fitting

		Bernoulli trial P_m = 0.82	**Observed**
Dyads	[*m*]	0.91	0.92
	[*r*]	0.09	0.08
Tetrads	[*rmr*]	0.02	0.01
	[*rmm*]/[*mmr*]	0.07	0.06
	[*mmm*]	0.75	0.76
	[*mrm*]	0.09	0.10

CONCLUSIONS OF CHAPTER 5

Zinc, cobalt and iron complexes were synthesized from readily available tripodal ligands. The catalysts revealed highly active and stereoselective in mild conditions for the ROP of *rac*-lactide. Microstructural analysis of the different PLAs formed revealed moderately to highly isotactic microstructures. Statistical analysis confirmed a chain end control mechanism.

In particular, for the first time, the achiral iron structures merge the three important features of high activity and high molecular weight with control of the polymer microstructure, producing isotactic PLAs.

These results are the object of a manuscript under review: *Iso-selective lactide polymerization with iron complexes: a new approach to stereocomplex formation.* P. Marin, M. J.-L. Tschan, F. Isnard, C. Robert, P. Haquette, X. Trivelli, T. Roisnel, L.-M. Chamoreau, V. Guérineau, I. del Rosal, L. Maron, V. Venditto, C. M. Thomas.

CHAPTER 6. EXPERIMENTAL PART.

6.1. GENERAL EXPERIMENTAL METHODS

Generals. All manipulations of air- and/or water-sensitive compounds were carried out under a dry nitrogen atmosphere using a Braun Labmaster glove-box or standard Schlenk line techniques. Glassware and vials used in the polymerization were dried in an oven at 120 °C overnight and exposed three times to vacuum–nitrogen cycles.

Reagents and Solvents. Benzene, hexane and THF (Sigma-Aldrich) were distilled under nitrogen over sodium/benzophenone. Toluene was distilled under nitrogen over sodium. CH_2Cl_2 was distilled over CaH_2. All solvents were stored over molecular sieves. The aluminum precursor $AlMe_3$ was purchased from Sigma-Aldrich and was used as received. Deuterated solvents were dried over molecular sieves. Cyclohexene oxide (CHO), Limonene Oxide (LO), ε-caprolactone (ε-CL), *rac*-β-butyrolactone (β-BL) were purchased from Sigma-Aldrich and freshly distilled over CaH_2. *rac*-lactide (*rac*-LA) and L-lactide (L-LA) was purchased from Sigma-Aldrich and dried in vacuo over P_2O_5 for 72 h, and afterward stored at - 20 °C in a glovebox. ^{i}PrOH was purified by distillation over sodium. All other chemicals were commercially available and used as received unless otherwise stated. The synthesis of complex **7** was performed according published procedure.[103c]

NMR analysis. NMR spectra were recorded on Bruker Advance 250, 300, 400 and 600 MHz spectrometers at 25 °C, unless otherwise stated. Chemical shifts (δ) are expressed as parts per million and coupling constants (J) in hertz. ^{1}H NMR spectra are referenced using the residual solvent peak at δ = 7.16 for C_6D_6 and δ = 7.27 for $CDCl_3$. ^{13}C NMR spectra are referenced using the residual solvent peak at δ = 128.06 for C_6D_6 and δ = 77.23 for $CDCl_3$. In the case of ^{19}F, resonances were automatically referenced versus $CF_3C_6H_5$ by the software. In the case of ^{31}P, resonances were automatically referenced versus triphenyl phosphate by the software.

GPC. Molecular weights (M_n) and molecular weight polydispersities were measured by gel permeation chromatography (GPC). The measurements were performed at 30 °C on a Waters 1525 binary system equipped with a Waters 2414 Refractive Index (RI) detector and a Waters 2487 Dual λ Absorbtion (UV, λ_{abs} = 220 nm) detector, using THF as eluent (1.0 mL.min^{-1}) and employing a system of four Styragel HR columns (7.8 x 300 mm; range 10^3 – 10^6 Å). Narrow polystyrene standards were used as reference and Waters Breeze v3.30 software for data processing.

MALDI-ToF-MS Analysis. Mass spectra were acquired using a Bruker solariX XR Fourier transform ion cyclotron resonance mass spectrometer (Bruker Daltonik GmbH, Bremen, Germany) equipped with a 7 T refrigerated actively-shielded superconducting magnet (Bruker Biospin, Wissembourg, France). The samples were ionized in positive ion mode using the MALDI ion source.

Matrix DHB. The mass range was set to *m/z* 800 – 5000. The laser power was 15% and 15 laser shots were used for each scan. The mass spectra were calibrated externally using a mix of peptide clusters in MALDI ionization positive ion mode. A linear calibration was applied. To improve the mass accuracy, the sample spectra were recalibrated internally by 2,5-dihydroxybenzoic acid matrix ionization (2,5-DHB). Samples were prepared by mixing 10 µL of analyte methanol solution (1mg/mL) with 10 µL of saturated (30 mg/mL) solution of 2,5-DHB. The mixed solution was hand-spotted on a stainless steel MALDI target and left to dry.

Matrix DCTB. The mass range was set to *m/z* 200 – 5000. The laser power was 12% and 18 laser shots were used for each scan. Mass spectra were calibrated externally using a mix of peptide clusters in MALDI ionization positive ion mode. A linear calibration was applied. The polymer samples were dissolved in THF at a concentration of 1 mg/mL. The cationization agent used was potassium trifluoroacetate (Fluka, > 99%) dissolved in THF at a concentration of 5 mg/mL. The matrix used was trans-2-[3-(4-tert-butylphenyl)-2-methyl-2-propenylidene]malononitrile (DCTB) (Fluka) and was dissolved in THF at a concentration of 40 mg/mL.

Solutions of matrix, salt and polymer were mixed in a volume ratio of 4:1:4, respectively. The mixed solution was hand-spotted on a stainless steel MALDI target and left to dry.

Thermal analysis. Melting points (T_m) and Glass transition temperature (T_g) of the polymers were measured by differential scanning calorimetry (DSC) using a DSC 2920 apparatus manufactured by TA Instruments under a nitrogen flux of 50 mL min^{-1} with a heating and cooling rate of 10 °C min^{-1} in the range −10 to 200 °C. All calorimetric data were reported for the second heating cycle.

X-ray. X-ray diffraction measurements were performed on a Philips PW1710 powder diffractometer using Ni-filtered CuKα radiation (λ = 1.5418 Å) at 40 kV and 20 mA. The scans were carried out, on as polymerized samples, in the 2Θ range of 3 to 40 °C with 0.05° step in 2Θ and an acquisition time of 3s. Data were processed with Origin 7.0 software.

6.2. Synthesis and characterization of the complexes

6.2.1. Dinuclear salen aluminum-alkyl complexes L-AL_2ME_4

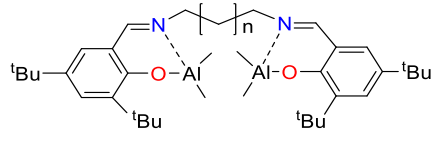

(1) n = 1
(2) n = 3
(3) n = 10

Complex 1. To a stirred solution containing $AlMe_3$ (0.056 g, 0.78 mmol) in benzene (2 mL) was added dropwise a solution of the corresponding ligand precursor (0.200 g, 0.39 mmol) in benzene (2 mL). The solution was stirred for 2 h at room temperature. The solvent was removed under vacuum, forming a pale yellow solid in almost quantitative yield (92%).

^{1}H NMR (600 MHz, C_6D_6, 298 K): δ 7.70 (d, J = 2.5 Hz, 2H, ArH), 7.15 (s, 2H, CH=N), 6.79 (d, J = 2.5 Hz, 2H, ArH), 2.84 (t, J = 7.0 Hz, 4H, N–CH_2), 1.72 (quin, J = 7.0 Hz, 2H, CH_2), 1.60 (s, 18H, *t*-Bu), 1.32 (s, 18H, *t*-Bu), −0.30 (s, 12H, Al–CH_3).
^{13}C NMR (63 MHz, C_6D_6, 298 K): δ 172.3, 162.0, 141.0, 139.3, 132.2, 128.9, 118.8 (Ar or ArCHN), 54.7 (N–CH_2), 35.6 ($C(CH_3)_3$), 34.1 ($C(CH_3)_3$), 31.5 ($C(CH_3)_3$), 29.5 ($C(CH_3)_3$), −8.8 (Al–CH_3).
Elemental analysis, calculated for $C_{37}H_{60}Al_2N_2O_2$ (%): C, 71.81; H, 9.77; N, 4.53. Found: C, 71.75; H, 9.89; N, 4.59.

Complex 2. To a stirred solution containing $AlMe_3$ (0.047 g, 0.68 mmol) in benzene (2 mL) was added dropwise a solution of the corresponding ligand precursor (0.180 g, 0.34 mmol) in benzene (2 mL). The solution was stirred for 2 h at room temperature.
The solvent was removed under vacuum, forming a pale yellow solid in almost quantitative yield (95%).
^{1}H NMR (250 MHz, C_6D_6, 298 K): δ 7.69 (d, J = 2.5 Hz, 2H, ArH), 7.26 (s, 2H, CH=N), 6.84 (d, J = 2.5 Hz, 2H, ArH), 2.87 (t, J = 7.2 Hz, 4H, N–CH_2), 1.60 (s, 18H, *t*-Bu), 1.32 (s, 18H, *t*-Bu), 1.23 (m, 4H), 0.77 (m, 2H, CH_2), −0.24 (s, 12H, Al–CH_3).
^{13}C NMR (63 MHz, C_6D_6, 298 K): δ 171.8, 161.9, 140.9, 139.0, 131.8, 128.9, 128.5, 128.2, 128.1, 118.8 (Ar or ArCHN), 57.3 (N–CH_2), 35.6 ($C(CH_3)_3$), 34.1 ($C(CH_3)_3$), 31.5 ($C(CH_3)_3$), 29.5 ($C(CH_3)_3$), −8.9 (Al–CH_3).
Elemental analysis, calculated for $C_{39}H_{64}Al_2N_2O_2$ (%): C, 72.41; H, 9.97; N, 4.33. Found: C, 72.37; H, 10.06; N, 4.44.

Complex 3. To a stirred solution containing $AlMe_3$ (0.034 g, 0.47 mmol) in benzene (2 mL) was added dropwise a solution of the corresponding ligand precursor (0.150 g, 0.23 mmol) in benzene (2 mL). The solution was stirred for 2 h at room temperature.
The solvent was removed under vacuum, forming a pale yellow solid in almost quantitative yield (94%).
^{1}H NMR (300 MHz, C_6D_6, 298 K): δ 7.69 (d, J = 2.5 Hz, 2H, ArH), 7.29 (s, 2H, CH=N), 6.79 (d, J = 2.5 Hz, 2H, ArH), 3.02 (t, J = 7.6 Hz, 4H, N–CH_2), 1.61 (s, 18H, *t*-Bu), 1.47 (m, 4H, CH_2), 1.32 (s,

18H, *t*-Bu), 1.29 (m, 4H, CH_2), 1.23 −1.22–1.07 (m, 16H, CH_2), −0.24 (s, 12H, Al–CH_3).
^{13}C NMR (101 MHz, C_6D_6, 298 K): δ 171.5, 162.0, 140.9, 138.8, 131.6, 128.8, 118.9 (Ar or ArCNH), 57.9 (N–CH_2), 35.6 ($C(CH_3)_3$), 34.1 ($C(CH_3)_3$), 31.5 ($C(CH_3)_3$), 30.4 (CH_2), 29.6 ($C(CH_3)_3$), 27.0 (CH_2), −8.9 (Al–CH_3).
Elemental analysis, calculated for $C_{46}H_{78}Al_2N_2O_2$ (%): C, 74.15; H, 10.55; N, 3.76. Found: C, 74.12; H, 10.61; N, 3.73.

6.2.2. PHENOXY-BASED DIMETHYL-ALUMINUM COMPLEXES L-ALME2

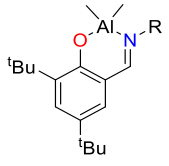

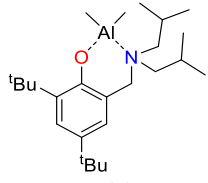

(6)

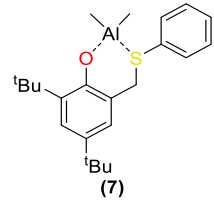

(7)

(4) R = *n*-propyl
(5a) R = Ph
(5b) R = 2,6-diisopropylphenyl
(5c) R = 2,6-dimethylphenyl
(5d) R = 4-methoxyphenyl
(5e) R = C_6F_5

Complex phenoxy-imine n-propyl (4). To a stirred solution containing 46 mg (0.61 mmol) of $AlMe_3$ in dry benzene (2 mL) was added dropwise a solution of the ligand (0.169 g, 0.61 mmol) in dry benzene (2 mL). The reaction mixture was stirred for 2 hours at room temperature. The solvent was removed under vacuum, forming a pale yellow solid in almost quantitative yield (96%).
^{1}H NMR (600 MHz, C_6D_6, 298 K): δ -0.26 (s, 6H, CH_3), 0.53 (t, J = 7.3 Hz, 3H, CH_3), 1.31 (s, 9H, CCH_3), 1.36 (m, 2H, CH_2), 1.59 (s, 9H, CCH_3), 2.85 (t, J = 7.3 Hz, 2H, CH_2), 6.75 (d, J = 2.6 Hz, 1H, ArH), 7.19 (s, 1H, CH=N), 7.66 (d, J = 2.6 Hz, 1H, ArH).
^{13}C NMR (150 MHz, C_6D_6, 298 K): δ - 9.0 (Al-CH_3), 11.1 (CH_3), 23.6 (CH_2), 29.6 ($C(CH_3)_3$), 31.6 ($C(CH_3)_3$), 34.2 ($C(CH_3)_3$), 35.6 ($C(CH_3)_3$), 59.4 (CH_2), 118.9 (Cq), 129.9 (CH), 131.6 (CH), 138.8 (Cq), 140.9 (Cq), 162,0 (Cq), 171.6 (CH).

General procedure for the synthesis of complexes 5a-e.

To a stirred solution containing 46 mg (0.61 mmol) of $AlMe_3$ (97% wt) in dry benzene (2 mL) was added dropwise a solution of the appropriate pro-ligand (0.61 mmol) in dry benzene (2 mL). The reaction mixture was stirred for 2 hours at room temperature. The solvent was removed under vacuum, forming a yellow solid in almost quantitative yield.

Complex phenoxy-imine phenyl (5a).[103a]

^{1}H NMR (300 MHz, C_6D_6, 298 K): δ -0.17 (s, 6H, Al-C*H*$_3$), 1.31 (s, 9H, CH(*CH*$_3$)$_2$), 1.60 (s, 9H, CH(*CH*$_3$)$_2$), 6.73 (d, J = 2.6 Hz, 1H, Ar-*H*), 6.94-6.96 (m, 5H, Ar-*H*), 7.42 (s, 1H, C*H*=N), 7.72 (d, J = 2.6 Hz, 1H, Ar-*H*).

^{13}C NMR (75 MHz, C_6D_6, 298 K): δ -8.6 (Al-*C*H$_3$), 29.6 (C(*C*H$_3$)), 31.5 (C(*C*H$_3$)), 34.2 (*C*(CH$_3$)), 35.6 (*C*(CH$_3$)), 119.4, 122.5, 129.8, 129.9, 132.9, 139.3, 141.2, 147.2 (all Ar-*C*, one peak obscured), 162.9 (*C*-O), 170.8 (*C*H=N).

Complex phenoxy-imine 2,6-diisopropylphenyl (5b).[103b]

^{1}H NMR (300 MHz, C_6D_6, 298 K): δ -0.23 (s, 6H, Al-C*H*$_3$), 0.79 (d, J = 6.7 Hz, 6H, CH(*CH*$_3$)$_2$), 1.18 (d, J = 6.7 Hz, 6H, CH(*CH*$_3$)$_2$), 1.24 (s, 9H, C(C*H*$_3$)), 1.60 (s, 9H, C(C*H*$_3$)), 3.11 (m, 2H, C*H*(CH$_3$)$_2$), 6.83 (d, J = 2.4 Hz, 1H, Ar-*H*), 6.96 (s, 1H, C*H*=N), 7.01 - 7.08 (m, 2H, Ar-*H*), 7.74 (d, J = 2.4 Hz, 1H, Ar-*H*), 7.85 (s, 1H, Ar-*H*).

^{13}C NMR (101 MHz, C_6D_6, 298 K): δ -8.9 (Al-*C*H$_3$), 22.9 (CH(*C*H$_3$)$_2$), 25.9 (CH(*C*H$_3$)$_2$), 28.5 (*C*H(CH$_3$)$_2$), 29.7 (C(*C*H$_3$)$_3$), 31.4 (C(CH$_3$)$_3$), 34.2 (*C*(CH$_3$)$_3$), 35.7 (*C*(CH$_3$)$_3$), 118.8, 124.5, 129.1, 133.4, 139.8, 141.6, 142.8, 142.9 (all Ar-*C*, one peak obscured), 163.2 (*C*-O), 174.5 (*C*H=N).

Complex phenoxy-imine 2,6-dimethylphenyl (5c).[103b]

^{1}H NMR (400 MHz, C_6D_6, 298 K): δ -0.29 (s, 6H, Al-C*H*$_3$), 1.29 (s, 9H, C(*CH*$_3$)), 1.60 (s, 9H, C(*CH*$_3$)), 1.97 (s, 6H, Ar-C*H*$_3$), 6.71 (d, J = 2.6 Hz, 1H, Ar-*H*), 6.82 - 6.88 (m, 3H, Ar-*H*), 7.17 (s, 1H, C*H*=N), 7.72 (d, J = 2.6 Hz, 1H, Ar-*H*).

^{13}C NMR (101 MHz, C_6D_6, 298 K): δ -8.4 (Al-*C*H$_3$), 18.5 (*C*H$_3$), 29.6 (C(*C*H$_3$)), 31.5 (C(*C*H$_3$)), 34.3 (*C*(CH$_3$)), 35.7 (*C*(CH$_3$)), 119.1, 127.4, 129.0, 129.5, 131.9, 133.1, 139.3, 141.4, 145.3, 163.1 (*C*-O), 174.9 (*C*H=N).

Single crystal X-ray structures of compounds **5b** and **5c** have been reported in the literature.[103b] In both structures, the aluminum centre has a distorted tetrahedral geometry.

Complex phenoxy-imine 4-methoxyphenyl (5d).
^{1}H NMR (400 MHz, C_6D_6, 298 K): δ -0.13 (s, 6H, Al-C*H*$_3$), 1.32 (s, 9H, C(*CH*$_3$)), 1.63 (s, 9H, C(*CH*$_3$)), 3.23 (s, 3H, OC*H*$_3$), 6.59 (d, J = 8.9 Hz, 2H, Ar-*H*), 6.77 (d, J = 2.4 Hz, 1H, Ar-*H*), 6.90 (d, J = 8.9 Hz, 2H, Ar-*H*), 7.52 (s, 1H, C*H*=N), 7.72 (d, J = 2.4 Hz, 1H, Ar-*H*).
^{13}C NMR (75 MHz, C_6D_6, 298 K): δ -8.6 (Al-*C*H$_3$), 29.6 (C(*C*H$_3$)), 31.5 (C(*C*H$_3$)), 34.2 (*C*(CH$_3$)), 35.6 (*C*(CH$_3$)), 59.0 (O*C*H$_3$), 117.9, 119.4, 123.9, 129.9, 132.9, 139.4, 141.1, 142.3, 157.7, 162.8 (*C*-O), 170.2 (*C*H=N).

Complex phenoxy-imine pentafluorophenyl (5e).
^{1}H NMR (400 MHz, C_6D_6, 298 K): δ -0.24 (s, 6H, Al-C*H*$_3$), 1.25 (s, 9H, C(C*H*$_3$)), 1.51 (s, 9H, C (C*H*$_3$)), 6.73 (d, J = 2.2 Hz, 1H, Ar-*H*), 7.18 (s, 1H, C*H*=N), 7.73 (d, J = 2.2 Hz, Ar-*H*).
^{13}C NMR (75 MHz, C_6D_6, 298 K): δ -9.8 (Al-*C*H$_3$), 29.4 (C(*C*H$_3$)), 31.2 (C(*C*H$_3$)), 34.1 (*C*(CH$_3$)), 35.6 (*C*(CH$_3$)), 118.6, 121.8 (*C*-N), 129.9, 135.5, 136.4 (*C*-F), 140.0, 140.3 (*C*-F), 142.0, 143.6 (*C*-F), 164.8 (*C*-O), 177.1 (*C*H=N).
^{19}F NMR (377 MHz, C_6D_6, 298 K): δ -160.72 (td, 2F, *o*-F)), -154.52 (t, 1F, *p*-F), -148.35 (d, 2F, *m*-F).

Complex phenoxy-amine (6). To a stirred solution containing 0.230 g (3.09 mmol) of $AlMe_3$ (97% wt) in dry benzene was added dropwise a solution of the ligand (1.00 g, 2.88 mmol) in dry benzene. The reaction mixture was stirred for 3 hours at room temperature. The solvent was removed under vacuum forming a gel, which was

successively washed with pentane. The complex was dried under vacuum, forming a white solid in almost quantitative yield.
^{1}H NMR (300 MHz, C_6D_6, 298 K): δ -0.28 (s, 6H, Al-CH_3), 0.55 (d, J = 6.8 Hz, 6H, CH(CH_3)$_2$), 0.68 (d, J = 6.6 Hz, 6H, CH(CH_3)$_2$), 1.41 (s, 9H, C(CH_3)), 1.71 (s, 9H, C(CH_3)), 1.77 (m, 2H, CH), 2.35 (dd, J = 4.9, 14.1 Hz, 2H, CH_2), 2.44 (dd, J = 6.0, 13.9 Hz, 2H, CH_2), 3.43 (s, 2H, N-CH_2-Ar), 6.75 (d, J = 2.4 Hz, 1H, Ar-H), 7.54 (d, J = 2.4 Hz, 1H, Ar-H).
^{13}C NMR (75 MHz, C_6D_6, 298 K): δ -8.7 (Al-CH$_3$), 22.8, 23.3, 23.5, 29.9, 32.1, 35.4, 58.7, 60.2, 119.9, 124.3, 125.4, 137.9, 138.3, 157.3 (C-O).

General procedure for the synthesis of the complexes with an additional donor.

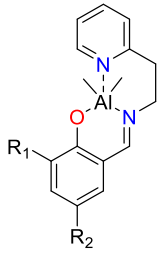

(8a) $R_1 = R_2 = {}^{t}Bu$
(8b) $R_1 = H$, $R_2 = OMe$
(8c) $R_1 = R_2 = F$
(8d) $R_1 = R_2 = NO_2$

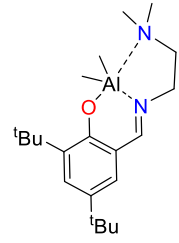

(9)

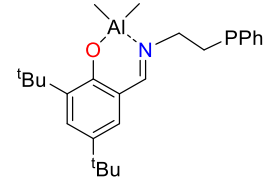

(10)

To a stirred solution containing 100 mg (1.3 mmol) of $AlMe_3$ (97% wt) in dry benzene (2 mL) was added dropwise a solution of the appropriate pro-ligand (1.3 mmol) in dry benzene (2 mL). The reaction mixture was stirred for 2 hours at room temperature. The solvent was then removed under vacuum, to yield a brown oil. The resulting oil was washed with dry hexane and dried *in vacuo*.

Complex phenoxy-imine with a pyridine donor (8a).

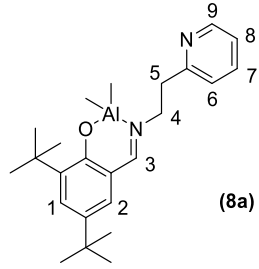

(8a)

^{1}H NMR (400 MHz, C_6D_6, 298 K): δ -0.22 (s, 6H, Al-CH_3), 1.27 (s, 9H, CCH_3), 1.58 (s, 9H, CCH_3), 2.9 (t, J = 7.3 Hz, 2H, CH_2), 3.68 (t, J = 7.3 Hz, 2H, N-CH_2), 6.52 (m, 1H, H8), 6.59 (m, 2H, H2, H6), 6.84 (m, 1H, H7), 7.31 (s, 1H, H3), 7.62 (d, J = 2.5 Hz, 1H, H1), 8.39 (d, J = 4.4 Hz, 1H, H9).

^{13}C NMR (75 MHz, C_6D_6, 298 K): δ -8.8 (Al-CH$_3$), 29.6 (C(CH$_3$)), 31.5 (C(CH$_3$)), 34.1 (C(CH$_3$)), 35.5 (C(CH$_3$)), 38.3, 56.3, 118.9, 121.6, 123.9, 128.2, 131.5, 136.2, 138.7, 140.6, 149.6, 157.9, 161.9, 172.7.

Complex (8b).

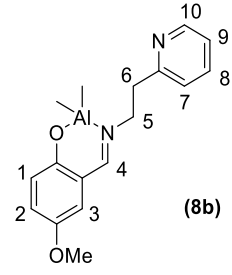

(8b)

^{1}H NMR (600 MHz, C_6D_6, 298 K): δ -0.22 (s, 6H, Al-CH_3), 2.89 (t, J = 7.2 Hz, 2H, CH_2), 3.27 (s, 3H, OMe), 3.68 (t, J = 7.2 Hz, 2H, N-CH_2), 6.12 (d, J = 3.3 Hz, 1H, H1), 6.53 (m, 1H, H9), 6.60 (d, J = 7.7 Hz, 1H, H7), 6.80 (dd, J = 3.3 Hz, 1H, H2), 6.85 (m, 1H, H8), 6.92 (m, 1H, H3), 7.20 (s, 1H, H4), 8.38 (d, J = 4.9 Hz, 1H, H10).

^{13}C NMR (75 MHz, C_6D_6, 298 K): δ -8.7 (Al-CH$_3$), 38.2, 55.5, 56.4, 116.1, 118.2, 121.7, 123.1, 124.0, 125.4, 136.3, 149.7, 151.1, 157.8, 159.7, 171.4.

Complex (8c). For complex **(8c)**, diluted solutions in dry THF were used for the complex synthesis because of the poor solubility of the pro-ligand in benzene.

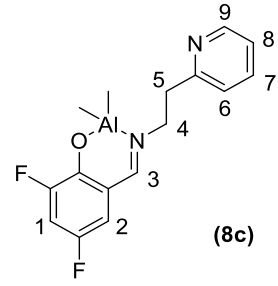

(8c)

^{1}H NMR (600 MHz, C_6D_6, 298 K): δ -0.33 (s, 6H, Al-CH_3), 2.79 (t, J = 7.1 Hz, 2H, CH_2), 3.59 (t, J = 7.1 Hz, 2H, N-CH_2), 5.94 (m, 1H, H2), 6.51-6.57 (m, 3H, H1, H6, H8), 6.86 (dt, J = 1.8, 7.7 Hz, 1H, H7), 7.00 (s, H, H3), 8.3 (d, J = 4.0 Hz, 1H, H9).
^{13}C NMR (63 MHz, C_6D_6, 298K): δ -8.8 (Al-CH$_3$), 37.5, 56.3, 111.0, 113.2, 119.0, 121.9, 124.0, 136.4, 149.6, 150.0, 151.4, 155.3, 157.3, 170.2.
^{19}F NMR (377 MHz, C_6D_6, 298K): δ -128.92 (d, *o*-F), -125.66 (t, *p*-F).

Complex (8d).

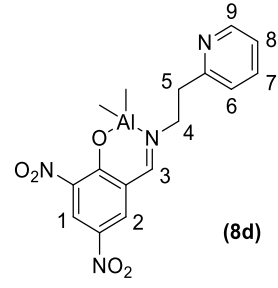

(8d)

^{1}H NMR (400 MHz, CD_2Cl_2, 298K): δ -0.76 (s, 6H, Al-CH_3), 3.32 (t, 2H, CH_2), 4.18 (t, 2H, N-CH_2), 7.23 (d, 1H), 7.29 (q, 1H), 7.69-7.73 (dt, 1H), 8.30-8.36 (m, 3H), 8.60 (d, 1H).

^{13}C NMR (75 MHz, C_6D_6, 298 K): δ -7.7 (Al-*C*H_3), 37.3, 58.6, 122.6, 124.4, 125.0, 126.1, 127.4, 133.6, 134.3, 137.8, 149.5, 158.9, 166.2, 170.6.

Complex phenoxy-imine with an amine donor (9).[117a]

^{1}H NMR (600 MHz, C_6D_6, 298K): δ -0.27 (s, 6H, Al-C*H*$_3$), 1.31 (s, 9H, CC*H*$_3$), 1.63 (s, 9H, CC*H*$_3$), 1.87 (s, 6H, N-(C*H*$_3$)$_2$), 2.11 (t, J = 6.7 Hz, 2H, C*H*$_2$), 2.90 (t, J = 6.7 Hz, 2H, HCN-C*H*$_2$), 6.80 (d, J = 2.6 Hz, 1H), 7.42 (s, 1H, N=CH), 7.66 (d, J = 2.6 Hz, 1H).

^{13}C NMR (75 MHz, C_6D_6, 298 K): δ -8.4 (Al-*C*H$_3$), 29.7 (C(*C*H$_3$)), 31.6 (C(*C*H$_3$)), 34.1 (*C*(CH$_3$)), 35.6 (*C*(CH$_3$)), 45.2, 54.1, 57.8, 118.5, 128.5, 131.5, 137.9, 140.9, 163.4, 172.8.

The crystal structure of complex **9** is reported, showing that the pendant arm donor is bound to the aluminum center.[117a]

Complex phenoxy-imine with a phosphine donor (10).

^{1}H NMR (400 MHz, C_6D_6, 298K): δ -0.28 (s, 6H, Al-C*H*$_3$), 1.30 (s, 9H, CC*H*$_3$), 1.57 (s, 9H, CC*H*$_3$), 2.29 (m, 2H, C*H*$_2$), 3.23 (m, 2H, N-C*H*$_2$), 6.67 (d, J = 2.3 Hz, 1H), 7.02-7.10 (m, 7H, PPh$_2$), 7.42 (m, 4H, PPh$_2$), 7.66 (d, J = 2.3 Hz, 1H).

^{13}C NMR (75 MHz, C_6D_6, 298 K): δ -8.7 (Al-*C*H$_3$), 29.6 (C(*C*H$_3$)), 29.9 (C(*C*H$_3$)), 31.6 (*C*(CH$_3$)), 34.2 (*C*(CH$_3$)), 35.6, 54.6, 118.9, 129.0, 129.1, 129.3, 131.7, 132.9, 133.2, 137.8, 138.0, 138.9, 140.8, 162.1, 171.9.

^{31}P NMR (162 MHz, C_6D_6, 298 K): δ -20.4.

6.3. SYNTHESIS OF THE POLYMERS

***rac*-Lactide polymerization.**

The polymerization was carried out under an inert atmosphere. In a Braun Labmaster glovebox, a magnetically stirred reactor vessel (10 mL) was charged with *rac*-lactide. Subsequently, a toluene solution of the metal-complex and ^{i}PrOH (0.1 M) was added. The reaction mixture was stirred at 70 °C. At desired times, small aliquots of the reaction mixture were sampled, dissolved in $CDCl_3$ and analyzed by ^{1}H NMR spectroscopy. At the end of the polymerization the product was precipitated in MeOH then filtered and dried in a vacuum oven.

β-BL and ε-CL polymerization.

The polymerizations were carried out in an inert atmosphere. In a Braun Labmaster glovebox, a reactor vessel (10 mL), equipped with a Teflon-coated stirring bar, was charged with the appropriate amount of the monomer dissolved in 1.8 mL of toluene. Subsequently, a toluene solution of the metal-complex and ^{i}PrOH (0.2 mL) was added. The reaction mixture was stirred at 70 °C. At desired times, small aliquots of the reaction mixture were sampled, dissolved in wet $CDCl_3$ and analyzed by ^{1}H NMR spectroscopy. At the end of the polymerization, the product was dissolved in chloroform to give a viscous solution, which was subsequently poured into excess methanol. The precipitated polymer was filtered and dried in a vacuum oven.

CHO polymerization.

Bulk. The polymerization was carried out under an inert atmosphere. In a Braun Labmaster glovebox, a magnetically stirred reactor vessel (10 mL) was charged with a solution of metal-complex (and ^{i}PrOH) in CHO. The reaction mixture was stirred at RT or at 70 °C. At desired times, small aliquots of the reaction mixture were sampled, dissolved in $CDCl_3$ and analyzed by ^{1}H NMR spectroscopy. At the

end of the polymerization the product was dissolved in hexane and then precipitated in HCl : ethanol 1 : 3.

Solution. The polymerization was carried out under an inert atmosphere. In a Braun Labmaster glovebox, a magnetically stirred reactor vessel (10 mL) was charged with a CH_2Cl_2 solution (2 mL) of metal-complex (and ^{i}PrOH) and CHO. The reaction mixture was stirred at RT. At desired times, small aliquots of the reaction mixture were sampled, dissolved in $CDCl_3$ and analyzed by ^{1}H NMR spectroscopy. At the end of the polymerization the product was dissolved in hexane and then precipitated in HCl : ethanol 1 : 3.

Synthesis of diblock copolymers.

The same procedure is followed for the synthesis of all diblock copolymers. In a typical polymerization, a magnetically stirred flame dried reaction vessel (10 cm^3) was charged with the first monomer (CHO) and the appropriate amount of catalyst/isopropanol and the solution was heated at 70 °C. The polymerization was performed until the required polymerization time. An aliquot (0.01 mL) was taken from the polymerization mixture and quenched in wet $CDCl_3$; completion of the reaction was deduced from the ^{1}H NMR spectroscopy. Subsequently, the second monomer (LA, ε-CL or β-BL) was added to the polymerization mixture and heated at the same temperature (70 °C). The polymerization was continued until complete monomer conversion. An aliquot was checked to verify the percentage of conversion of the second monomer. The polymerization was terminated by the addition of 5 mL of CH_3OH. The reaction mixture was dissolved in chloroform and precipitated in hexane. The resulting polymer (white solid) was filtered, washed with methanol, dried in a vacuum.

Kinetic studies for homopolymers.

In a typical experiment carried out in the nitrogen filled glovebox, 0.1 mL of a stock solution of the complex (5 μmol) in deuterated

toluene was added to a J-Young NMR tube containing 100 equiv. of an appropriate monomer (β-butyrolactone, or ε-caprolactone). Next, 0.4 mL of deuterated toluene was added to adjust the total volume to 0.5 mL. The NMR tube was then placed into the preheated NMR spectrometer at the corresponding temperature (70 ° C), and the % conversion was investigated from the integration of the polymer and monomer signals.

Kinetic studies for copolymers.

In a typical experiment carried out in the nitrogen filled glovebox, 50 equivalents of each monomer and 0.1 mL of a stock solution of ^{i}PrOH in toluene were added to a J-Young NMR tube containing of the catalyst. Next, 0.4 mL of deuterated toluene was added to adjust the total volume to 0.5 mL. The NMR tube was then placed into the preheated NMR spectrometer at the corresponding temperature (70 °C) and the % conversion was investigated from the integration of polymer and monomer signals.

The characteristic chemical shift ^{1}H NMR (400 MHz, tol-d8) for each monomer is:
Lactide = 4.12 (q, –CH–)
β-butyrolactone = 3.93 (m, –CH–)
ε-caprolactone = 3.63 (m, CH_2)
The characteristic chemical shift for each polymer is:
Poly-β-butyrolactone = 5.31 (m, –CH–)
Polylactide = 5.12 (q, –CH–)
Poly-ε-caprolactone = 4.00 (t, –CH_2–).

General procedure for the co-polymerization of epoxides with cyclic anhydrides.

In bulk. In a Braun Labmaster glovebox, a magnetically stirred reactor vessel (10 mL) was charged with the anhydride. Subsequently, a solution of catalyst and cocatalyst dissolved in neat epoxide was added. The reaction mixture was stirred at the desired

temperature. At desired times, small aliquots of the reaction mixture were sampled, dissolved in $CDCl_3$ and analyzed by ^1H NMR spectroscopy. At the end of the polymerization, the product was dissolved in CH_2Cl_2 and dried under vacuum oven. All analyses were performed on crude samples.

In solution. The copolymerization was performed at the desired temperature in 1 mL toluene. In a Braun Labmaster glovebox, a magnetically stirred reactor vessel (10 mL) was charged with the anhydride. Subsequently, a solution of catalyst, cocatalyst and epoxide in 1 mL of toluene was added. The reaction mixture was stirred at 110 °C. At desired times, small aliquots of the reaction mixture were sampled, dissolved in $CDCl_3$ and analyzed by ^1H NMR spectroscopy. At the end of the polymerization, the product was dissolved in CH_2Cl_2 and dried under vacuum oven. All analyses were performed on crude samples.

The characteristic chemical shift for each monomer is:
Succinic anhydride = ^1H NMR (300 MHz, $CDCl_3$): δ 3.01 (s, 4H)
Phthalic anhydride = ^1H NMR (300 MHz, $CDCl_3$): δ 7.97 (m, 2H), 7.86 (m, 2H)
Maleic anhydride = ^1H NMR (300 MHz, $CDCl_3$): δ 6.43 (s, 2H)
Cyclohexene oxide = ^1H NMR (400 MHz, $CDCl_3$): δ 3.12 (s, 2H); ^1H NMR (300 MHz, C_6D_6): δ 2.78 (s, 2H)
Limonene oxide = ^1H NMR (400 MHz, $CDCl_3$): δ 4.68 (s, 1H), 4.62 (s, 1H)

APPENDIX 1. STRUCTURE OF THE COMPLEXES **1-10**.

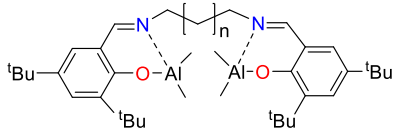

(1) n = 1
(2) n = 3
(3) n = 10

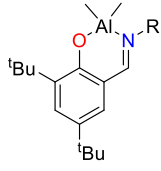

(4) R = *n*-propyl
(5a) R = Ph
(5b) R = 2,6-diisopropylphenyl
(5c) R = 2,6-dimethylphenyl
(5d) R = 4-methoxyphenyl
(5e) R = C_6F_5

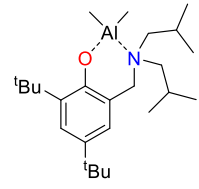

(6)

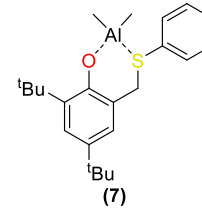

(7)

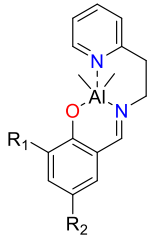

(8a) $R_1 = R_2 = {}^t$Bu
(8b) R_1 = H, R_2 = OMe
(8c) $R_1 = R_2$ = F
(8d) $R_1 = R_2 = NO_2$

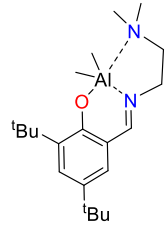

(9)

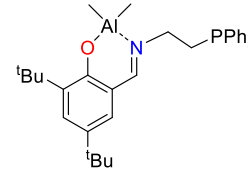

(10)

APPENDIX 2. THERMAL AND X-RAY ANALYSIS OF COPOLYMERS.

PCL/PLA

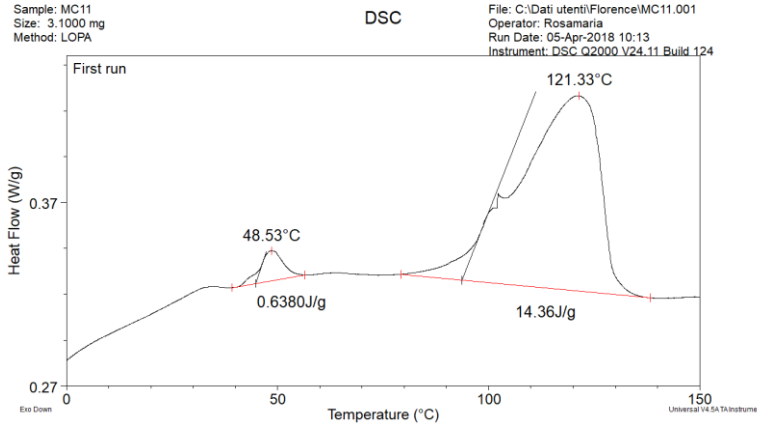

Figure A2.1. DSC thermogram of PCL/PLA copolymer.

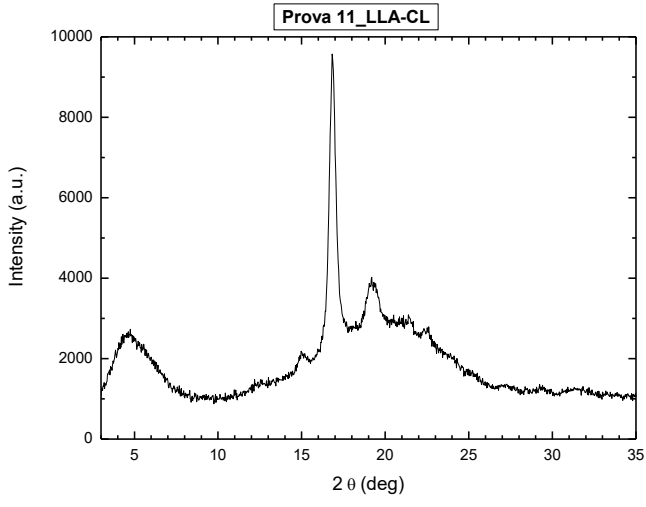

Figure A2.2. WAXD analysis of the PCL/PLA copolymer.

PHB/PLA

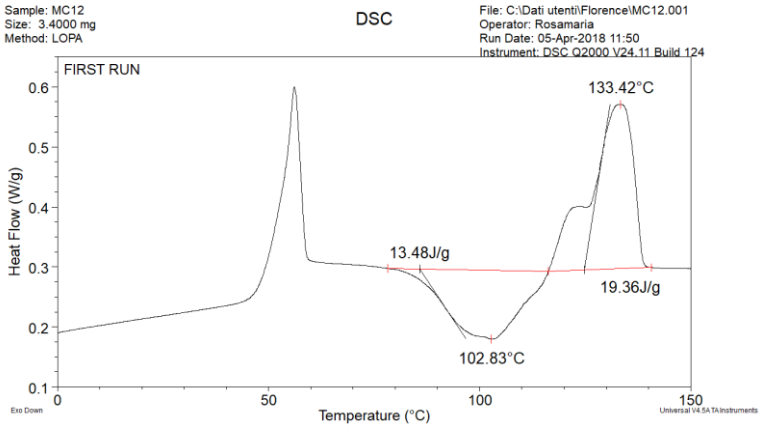

Figure A2.3. DSC thermogram of PHB/PLA copolymer.

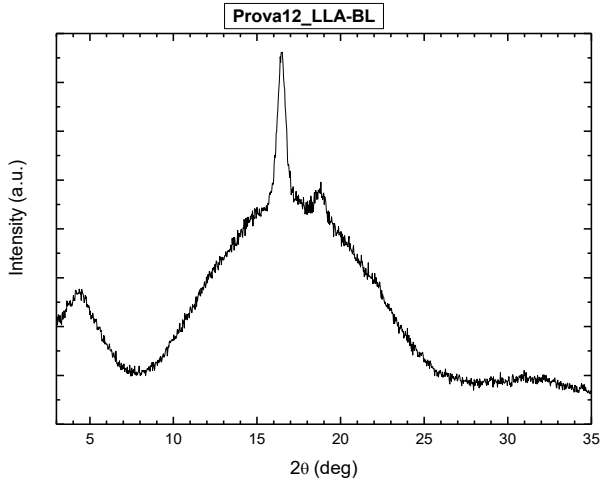

Figure A24. WAXD analysis of PHB/PLA copolymer.

APPENDIX 3. CATALYST ACTIVITY AND SELECTIVITY IN THE ROCOP BETWEEN EPOXIDES /ANHYDRIDES.

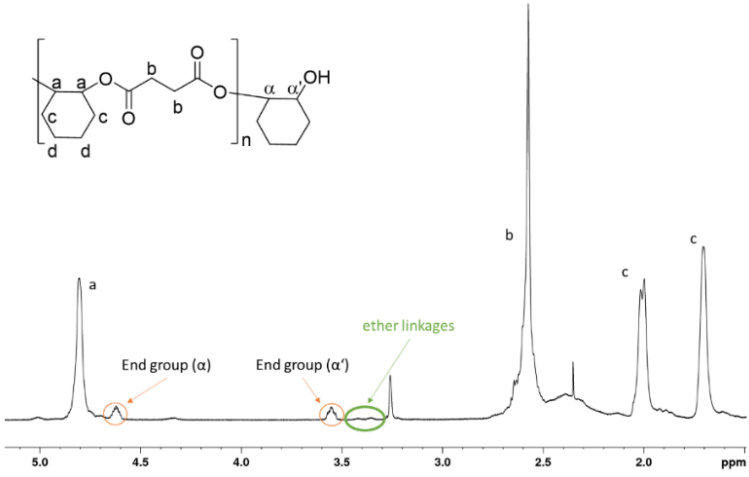

Figure A3.1. ^{1}H NMR spectrum (600 MHz, $CDCl_3$) of the CHO/SA copolymer.

On the ^{1}H NMR spectrum, conversions of both monomers can be calculated. It is quite simple with the anhydride since it transforms only in polyester. On the other hand, the epoxide can form ester and ether linkages. In $CDCl_3$, ether linkages from CHO range from 3.31 to 3.47 ppm, whereas ester linkages from CHO (Ha + Hα) range from 4.58 to 4.90 ppm (including end-group from 4.58 to 4.67 ppm).

$$\text{Anhydride conversion} = \frac{[\text{Anhydride polyester Hb}]}{[\text{Anhydride polyester Hb}] + [\text{Anhydride monomer}]}$$

$$\text{Epoxide conversion} = \frac{[\text{Epoxide polyester}] + [\text{Epoxide polyether}]}{[\text{Epoxide polyester}] + [\text{Epoxide polyether}] + [\text{Epoxide monomer}]}$$

The percentage of ester linkages in comparison to ether linkages (formed by sequential enchainment of epoxides) determines the selectivity of the copolymerization:

$$\text{Selectivity} = \frac{[\text{Epoxide polyester (Ha+H}\alpha)]}{[\text{Epoxide polyester (Ha+H}\alpha)] + [\text{Epoxide polyether}]}$$

The activity can also be expressed by the TOF, turnover frequency: the number of equivalents of monomer that can be converted by the catalyst per unit of time. We decided to calculate the TOF on the anhydride conversion, to exclude the homopolymerization reaction.

REFERENCES.

1. (a) Gandini, A., The irruption of polymers from renewable resources on the scene of macromolecular science and technology. *Green Chem.* **2011,** *13* (5), 1061-1083; (b) Tschan, M. J.-L.; Brulé, E.; Haquette, P.; Thomas, C. M., Synthesis of biodegradable polymers from renewable resources. *Polym. Chem.* **2012,** *3* (4), 836-851.

2. (a) Thomas, C. M., Stereocontrolled ring-opening polymerization of cyclic esters: synthesis of new polyester microstructures. *Chem. Soc. Rev.* **2010,** *39* (1), 165-173; (b) Dijkstra, P. J.; Du, H.; Feijen, J., Single site catalysts for stereoselective ring-opening polymerization of lactides. *Polym. Chem.* **2011,** *2* (3), 520-527; (c) Platel, R. H.; Hodgson, L. M.; Williams, C. K., Biocompatible initiators for lactide polymerization. *Polym. Rev.* **2008,** *48* (1), 11-63.

3. (a) Li, W.; Ouyang, H.; Chen, L.; Yuan, D.; Zhang, Y.; Yao, Y., A Comparative Study on Dinuclear and Mononuclear Aluminum Methyl Complexes Bearing Piperidyl-Phenolato Ligands in ROP of Epoxides. *Inorg. Chem.* **2016,** *55* (13), 6520-4; (b) Thevenon, A.; Romain, C.; Bennington, M. S.; White, A. J.; Davidson, H. J.; Brooker, S.; Williams, C. K., Dizinc lactide polymerization catalysts: hyperactivity by control of ligand conformation and metallic cooperativity. *Angew. Chem. Int. Ed.* **2016,** *55* (30), 8680-8685; (c) Tseng, H.-C.; Chen, H.-Y.; Huang, Y.-T.; Lu, W.-Y.; Chang, Y.-L.; Chiang, M. Y.; Lai, Y.-C.; Chen, H.-Y., Improvement in Titanium Complexes Bearing Schiff Base Ligands in the Ring-Opening Polymerization of L-Lactide: A Dinuclear System with Hydrazine-Bridging Schiff Base Ligands. *Inorg. Chem.* **2016,** *55* (4), 1642-1650; (d) Chen, L.; Li, W.; Yuan, D.; Zhang, Y.; Shen, Q.; Yao, Y., Syntheses of mononuclear and dinuclear aluminum complexes stabilized by phenolato ligands and their applications in the polymerization of ε-caprolactone: a comparative study. *Inorg. Chem.* **2015,** *54* (10), 4699-4708; (e) Chen, H.-Y.; Liu, M.-Y.; Sutar, A. K.; Lin, C.-C., Synthesis and structural studies of heterobimetallic alkoxide complexes supported by bis (phenolate) ligands: Efficient catalysts for ring-opening polymerization of L-lactide. *Inorg. Chem.* **2009,** *49* (2), 665-674; (f) Sarazin, Y.; Howard, R. H.; Hughes, D. L.; Humphrey, S. M.; Bochmann, M., Titanium, zinc and alkaline-earth metal complexes supported by bulky O, N, N, O-multidentate

ligands: syntheses, characterisation and activity in cyclic ester polymerisation. *Dalton Trans.* **2006,** (2), 340-350; (g) Bukhaltsev, E.; Frish, L.; Cohen, Y.; Vigalok, A., Single-site catalysis by bimetallic zinc calixarene inclusion complexes. *Org. Lett.* **2005,** *7* (23), 5123-5126.
4. Liu, J.; Bao, Y.-Y.; Liu, Y.; Ren, W.-M.; Lu, X.-B., Binuclear chromium-salan complex catalyzed alternating copolymerization of epoxides and cyclic anhydrides. *Polym. Chem.* **2013,** *4* (5), 1439-1444.
5. Li, J.; Liu, Y.; Ren, W.-M.; Lu, X.-B., Asymmetric Alternating Copolymerization of Meso-epoxides and Cyclic Anhydrides: Efficient Access to Enantiopure Polyesters. *J. Am. Chem. Soc.* **2016,** *138* (36), 11493-11496.
6. (a) Han, H.-L.; Liu, Y.; Liu, J.-Y.; Nomura, K.; Li, Y.-S., Synthesis of binuclear phenoxyimino organoaluminum complexes and their use as the catalyst precursors for efficient ring-opening polymerisation of ε-caprolactone. *Dalton Trans.* **2013,** *42* (34), 12346-12353; (b) Li, L.; Liu, B.; Liu, D.; Wu, C.; Li, S.; Liu, B.; Cui, D., Copolymerization of ε-caprolactone and L-lactide catalyzed by multinuclear aluminum complexes: an immortal approach. *Organometallics* **2014,** *33* (22), 6474-6480.
7. Isnard, F.; Lamberti, M.; Lettieri, L.; D'auria, I.; Press, K.; Troiano, R.; Mazzeo, M., Bimetallic salen aluminum complexes: cooperation between reactive centers in the ring-opening polymerization of lactides and epoxides. *Dalton Trans.* **2016,** *45* (40), 16001-16010.
8. Isnard, F.; Carratù, M.; Lamberti, M.; Venditto, V.; Mazzeo, M., Copolymerization of cyclic esters, epoxides and anhydrides: evidence of the dual role of the monomers in the reaction mixture. *Catal. Sci. Technol.* **2018**.
9. Isnard, F.; Lamberti, M.; Pellecchia, C.; Mazzeo, M., Ring-Opening Copolymerization of Epoxides with Cyclic Anhydrides Promoted by Bimetallic and Monometallic Phenoxy-Imine Aluminum complexes. *ChemCatChem* **2017,** *9* (15), 2972-2979.
10. https://www.plasticseurope.org/en/resources/market-data (accessed in October 2018).
11. Zhang, X.; Fevre, M.; Jones, G. O.; Waymouth, R. M., Catalysis as an Enabling Science for Sustainable Polymers. *Chem. Rev.* **2018,** *118* (2), 839-885.
12. Auras, R.; Harte, B.; Selke, S., An overview of polylactides as packaging materials. *Macromol. Biosci.* **2004,** *4* (9), 835-864.

13. Miller, S. A., Sustainable polymers: opportunities for the next decade. ACS Publications: 2013.
14. Vink, E. T.; Rábago, K. R.; Glassner, D. A.; Springs, B.; O'Connor, R. P.; Kolstad, J.; Gruber, P. R., The sustainability of NatureWorks™ polylactide polymers and Ingeo™ polylactide fibers: an update of the future. *Macromol. Biosci.* **2004,** *4* (6), 551-564.
15. Place, E. S.; George, J. H.; Williams, C. K.; Stevens, M. M., Synthetic polymer scaffolds for tissue engineering. *Chem. Soc. Rev.* **2009,** *38* (4), 1139-1151.
16. http://www.european-bioplastics.org/market/ (accessed in October 2018).
17. Brulé, E.; Robert, C.; Thomas, C. M. In *Sequence-Controlled Ring-Opening Polymerization: Synthesis of New Polyester Structure*, ACS Symp. Ser, 2014; pp 349-368.
18. Dubois, P.; Jacobs, C.; Jerome, R.; Teyssie, P., Macromolecular engineering of polylactones and polylactides. 4. Mechanism and kinetics of lactide homopolymerization by aluminum isopropoxide. *Macromolecules* **1991,** *24* (9), 2266-2270.
19. Inoue, S., Immortal polymerization: The outset, development, and application. *J. Polym. Sci., Part A: Polym. Chem.* **2000,** *38* (16), 2861-2871.
20. (a) Le Borgne, A.; Vincens, V.; Jouglard, M.; Spassky, N. In *Ring-opening oligomerization reactions using aluminium complexes of schiff's bases as initiators*, Makromolekulare Chemie. Macromolecular Symposia, Wiley Online Library: 1993; pp 37-46; (b) Ovitt, T. M.; Coates, G. W., Stereochemistry of lactide polymerization with chiral catalysts: new opportunities for stereocontrol using polymer exchange mechanisms. *J. Am. Chem. Soc.* **2002,** *124* (7), 1316-1326; (c) Nomura, N.; Ishii, R.; Akakura, M.; Aoi, K., Stereoselective ring-opening polymerization of racemic lactide using aluminum-achiral ligand complexes: Exploration of a chain-end control mechanism. *J. Am. Chem. Soc.* **2002,** *124* (21), 5938-5939; (d) Zhong, Z.; Dijkstra, P. J.; Feijen, J., Controlled and stereoselective polymerization of lactide: Kinetics, selectivity, and microstructures. *J. Am. Chem. Soc.* **2003,** *125* (37), 11291-11298; (e) Nomura, N.; Ishii, R.; Yamamoto, Y.; Kondo, T., Stereoselective ring-opening polymerization of a racemic lactide by using achiral salen- and homosalen-aluminum complexes. *Chem. - Eur. J.* **2007,** *13* (16), 4433-4451.

21. Dubois, P.; Coulembier, O.; Raquez, J.-M., *Handbook of ring-opening polymerization*. John Wiley & Sons: 2009.
22. (a) Paul, S.; Zhu, Y.; Romain, C.; Brooks, R.; Saini, P. K.; Williams, C. K., Ring-opening copolymerization (ROCOP): synthesis and properties of polyesters and polycarbonates. *Chem. Commun.* **2015,** *51* (30), 6459-6479; (b) Longo, J. M.; Sanford, M. J.; Coates, G. W., Ring-opening copolymerization of epoxides and cyclic anhydrides with discrete metal complexes: structure–property relationships. *Chem. Rev.* **2016,** *116* (24), 15167-15197.
23. Inoue, S.; Kitamura, K.; Tsuruta, T., Alternating copolymerization of phthalic anhydride and propylene oxide by dialkylzinc. *Die Makromolekulare Chemie* **1969,** *126* (1), 250-265.
24. Jeske, R. C.; DiCiccio, A. M.; Coates, G. W., Alternating Copolymerization of Epoxides and Cyclic Anhydrides: An Improved Route to Aliphatic Polyesters. *J. Am. Chem. Soc.* **2007,** *129* (37), 11330-11331.
25. Aida, T.; Inoue, S., Catalytic reaction on both sides of a metalloporphyrin plane. Alternating copolymerization of phthalic anhydride and epoxypropane with an aluminum porphyrin-quaternary salt system. *J. Am. Chem. Soc.* **1985,** *107* (5), 1358-1364.
26. Huijser, S.; Hosseini Nejad, E.; Sablong, R.; de Jong, C.; Koning, C. E.; Duchateau, R., Ring-Opening Co- and Terpolymerization of an Alicyclic Oxirane with Carboxylic Acid Anhydrides and CO2in the Presence of Chromium Porphyrinato and Salen Catalysts. *Macromolecules* **2011,** *44* (5), 1132-1139.
27. DiCiccio, A. M.; Coates, G. W., Ring-Opening Copolymerization of Maleic Anhydride with Epoxides: A Chain-Growth Approach to Unsaturated Polyesters. *J. Am. Chem. Soc.* **2011,** *133* (28), 10724-10727.
28. Van Zee, N. J.; Coates, G. W., Alternating Copolymerization of Propylene Oxide with Biorenewable Terpene-Based Cyclic Anhydrides: A Sustainable Route to Aliphatic Polyesters with High Glass Transition Temperatures. *Angew. Chem. Int. Ed.* **2015,** *54* (9), 2665-2668.
29. Hosseini Nejad, E.; van Melis, C. G. W.; Vermeer, T. J.; Koning, C. E.; Duchateau, R., Alternating Ring-Opening Polymerization of Cyclohexene Oxide and Anhydrides: Effect of Catalyst, Cocatalyst, and Anhydride Structure. *Macromolecules* **2012,** *45* (4), 1770-1776.
30. Nejad, E. H.; Paoniasari, A.; van Melis, C. G.; Koning, C. E.; Duchateau, R., Catalytic ring-opening copolymerization of

limonene oxide and phthalic anhydride: Toward partially renewable polyesters. *Macromolecules* **2013,** *46* (3), 631-637.
31. (a) Jutz, F.; Buchard, A.; Kember, M. R.; Fredriksen, S. B.; Williams, C. K., Mechanistic Investigation and Reaction Kinetics of the Low-Pressure Copolymerization of Cyclohexene Oxide and Carbon Dioxide Catalyzed by a Dizinc Complex. *J. Am. Chem. Soc.* **2011,** *133* (43), 17395-17405; (b) Buchard, A.; Jutz, F.; Kember, M. R.; White, A. J. P.; Rzepa, H. S.; Williams, C. K., Experimental and Computational Investigation of the Mechanism of Carbon Dioxide/Cyclohexene Oxide Copolymerization Using a Dizinc Catalyst. *Macromolecules* **2012,** *45* (17), 6781-6795.
32. (a) Thevenon, A.; Garden, J. A.; White, A. J. P.; Williams, C. K., Dinuclear Zinc Salen Catalysts for the Ring Opening Copolymerization of Epoxides and Carbon Dioxide or Anhydrides. *Inorg. Chem.* **2015,** *54* (24), 11906-11915; (b) Klaus, S.; Lehenmeier, M. W.; Herdtweck, E.; Deglmann, P.; Ott, A. K.; Rieger, B., Mechanistic Insights into Heterogeneous Zinc Dicarboxylates and Theoretical Considerations for CO2–Epoxide Copolymerization. *J. Am. Chem. Soc.* **2011,** *133* (33), 13151-13161; (c) Cheng, M.; Moore, D. R.; Reczek, J. J.; Chamberlain, B. M.; Lobkovsky, E. B.; Coates, G. W., Single-Site β-Diiminate Zinc Catalysts for the Alternating Copolymerization of CO2 and Epoxides: Catalyst Synthesis and Unprecedented Polymerization Activity. *J. Am. Chem. Soc.* **2001,** *123* (36), 8738-8749; (d) Robert, C.; Ohkawara, T.; Nozaki, K., Manganese-Corrole Complexes as Versatile Catalysts for the Ring-Opening Homo- and Co-Polymerization of Epoxide. *Chem. - Eur. J.* **2014,** *20* (16), 4789-4795.
33. Garden, J. A.; Saini, P. K.; Williams, C. K., Greater than the Sum of Its Parts: A Heterodinuclear Polymerization Catalyst. *J. Am. Chem. Soc.* **2015,** *137* (48), 15078-15081.
34. F. Isnard, M. Mazzeo, C. M. Thomas. Novel polyesters from renewable ressources. L'actualité chimique, 2018, 427-428, 50.
35. https://www.plasticseurope.org/en/resources/market-data (accessed in October 2018).
36. Zhu, Y.; Romain, C.; Williams, C. K., Sustainable polymers from renewable resources. *Nature* **2016,** *540* (7633), 354.
37. Maeda, Y.; Nakayama, A.; Kawasaki, N.; Hayashi, K.; Aiba, S.; Yamamoto, N., Ring-opening copolymerization of succinic anhydride with ethylene oxide initiated by magnesium diethoxide. *Polymer* **1997,** *38* (18), 4719-4725.

38. Robert, C.; De Montigny, F.; Thomas, C. M., Tandem synthesis of alternating polyesters from renewable resources. *Nat. Commun.* **2011,** *2*, 586.
39. Mahmoud, E.; Watson, D. A.; Lobo, R. F., Renewable production of phthalic anhydride from biomass-derived furan and maleic anhydride. *Green Chem.* **2014,** *16* (1), 167-175.
40. Winkler, M.; Romain, C.; Meier, M. A.; Williams, C. K., Renewable polycarbonates and polyesters from 1, 4-cyclohexadiene. *Green Chem.* **2015,** *17* (1), 300-306.
41. Burdock, G. A., *Fenaroli's handbook of flavor ingredients*. CRC press: 2016.
42. Nonino, E. A., Where is the citrus industry going? *Perfumer & flavorist* **1997,** *22* (2), 53-58.
43. Schrader, J.; Bohlmann, J., Biotechnology of Isoprenoids Preface. SPRINGER INT PUBLISHING AG GEWERBESTRASSE 11, CHAM, CH-6330, SWITZERLAND: 2015.
44. Fournier, L.; Robert, C.; Pourchet, S.; Gonzalez, A.; Williams, L.; Prunet, J.; Thomas, C. M., Facile and efficient chemical functionalization of aliphatic polyesters by cross metathesis. *Polym. Chem.* **2016,** *7* (22), 3700-3704.
45. Sanford, M. J.; Peña Carrodeguas, L.; Van Zee, N. J.; Kleij, A. W.; Coates, G. W., Alternating Copolymerization of Propylene Oxide and Cyclohexene Oxide with Tricyclic Anhydrides: Access to Partially Renewable Aliphatic Polyesters with High Glass Transition Temperatures. *Macromolecules* **2016,** *49* (17), 6394-6400.
46. Spassky, N.; Wisniewski, M.; Pluta, C.; Le Borgne, A., Highly stereoelective polymerization of rac-(D, L)-lactide with a chiral schiff's base/aluminium alkoxide initiator. *Macromol. Chem. Phys.* **1996,** *197* (9), 2627-2637.
47. Hormnirun, P.; Marshall, E. L.; Gibson, V. C.; Pugh, R. I.; White, A. J., Study of ligand substituent effects on the rate and stereoselectivity of lactide polymerization using aluminum salen-type initiators. *Proc. Natl. Acad. Sci.* **2006,** *103* (42), 15343-15348.
48. (a) Hormnirun, P.; Marshall, E. L.; Gibson, V. C.; White, A. J.; Williams, D. J., Remarkable stereocontrol in the polymerization of racemic lactide using aluminum initiators supported by tetradentate aminophenoxide ligands. *J. Am. Chem. Soc.* **2004,** *126* (9), 2688-2689; (b) Du, H.; Velders, A. H.; Dijkstra, P. J.; Sun, J.; Zhong, Z.; Chen, X.; Feijen, J., Chiral salan aluminium ethyl complexes and their application in lactide polymerization. *Chem. Eur. J.* **2009,** *15* (38), 9836-9845; (c) Ikpo, N.; Barbon, S. M.;

Drover, M. W.; Dawe, L. N.; Kerton, F. M., Aluminum Methyl and Chloro Complexes Bearing Monoanionic Aminephenolate Ligands: Synthesis, Characterization, and Use in Polymerizations. *Organometallics* **2012,** *31* (23), 8145-8158.
49. (a) Whitelaw, E. L.; Loraine, G.; Mahon, M. F.; Jones, M. D., Salalen aluminium complexes and their exploitation for the ring opening polymerisation of rac-lactide. *Dalton Trans.* **2011,** *40* (43), 11469-11473; (b) Hancock, S. L.; Mahon, M. F.; Jones, M. D., Aluminium salalen complexes based on 1, 2-diaminocyclohexane and their exploitation for the polymerisation of rac-lactide. *Dalton Trans.* **2013,** *42* (25), 9279-9285; (c) Pilone, A.; De Maio, N.; Press, K.; Venditto, V.; Pappalardo, D.; Mazzeo, M.; Pellecchia, C.; Kol, M.; Lamberti, M., Ring-opening homo- and co-polymerization of lactides and ε-caprolactone by salalen aluminum complexes. *Dalton Trans.* **2015,** *44* (5), 2157-2165.
50. (a) Bouyahyi, M.; Grunova, E.; Marquet, N.; Kirillov, E.; Thomas, C. M.; Roisnel, T.; Carpentier, J.-F., Aluminum complexes of fluorinated dialkoxy-diimino salen-like ligands: Syntheses, structures, and use in ring-opening polymerization of cyclic esters. *Organometallics* **2008,** *27* (22), 5815-5825; (b) Alaaeddine, A.; Thomas, C. M.; Roisnel, T.; Carpentier, J.-F., Aluminum and yttrium complexes of an unsymmetrical mixed fluorous alkoxy/phenoxy-diimino ligand: synthesis, structure, and ring-opening polymerization catalysis. *Organometallics* **2009,** *28* (5), 1469-1475.
51. Press, K.; Goldberg, I.; Kol, M., Mechanistic insight into the stereochemical control of lactide polymerization by salan–aluminum catalysts. *Angew. Chem. Int. Ed.* **2015,** *127* (49), 15071-15074.
52. Pilone, A.; Press, K.; Goldberg, I.; Kol, M.; Mazzeo, M.; Lamberti, M., Gradient Isotactic Multiblock Polylactides from Aluminum Complexes of Chiral Salalen Ligands. *J. Am. Chem. Soc.* **2014,** *136* (8), 2940-2943.
53. (a) Pang, X.; Duan, R.; Li, X.; Chen, X., Bimetallic salen–aluminum complexes: synthesis, characterization and their reactivity with rac-lactide and ε-caprolactone. *Polym. Chem.* **2014,** *5* (12), 3894-3900; (b) Qu, Z.; Duan, R.; Pang, X.; Gao, B.; Li, X.; Tang, Z.; Wang, X.; Chen, X., Living and stereoselective polymerization of rac-lactide by bimetallic aluminum Schiff-Base complexes. *J. Polym. Sci., Part A: Polym. Chem.* **2014,** *52* (9), 1344-1352; (c) Darensbourg, D. J.; Karroonnirun, O., Stereoselective Ring-Opening Polymerization of rac-Lactides Catalyzed by Chiral and Achiral Aluminum Half-Salen Complexes. *Organometallics* **2010,** *29* (21),

5627-5634; (d) Li, W.; Wu, W.; Wang, Y.; Yao, Y.; Zhang, Y.; Shen, Q., Bimetallic aluminum alkyl complexes as highly active initiators for the polymerization of ε-caprolactone. *Dalton Trans.* **2011,** *40* (43), 11378-11381; (e) Sun, Z.; Duan, R.; Yang, J.; Zhang, H.; Li, S.; Pang, X.; Chen, W.; Chen, X., Bimetallic Schiff base complexes for stereoselective polymerisation of racemic-lactide and copolymerisation of racemic-lactide with ε-caprolactone. *Rsc Advances* **2016,** *6* (21), 17531-17538.
54. Maudoux, N.; Roisnel, T.; Dorcet, V.; Carpentier, J. F.; Sarazin, Y., Chiral (1, 2)-Diphenylethylene-Salen Complexes of Triel Metals: Coordination Patterns and Mechanistic Considerations in the Isoselective ROP of Lactide. *Chem. Eur. J.* **2014,** *20* (20), 6131-6147.
55. Kan, C.; Ge, J.; Ma, H., Aluminum methyl, alkoxide and α-alkoxy ester complexes supported by 6,6′-dimethylbiphenyl-bridged salen ligands: synthesis, characterization and catalysis for rac-lactide polymerization. *Dalton Trans.* **2016,** *45* (15), 6682-6695.
56. Wang, Y.; Ma, H., Exploitation of dinuclear salan aluminum complexes for versatile copolymerization of ε-caprolactone and l-lactide. *Chem. Commun.* **2012,** *48* (53), 6729-6731.
57. Van Aelstyn, M. A.; Keizer, T. S.; Klopotek, D. L.; Liu, S.; Munoz-Hernandez, M.-A.; Wei, P.; Atwood, D. A., Bimetallic aluminum and gallium chelates with N2O2 ligands. *Organometallics* **2000,** *19* (9), 1796-1801.
58. Baran, J.; Duda, A.; Kowalski, A.; Szymanski, R.; Penczek, S., Intermolecular chain transfer to polymer with chain scission: general treatment and determination of kp/ktr in l, l-lactide polymerization. *Macromol. Rapid Commun.* **1997,** *18* (4), 325-333.
59. Normand, M.; Roisnel, T.; Carpentier, J. F.; Kirillov, E., Dinuclear vs. mononuclear complexes: accelerated, metal-dependent ring-opening polymerization of lactide. *Chem. Commun.* **2013,** *49* (99), 11692-11694.
60. Normand, M.; Dorcet, V.; Kirillov, E.; Carpentier, J.-F., {Phenoxy-imine}aluminum versus -indium Complexes for the Immortal ROP of Lactide: Different Stereocontrol, Different Mechanisms. *Organometallics* **2013,** *32* (6), 1694-1709.
61. (a) Zhang, W.; Wang, Y.; Sun, W.-H.; Wang, L.; Redshaw, C., Dimethylaluminium aldiminophenolates: synthesis, characterization and ring-opening polymerization behavior towards lactides. *Dalton Trans.* **2012,** *41* (38), 11587-11596; (b) Maudoux, N.; Roisnel, T.; Dorcet, V.; Carpentier, J.-F.; Sarazin, Y., Chiral

(1,2)-Diphenylethylene-Salen Complexes of Triel Metals: Coordination Patterns and Mechanistic Considerations in the Isoselective ROP of Lactide. *Chem. - Eur. J.* **2014,** *20* (20), 6131-6147.
62. Wang, Y.; Ma, H., Aluminum complexes of bidentate phenoxy-amine ligands: Synthesis, characterization and catalysis in ring-opening polymerization of cyclic esters. *J. Organomet. Chem.* **2013,** *731*, 23-28.
63. Jacobs, C.; Dubois, P.; Jerome, R.; Teyssie, P., Macromolecular engineering of polylactones and polylactides. 5. Synthesis and characterization of diblock copolymers based on poly-iε-caprolactone and poly(L,L or D,L)lactide by aluminum alkoxides. *Macromolecules* **1991,** *24* (11), 3027-3034.
64. (a) Lewiński, J.; Horeglad, P.; Wójcik, K.; Justyniak, I., Chelation Effect in Polymerization of Cyclic Esters by Metal Alkoxides: Structure Characterization of the Intermediate Formed by Primary Insertion of Lactide into the Al−OR Bond of an Organometallic Initiator. *Organometallics* **2005,** *24* (19), 4588-4593; (b) Klitzke, J. S.; Roisnel, T.; Kirillov, E.; Casagrande, O. d. L.; Carpentier, J.-F., Discrete O-Lactate and β-Alkoxybutyrate Aluminum Pyridine–Bis(naphtholate) Complexes: Models for Mechanistic Investigations in the Ring-Opening Polymerization of Lactides and β-Lactones. *Organometallics* **2014,** *33* (20), 5693-5707.
65. (a) Tschan, M. J. L.; Brule, E.; Haquette, P.; Thomas, C. M., Synthesis of biodegradable polymers from renewable resources. *Polym. Chem.* **2012,** *3* (4), 836-851; (b) Carpentier, J.-F., Discrete Metal Catalysts for Stereoselective Ring-Opening Polymerization of Chiral Racemic β-Lactones. *Macromol. Rapid Commun.* **2010,** *31* (19), 1696-1705; (c) García-Valle, F. M.; Tabernero, V.; Cuenca, T.; Mosquera, M. E. G.; Cano, J.; Milione, S., Biodegradable PHB from rac-β-Butyrolactone: Highly Controlled ROP Mediated by a Pentacoordinated Aluminum Complex. *Organometallics* **2018,** *37* (6), 837-840.
66. A. Duda and A. Kowalski, i. e. P. D., O. Coulembier and; J. M. Raquez; . Handbook of Ring-Opening Polymerization, . *Wiley-VCHVerlag GmbH* **2009**, 1–51.
67. (a) Liu, Y.; Dong, W.-S.; Liu, J.-Y.; Li, Y.-S., Living ring-opening homo- and copolymerization of ε-caprolactone and L-lactide by cyclic β-ketiminato aluminum complexes. *Dalton Trans.* **2014,** *43* (5), 2244-2251; (b) Dagorne, S.; Wehmschulte, R., Recent

Developments on the Use of Group 13 Metal Complexes in Catalysis. *ChemCatChem* **2018,** *10* (12), 2509-2520.
68. (a) Childers, M. I.; Longo, J. M.; Van Zee, N. J.; LaPointe, A. M.; Coates, G. W., Stereoselective Epoxide Polymerization and Copolymerization. *Chem. Rev.* **2014,** *114* (16), 8129-8152; (b) Braune, W.; Okuda, J., An Efficient Method for Controlled Propylene Oxide Polymerization: The Significance of Bimetallic Activation in Aluminum Lewis Acids. *Angew. Chem. Int. Ed.* **2003,** *42* (1), 64-68.
69. (a) Baker, R. J.; Walshe, A., New reactivity of the uranyl ion: ring opening polymerisation of epoxides. *Chem. Commun.* **2012,** *48* (7), 985-987; (b) Fang, J.; Walshe, A.; Maron, L.; Baker, R. J., Ring-Opening Polymerization of Epoxides Catalyzed by Uranyl Complexes: An Experimental and Theoretical Study of the Reaction Mechanism. *Inorg. Chem.* **2012,** *51* (16), 9132-9140.
70. (a) Vandenberg, E. J., Organometallic catalysts for polymerizing monosubstituted epoxides. *J. Polym. Sci. Pol. Chem.* **1960,** *47* (149), 486-489; (b) Vandenberg, E. J.; Salamone, J. C. In *Catalysis in polymer synthesis*, United States, 1992-01-01; Washington, DC (United States); American Chemical Society: United States, 1992; (c) Mason, M. R.; Perkins, A. M., Alkylaluminophosphonate-catalyzed ring-opening homopolymerization of epichlorohydrin and propylene oxide. *J. Organomet. Chem.* **2000,** *599* (2), 200-207.
71. Pappuru, S.; Chokkapu, E. R.; Chakraborty, D.; Ramkumar, V., Group iv complexes containing the benzotriazole phenoxide ligand as catalysts for the ring-opening polymerization of lactides, epoxides and as precatalysts for the polymerization of ethylene. *Dalton Trans.* **2013,** *42* (46), 16412-16427.
72. Cui, D.; Nishiura, M.; Hou, Z., Alternating Copolymerization of Cyclohexene Oxide and Carbon Dioxide Catalyzed by Organo Rare Earth Metal Complexes. *Macromolecules* **2005,** *38* (10), 4089-4095.
73. Plommer, H.; Reim, I.; Kerton, F. M., Ring-opening polymerization of cyclohexene oxide using aluminum amine-phenolate complexes. *Dalton Trans* **2015,** *44* (27), 12098-102.
74. Martínez, G.; Pedrosa, S.; Tabernero, V.; Mosquera, M. E. G.; Cuenca, T., Controlled Synthesis of Novel Aryloxide Polynuclear Aluminum Species. Study of Their Catalytic Properties in Polymerization Processes. *Organometallics* **2008,** *27* (10), 2300-2305.

75. (a) Hild, F.; Neehaul, N.; Bier, F.; Wirsum, M.; Gourlaouen, C.; Dagorne, S., Synthesis and structural characterization of various N,O,N-chelated aluminum and gallium complexes for the efficient ROP of cyclic esters and carbonates: how do aluminum and gallium derivatives compare? *Organometallics* **2013,** *32* (2), 587-598; (b) Darensbourg, D. J.; Karroonnirun, O.; Wilson, S. J., Ring-Opening Polymerization of Cyclic Esters and Trimethylene Carbonate Catalyzed by Aluminum Half-Salen Complexes. *Inorg. Chem.* **2011,** *50* (14), 6775-6787.
76. Van Zee, N. J.; Coates, G. W., Alternating copolymerization of dihydrocoumarin and epoxides catalyzed by chromium salen complexes: a new route to functional polyesters. *Chem. Commun.* **2014,** *50* (48), 6322-6325.
77. Fernández-Millán, M.; Temprado, M.; Cano, J.; Cuenca, T.; Mosquera, M. E., Synthesis of novel chiral heterometallic terpene oximates: unusual generation of an aluminium enolate by a cooperative effect. *Dalton Trans.* **2016,** *45* (26), 10514-10518.
78. (a) Arbaoui, A.; Redshaw, C.; Hughes, D. L., Multinuclear alkylaluminium macrocyclic Schiff base complexes: influence of procatalyst structure on the ring opening polymerisation of ε-caprolactone. *Chem. Commun.* **2008,** (39), 4717-4719; (b) Kirk, S. M.; Quilter, H. C.; Buchard, A.; Thomas, L. H.; Kociok-Kohn, G.; Jones, M. D., Monomeric and dimeric Al (III) complexes for the production of polylactide. *Dalton Trans.* **2016,** *45* (35), 13846-13852; (c) Pang, X.; Duan, R.; Li, X.; Hu, C.; Wang, X.; Chen, X., Breaking the Paradox between Catalytic Activity and Stereoselectivity: rac-Lactide Polymerization by Trinuclear Salen–Al Complexes. *Macromolecules* **2018,** *51* (3), 906-913; (d) Gong, S.; Du, P.; Ma, H., Binuclear aluminum complexes supported by linked bis (β-diketiminate) ligands for ring-opening polymerization of cyclic esters. *Chin. J. Polym. Sci.* **2018,** *36* (2), 190-201; (e) Pang, X.; Duan, R.; Li, X.; Gao, B.; Sun, Z.; Wang, X.; Chen, X., Bimetallic Schiff-base aluminum complexes based on pentaerythrityl tetramine and their stereoselective polymerization of racemic lactide. *RSC Advances* **2014,** *4* (43), 22561-22566.
79. (a) Kan, C.; Ma, H., Copolymerization of l-lactide and ε-caprolactone catalyzed by mono-and dinuclear salen aluminum complexes bearing bulky 6, 6′-dimethylbipheyl-bridge: random and tapered copolymer. *RSC Advances* **2016,** *6* (53), 47402-47409; (b) Osorio Meléndez, D.; Castro-Osma, J. A.; Lara-Sánchez, A.; Rojas, R. S.; Otero, A., Ring-opening polymerization and copolymerization

of cyclic esters catalyzed by amidinate aluminum complexes. *J. Polym. Sci., Part A: Polym. Chem.* **2017,** *55* (14), 2397-2407.
80. Albertsson, A.-C.; Varma, I. K., Recent Developments in Ring Opening Polymerization of Lactones for Biomedical Applications. *Biomacromolecules* **2003,** *4* (6), 1466-1486.
81. Dobroth, Z. T.; Hu, S.; Coats, E. R.; McDonald, A. G., Polyhydroxybutyrate synthesis on biodiesel wastewater using mixed microbial consortia. *Bioresour. Technol.* **2011,** *102* (3), 3352-3359.
82. Vanhoorne, P.; Dubois, P.; Jerome, R.; Teyssie, P., Macromolecular engineering of polylactones and polylactides. 7. Structural analysis of copolyesters of iε-caprolactone and L- or D,L-lactide initiated by triisopropoxyaluminum. *Macromolecules* **1992,** *25* (1), 37-44.
83. Crystallinity degree was calculated by comparing the observed melting enthalpy with the value of 142 J/g of a PLLA crystal of infinite size.
84. Tsuji, H., Poly (lactide) stereocomplexes: formation, structure, properties, degradation, and applications. *Macromol. Biosci.* **2005,** *5* (7), 569-597.
85. Abe, H.; Doi, Y.; Aoki, H.; Akehata, T.; Hori, Y.; Yamaguchi, A., Physical properties and enzymic degradability of copolymers of (R)-3-hydroxybutyric and 6-hydroxyhexanoic acids. *Macromolecules* **1995,** *28* (23), 7630-7637.
86. Chen, C.; Fei, B.; Peng, S.; Wu, H.; Zhuang, Y.; Chen, X.; Dong, L.; Feng, Z., Synthesis and characterization of poly (β-hydroxybutyrate) and poly (ϵ-caprolactone) copolyester by transesterification. *J. Polym. Sci., Part B: Polym. Phys.* **2002,** *40* (17), 1893-1903.
87. (a) Hori, Y.; Takahashi, Y.; Yamaguchi, A.; Nishishita, T., Ring-opening copolymerization of optically active .beta.-butyrolactone with several lactones catalyzed by distannoxane complexes: synthesis of new biodegradable polyesters. *Macromolecules* **1993,** *26* (16), 4388-4390; (b) Reeve, M. S.; McCarthy, S. P.; Gross, R. A., Preparation and characterization of (R)-poly(.beta.-hydroxybutyrate)-poly(.epsilon.-caprolactone) and (R)-poly(.beta.-hydroxybutyrate)-poly(lactide) degradable diblock copolymers. *Macromolecules* **1993,** *26* (5), 888-894; (c) Aluthge, D. C.; Xu, C.; Othman, N.; Noroozi, N.; Hatzikiriakos, S. G.; Mehrkhodavandi, P., PLA–PHB–PLA Triblock Copolymers: Synthesis by Sequential Addition and Investigation of Mechanical and Rheological Properties. *Macromolecules* **2013,** *46* (10), 3965-

3974; (d) Jeffery, B. J.; Whitelaw, E. L.; Garcia-Vivo, D.; Stewart, J. A.; Mahon, M. F.; Davidson, M. G.; Jones, M. D., Group 4 initiators for the stereoselective ROP of rac-[small beta]-butyrolactone and its copolymerization with rac-lactide. *Chem. Commun.* **2011,** *47* (45), 12328-12330; (e) Agatemor, C.; Arnold, A. E.; Cross, E. D.; Decken, A.; Shaver, M. P., Aluminium salophen and salen initiators in the ring-opening polymerization of rac-lactide and rac-β-butyrolactone: Electronic effects on stereoselectivity and polymerization rates. *J. Organomet. Chem.* **2013,** *745-746*, 335-340.
88. Saini, P. K.; Romain, C.; Zhu, Y.; Williams, C. K., Di-magnesium and zinc catalysts for the copolymerization of phthalic anhydride and cyclohexene oxide. *Polym. Chem.* **2014,** *5* (20), 6068-6075.
89. Yu, C.-Y.; Chuang, H.-J.; Ko, B.-T., Bimetallic bis(benzotriazole iminophenolate) cobalt, nickel and zinc complexes as versatile catalysts for coupling of carbon dioxide with epoxides and copolymerization of phthalic anhydride with cyclohexene oxide. *Catal. Sci. Technol.* **2016,** *6* (6), 1779-1791.
90. (a) Rieth , L. R. M., D. R.; Lobkovsky , E. B.; Coates, G. W., Single-Site β-Diiminate Zinc Catalysts for the Ring-Opening Polymerization of β-Butyrolactone and β-Valerolactone to Poly(3-hydroxyalkanoates). *J. Am. Chem. Soc.* **2002,** *124*, 15239–15248; (b) Vagin, S. I.; Reichardt, R.; Klaus, S.; Rieger, B., Conformationally Flexible Dimeric Salphen Complexes for Bifunctional Catalysis. *J. Am. Chem. Soc.* **2010,** *132* (41), 14367-14369; (c) Aida, T.; Sanuki, K.; Inoue, S., Well-controlled polymerization by metalloporphyrin. Synthesis of copolymer with alternating sequence and regulated molecular weight from cyclic acid anhydride and epoxide catalyzed by the system of aluminum porphyrin coupled with quaternary organic salt. *Macromolecules* **1985,** *18* (6), 1049-55; (d) Coulembier, O.; Moins, S.; Todd, R.; Dubois, P., External and Reversible CO2 Regulation of Ring-Opening Polymerizations Based on a Primary Alcohol Propagating Species. *Macromolecules* **2014,** *47* (2), 486-491; (e) Nejad, E. H.; van Melis, C. G. W.; Vermeer, T. J.; Koning, C. E.; Duchateau, R., Alternating Ring-Opening Polymerization of Cyclohexene Oxide and Anhydrides: Effect of Catalyst, Cocatalyst, and Anhydride Structure. *Macromolecules* **2012,** *45* (4), 1770-1776.
91. (a) Romain, C.; Zhu, Y.; Dingwall, P.; Paul, S.; Rzepa, H. S.; Buchard, A.; Williams, C. K., Chemoselective Polymerizations from Mixtures of Epoxide, Lactone, Anhydride, and Carbon Dioxide. *J. Am. Chem. Soc.* **2016,** *138* (12), 4120-4131; (b) Paul, S.; Romain, C.;

Shaw, J.; Williams, C. K., Sequence Selective Polymerization Catalysis: A New Route to ABA Block Copoly(ester-b-carbonate-b-ester). *Macromolecules* **2015,** *48* (17), 6047-6056; (c) Romain, C.; Williams, C. K., Chemoselective Polymerization Control: From Mixed-Monomer Feedstock to Copolymers. *Angew. Chem., Int. Ed.* **2014,** *53* (6), 1607-1610; (d) Tim, S.; K., W. C., Selective Polymerization Catalysis from Monomer Mixtures: Using a Commercial Cr-Salen Catalyst To Access ABA Block Polyesters. *Angew. Chem. Int. Ed. 0* (0); (e) Zhu, Y.; Radlauer, M. R.; Schneiderman, D. K.; Shaffer, M. S. P.; Hillmyer, M. A.; Williams, C. K., Multiblock Polyesters Demonstrating High Elasticity and Shape Memory Effects. *Macromolecules* **2018,** *51* (7), 2466-2475; (f) Stößer, T.; Williams, C. K., Selective Polymerization Catalysis from Monomer Mixtures: Using a Commercial Cr-Salen Catalyst To Access ABA Block Polyesters. *Angew. Chem. Int. Ed.* **2018,** *57* (21), 6337-6341.

92. Kernbichl, S.; Reiter, M.; Adams, F.; Vagin, S.; Rieger, B., CO2-Controlled One-Pot Synthesis of AB, ABA Block, and Statistical Terpolymers from β-Butyrolactone, Epoxides, and CO2. *J. Am. Chem. Soc.* **2017,** *139* (20), 6787-6790.

93. (a) Darensbourg, D. J.; Mackiewicz, R. M.; Rodgers, J. L.; Phelps, A. L., (Salen)CrIIIX Catalysts for the Copolymerization of Carbon Dioxide and Epoxides: Role of the Initiator and Cocatalyst. *Inorg. Chem.* **2004,** *43* (6), 1831-1833; (b) Darensbourg, D. J.; Mackiewicz, R. M., Role of the Cocatalyst in the Copolymerization of CO2 and Cyclohexene Oxide Utilizing Chromium Salen Complexes. *J. Am. Chem. Soc.* **2005,** *127* (40), 14026-14038.

94. The importance of the use of a Lewis base as co-catalyst to reprime the epoxide homopolymerization is exemplified by the catalytic behaviour of tetraphenylporphyrin aluminium and e cobalt complexes in CO2/ epoxide copolymerization. See P. Pescarmona, M. Taherimehr Catal. Sci. Technol., 2012, 2, 2169–2187

95. Analogous results in terms of the molecular weighs were obtained by using SA purified by sublimation or crystallization.

96. (a) Hauenstein, O.; Reiter, M.; Agarwal, S.; Rieger, B.; Greiner, A., Bio-based polycarbonate from limonene oxide and CO2 with high molecular weight, excellent thermal resistance, hardness and transparency. *Green Chem.* **2016,** *18* (3), 760-770; (b) Li, C.; Sablong, R. J.; Koning, C. E., Chemoselective Alternating Copolymerization of Limonene Dioxide and Carbon Dioxide: A New Highly Functional Aliphatic Epoxy Polycarbonate. *Angew.*

Chem. Int. Ed. **2016,** *55* (38), 11572-11576; (c) Byrne, C. M.; Allen, S. D.; Lobkovsky, E. B.; Coates, G. W., Alternating Copolymerization of Limonene Oxide and Carbon Dioxide. *J. Am. Chem. Soc.* **2004,** *126* (37), 11404-11405.
97. (a) Martín, C.; Pizzolante, A.; Escudero-Adán, E. C.; Kleij, A. W., Bifunctional Aminotriphenolate Complexes as One-Component Catalysts for the Ring-Opening Copolymerization of Cyclic Anhydrides and Epoxides. *Eur. J. Inorg. Chem.* **2018,** *2018* (18), 1921-1927; (b) Peña Carrodeguas, L.; Martín, C.; Kleij, A. W., Semiaromatic Polyesters Derived from Renewable Terpene Oxides with High Glass Transitions. *Macromolecules* **2017,** *50* (14), 5337-5345.
98. Nejad, E. H.; Paoniasari, A.; van Melis, C. G. W.; Koning, C. E.; Duchateau, R., Catalytic Ring-Opening Copolymerization of Limonene Oxide and Phthalic Anhydride: Toward Partially Renewable Polyesters. *Macromolecules* **2013,** *46* (3), 631-637.
99. (a) Darensbourg, D. J.; Poland, R. R.; Escobedo, C., Kinetic Studies of the Alternating Copolymerization of Cyclic Acid Anhydrides and Epoxides, and the Terpolymerization of Cyclic Acid Anhydrides, Epoxides, and CO2 Catalyzed by (salen)CrIIICl. *Macromolecules* **2012,** *45* (5), 2242-2248; (b) Jeske, R. C.; Rowley, J. M.; Coates, G. W., Pre-rate-determining selectivity in the terpolymerization of epoxides, cyclic anhydrides, and CO2: a one-step route to diblock copolymers. *Angew. Chem. Int. Ed.* **2008,** *47* (32), 6041-6044, S6041/1-S6041/16.
100. Cozzolino, M.; Rosen, T.; Goldberg, I.; Mazzeo, M.; Lamberti, M., Selective Synthesis of Cyclic Carbonate by Salalen–Aluminum Complexes and Mechanistic Studies. *ChemSusChem* **2017**, n/a-n/a.
101. Zhu, Y.; Romain, C.; Williams, C. K., Selective Polymerization Catalysis: Controlling the Metal Chain End Group to Prepare Block Copolyesters. *J. Am. Chem. Soc.* **2015,** *137* (38), 12179-12182.
102. (a) Pilone, A.; Lamberti, M.; Mazzeo, M.; Milione, S.; Pellecchia, C., Ring-opening polymerization of cyclic esters by phenoxy-thioether complexes derived from biocompatible metals. *Dalton Trans.* **2013,** *42* (36), 13036-13047; (b) Pappalardo, D.; Annunziata, L.; Pellecchia, C., Living Ring-Opening Homo- and Copolymerization of ε-Caprolactone and l- and d,l-Lactides by Dimethyl(salicylaldiminato)aluminum Compounds. *Macromolecules* **2009,** *42* (16), 6056-6062; (c) Wang, X.; Zhao, K.-

Q.; Al-Khafaji, Y.; Mo, S.; Prior, T. J.; Elsegood, M. R. J.; Redshaw, C., Organoaluminium Complexes Derived from Anilines or Schiff Bases for the Ring-Opening Polymerization of ε-Caprolactone, δ-Valerolactone and rac-Lactide. *Eur. J. Inorg. Chem.* **2017,** *2017* (13), 1951-1965; (d) Iwasa, N.; Fujiki, M.; Nomura, K., Ring-opening polymerization of various cyclic esters by Al complex catalysts containing a series of phenoxy-imine ligands: Effect of the imino substituents for the catalytic activity. *J. Mol. Catal. A: Chem.* **2008,** *292* (1-2), 67-75; (e) Iwasa, N.; Katao, S.; Liu, J.; Fujiki, M.; Furukawa, Y.; Nomura, K., Notable Effect of Fluoro Substituents in the Imino Group in Ring-Opening Polymerization of ϵ-Caprolactone by Al Complexes Containing Phenoxyimine Ligands. *Organometallics* **2009,** *28* (7), 2179-2187.

103. (a) Sugimoto, H.; Ohtsuka, H.; Inoue, S., Alternating copolymerization of carbon dioxide and epoxide catalyzed by an aluminum Schiff base–ammonium salt system. *J. Polym. Sci., Part A: Polym. Chem.* **2005,** *43* (18), 4172-4186; (b) Cameron, P. A.; Gibson, V. C.; Redshaw, C.; Segal, J. A.; Solan, G. A.; White, A. J. P.; Williams, D. J., Synthesis and characterisation of neutral dialkylaluminium complexes stabilised by salicylaldiminato ligands, and their conversion to monoalkylaluminium cations*J. Chem. Soc., Dalton Trans.* **2001,** (9), 1472-1476; (c) Lamberti, M.; D'Auria, I.; Mazzeo, M.; Milione, S.; Bertolasi, V.; Pappalardo, D., Phenoxy-Thioether Aluminum Complexes as ε-Caprolactone and Lactide Polymerization Catalysts. *Organometallics* **2012,** *31* (15), 5551-5560.

104. Van Zee, N. J.; Sanford, M. J.; Coates, G. W., Electronic Effects of Aluminum Complexes in the Copolymerization of Propylene Oxide with Tricyclic Anhydrides: Access to Well-Defined, Functionalizable Aliphatic Polyesters. *J. Am. Chem. Soc.* **2016,** *138* (8), 2755-2761.

105. Analogous results in terms of the molecular weighs were obtained by using SA purified by sublimation or crystallization.

106. The polymer chains initiated by DMAP are intrinsically charged thus, in the MALDI-ToF-MS spectra, they can totally obscure the originally uncharged chains formed by inititiation by methyl groups.

107. Fieser, M. E.; Sanford, M. J.; Mitchell, L. A.; Dunbar, C. R.; Mandal, M.; Van Zee, N. J.; Urness, D. M.; Cramer, C. J.; Coates, G. W.; Tolman, W. B., Mechanistic Insights into the Alternating Copolymerization of Epoxides and Cyclic Anhydrides Using a

(Salph)AlCl and Iminium Salt Catalytic System. *J. Am. Chem. Soc.* **2017,** *139* (42), 15222-15231.
108. The experiment was repeated in the presence of two equivalents of DMAP , also in this case no opening of the monomer was achieved at room temperature, the DMAP was not coordinated. After heating at 70 °C, the complete conversion of complex 1 into species 1a occurred within the same time.
109. (a) Dzugan, S. J.; Goedken, V. L., Factors affecting aluminum-carbon bond reactivity of tetradentate Schiff-base organoaluminum complexes. *Inorg. Chem.* **1986,** *25* (16), 2858-2864; (b) Rutherford, D.; Atwood, D. A., Five-Coordinate Aluminum Amides. *Organometallics* **1996,** *15* (21), 4417-4422.
110. Balskus, E. P.; Jacobsen, E. N., α,β-Unsaturated β-Silyl Imide Substrates for Catalytic, Enantioselective Conjugate Additions: A Total Synthesis of (+)-Lactacystin and the Discovery of a New Proteasome Inhibitor. *J. Am. Chem. Soc.* **2006,** *128* (21), 6810-6812.
111. Meléndez, J.; North, M.; Pasquale, R., Synthesis of Cyclic Carbonates from Atmospheric Pressure Carbon Dioxide Using Exceptionally Active Aluminium(salen) Complexes as Catalysts. *Eur. J. Inorg. Chem.* **2007,** *2007* (21), 3323-3326.
112. Mason, M. R.; Smith, J. M.; Bott, S. G.; Barron, A. R., Hydrolysis of tri-tert-butylaluminum: the first structural characterization of alkylalumoxanes [(R2Al)2O]n and (RAlO)n. *J. Am. Chem. Soc.* **1993,** *115* (12), 4971-4984.
113. Nakano, K.; Kamada, T.; Nozaki, K., Selective Formation of Polycarbonate over Cyclic Carbonate: Copolymerization of Epoxides with Carbon Dioxide Catalyzed by a Cobalt(III) Complex with a Piperidinium End-Capping Arm. *Angew. Chem. Int. Ed.* **2006,** *118* (43), 7432-7435.
114. Rulev, Y. A.; Gugkaeva, Z.; Maleev, V. I.; North, M.; Belokon, Y. N., Robust bifunctional aluminium-salen catalysts for the preparation of cyclic carbonates from carbon dioxide and epoxides. *Beilstein J Org Chem* **2015,** *11*, 1614-23.
115. Jeon, J. Y.; Eo, S. C.; Varghese, J. K.; Lee, B. Y., Copolymerization and terpolymerization of carbon dioxide/propylene oxide/phthalic anhydride using a (salen)Co(III) complex tethering four quaternary ammonium salts. *Beilstein J Org Chem* **2014,** *10*, 1787-95.
116. Sujith, S.; Min, J. K.; Seong, J. E.; Na, S. J.; Lee, B. Y., A highly active and recyclable catalytic system for CO2/propylene

oxide copolymerization. *Angew. Chem. Int. Ed.* **2008,** *47* (38), 7306-9.
117. (a) Cameron, P. A.; Gibson, V. C.; Redshaw, C.; Segal, J. A.; White, A. J. P.; Williams, D. J., Synthesis and characterisation of neutral and cationic alkyl aluminium complexes bearing N,O-Schiff base chelates with pendant donor arms. *J. Chem. Soc., Dalton Trans.* **2002,** (3), 415-422; (b) Yankey, M.; Obuah, C.; Darkwa, J., Phenoxysalicylaldimine-Bearing Chromium (III) Precatalysts for Ethylene Polymerization. *Macromol. Chem. Phys.* **2014,** *215* (18), 1767-1775; (c) Asadi, M.; Hemmateenejad, B.; Mohammadikish, M., Synthesis, characterization, and formation constant of hexacoordinate iron (III) complexes. *J. Coord. Chem.* **2010,** *63* (1), 124-135.
118. Tschan, M. J.-L.; Guo, J.; Raman, S. K.; Brulé, E.; Roisnel, T.; Rager, M.-N.; Legay, R.; Durieux, G.; Rigaud, B.; Thomas, C. M., Zinc and cobalt complexes based on tripodal ligands: synthesis, structure and reactivity toward lactide. *Dalton Trans.* **2014,** *43* (11), 4550-4564.
119. Abdel-Magid, A. F.; Carson, K. G.; Harris, B. D.; Maryanoff, C. A.; Shah, R. D., Reductive amination of aldehydes and ketones with sodium triacetoxyborohydride. studies on direct and indirect reductive amination procedures1. *J. Org. Chem.* **1996,** *61* (11), 3849-3862.
120. Kochnev, A.; Oleynik, I.; Oleynik, I.; Ivanchev, S.; Tolstikov, G., Synthesis of salicylaldehydes bearing bulky substituents in the positions 3 and 5. *Russ. Chem. Bull.* **2007,** *56* (6), 1125-1129.
121. Andersen, R.; Faegri Jr, K.; Green, J. C.; Haaland, A.; Lappert, M.; Leung, W. P.; Rypdal, K., Synthesis of bis [bis (trimethylsilyl) amido] iron (II). Structure and bonding in M [N (SiMe3) 2] 2 (M= manganese, iron, cobalt): two-coordinate transition-metal amides. *Inorg. Chem.* **1988,** *27* (10), 1782-1786.
122. (a) Thakur, K. A.; Kean, R. T.; Hall, E. S.; Kolstad, J. J.; Lindgren, T. A.; Doscotch, M. A.; Siepmann, J. I.; Munson, E. J., High-resolution 13C and 1H solution NMR study of poly (lactide). *Macromolecules* **1997,** *30* (8), 2422-2428; (b) Thakur, K. A.; Kean, R. T.; Hall, E. S.; Kolstad, J. J.; Munson, E. J., Stereochemical aspects of lactide stereo-copolymerization investigated by 1H NMR: a case of changing stereospecificity. *Macromolecules* **1998,** *31* (5), 1487-1494; (c) Zell, M. T.; Padden, B. E.; Paterick, A. J.; Thakur, K. A.; Kean, R. T.; Hillmyer, M. A.; Munson, E. J., Unambiguous

determination of the 13C and 1H NMR stereosequence assignments of polylactide using high-resolution solution NMR spectroscopy. *Macromolecules* **2002,** *35* (20), 7700-7707; (d) Thakur, K. A.; Kean, R. T.; Zell, M. T.; Padden, B. E.; Munson, E. J., An alternative interpretation of the HETCOR NMR spectra of poly (lactide). *Chem. Commun.* **1998,** (17), 1913-1914; (e) Chisholm, M. H.; Iyer, S. S.; McCollum, D. G.; Pagel, M.; Werner-Zwanziger, U., Microstructure of Poly (lactide). Phase-Sensitive HETCOR Spectra of Poly (meso-lactide), Poly (r ac-lactide), and Atactic Poly (lactide). *Macromolecules* **1999,** *32* (4), 963-973; (f) Amgoune, A.; Thomas, C. M.; Roisnel, T.; Carpentier, J. F., Ring-opening polymerization of lactide with group 3 metal complexes supported by dianionic alkoxy-amino-bisphenolate ligands: combining high activity, productivity, and selectivity. *Chem. Eur. J.* **2006,** *12* (1), 169-179; (g) Amgoune, A.; Thomas, C. M.; Carpentier, J. F., Yttrium complexes as catalysts for living and immortal polymerization of lactide to highly heterotactic PLA. *Macromol. Rapid Commun.* **2007,** *28* (6), 693-697.
123. Coudane, J.; Ustariz-Peyret, C.; Schwach, G.; Vert, M., More about the stereodependence of DD and LL pair linkages during the ring-opening polymerization of racemic lactide. *J. Polym. Sci., Part A: Polym. Chem.* **1997,** *35* (9), 1651-1658.

PHD COURSE ACTIVITY SUMMARY.

Candidate: Florence Isnard

ATTENDED COURSES:

- Physical Methods of Organic Chemistry - Prof. Carmine Gaeta.
- Laboratory of Characterization of Polymeric Materials - Prof. Paola Rizzo.
- Theoretical and practical course for the use of DSC and TGA - Marco Coletti (TA instruments).
- Uses and Applications of Crystallographic Data in Structural Chemistry and Drug Discovery - The Cambridge Crystallographic Data Centre.
- Introductory course about statistics with R - Prof. Emmanuelle Becker.

VISITING PERIOD:

July 2017 - February 2018 at Organometallic Chemistry and Polymerization Catalysis group at IRCP (Institut de Recherche de Chimie Paris) - Prof. C. M. Thomas.

PUBLICATIONS:

- Copolymerization of cyclic esters, epoxides and anhydrides by a bimetallic salen aluminum complex. Evidences of a dual role of the monomers in the reaction mixture. F. Isnard, M. Carratu , M. Lamberti, V. Venditto, M. Mazzeo. *Catal. Sci. Technol.*, **2018**, *8*, 5034.
- Novel polyesters from renewable resources. F. Isnard, M. Mazzeo, C. M. Thomas. *L'actualité chimique*, **2018**, *427-428*, 50.
- Ring-opening copolymerization of epoxides with cyclic anhydrides promoted by bimetallic and monometallic phenoxy–imine aluminum complexes. F. Isnard, M. Lamberti, C. Pellecchia, M. Mazzeo. *ChemCatChem*, **2017**, *9(15)*, 2972.
- Bimetallic salen aluminum complexes: cooperation between reactive centers in the ring-opening polymerization of lactides

and epoxides. F. Isnard, M. Lamberti, L. Lettieri, M. Mazzeo. *Dalton Trans.*, **2016**, *45(40)*, 16001.

- Phenoxy-based Aluminum Complexes: Simple and Efficient Catalysts for the Ring-Opening Copolymerization of Epoxides and Anhydrides. F. Isnard, F. Santulli, M. Cozzolino, M. Lamberti, M. Mazzeo. Manuscript submitted.
- Iso-selective lactide polymerization with iron complexes: a new approach to stereocomplex formation. P. Marin, M. J.-L. Tschan, F. Isnard, C. Robert, P. Haquette, X. Trivelli, T. Roisnel, L.-M. Chamoreau, V. Guérineau, I. del Rosal, L. Maron, V. Venditto, C. M. Thomas. Manuscript submitted.
- Bifunctional aluminum catalysts for the selective Ring-Opening Co-Polymerization of Epoxides and Cyclic Anhydrides. F. Isnard, S. Russo, R. Zeolla, M. Lamberti, M. Mazzeo. Manuscript in preparation.

ATTENDED CONGRESSES:

- Merck Young Chemist Symposium.
  F. Isnard, M. Lamberti, M. Mazzeo. "Homo- and Co-Polymerization of Epoxides and Anhydrides promoted by bimetallic salen aluminum complexes: role of the cooperation between the two reactive metal center". POSTER, p. 142. Rimini, October 25-27th 2016.

- Nanomeetsbio@nanomates workshop.
  F. Isnard, M. Lamberti, M. Mazzeo. "Bio-based Polyesters from the Co-Polymerization of Epoxides and Anhydrides". POSTER, p. 8. Salerno, Febbruary 16th 2017.

- XIV PhD Day Inter-university Consortium Chemical Reactivity and Catalysis.
  F. Isnard, M. Lamberti, M. Mazzeo, C. Pellecchia. "Polyesters from the alternating copolymerization of epoxides and cyclic anhydrides". ORAL PRESENTATION. Bari, March 30-31st 2017.

ACKNOWLEDGEMENTS.

First of all, I would like to thank everybody at the University of Salerno for the kind welcome I have had in South Italy. These three years have been full of surprises and adventures, and I believe I have learned and changed a lot! I will definitely miss pizza and mozzarella!

The work presented in this thesis has been conducted in the Laboratory of Prof. Claudio Pellecchia, and I would like to thank him for the opportunity to carry out my PhD in his laboratory.

I am truly thankful to my tutor Mina who has always been full of enthusiasm, optimism and even ready to help me settle in Italy. She has been giving me a wonderful guidance during these years of research and made it a pleasure doing my PhD.

I would like to express my gratitude to Marina for her kindness, her help and good advice.

I acknowledge the Cariplo Foundation (Apollo project 2016-0643) for financial support.

I wish to express my sincere gratitude to Prof. Christophe Thomas, first for giving me the opportunity to get in contact with Mina and Marina, and also for welcoming me in his lab for 7 months where I learned a lot.

An immense thanks to Lab3, especially Ilaria and Mariachiara whom I have been putting up with for three years (yes, they put up with me too)! It has been awesome working with you, I will be forever grateful for your welcome, your help, your jokes (well not when you were joking on me!) and the good atmosphere! Mariachiara for being a real friend during this adventure and helping me understand the Italian life!

Thank you to my dear Marco and Flavia for their great company, all the interns who have worked with me and they have been numerous, especially Federica for coming back after the first experience!

Thank you to all my friends from all over the world who were in Salerno, to all my French friends who came to see me (and the beautiful Amalfi Coast…).

Lastly, a huge thanks to my family who was a constant support, even from a distance and came to see me several times. And I am truly grateful to my boyfriend for his love and comprehension, even when he thought I was crazy while writing this thesis, and his family who made me feel at home far away from home!